

Intro



Gianluca Geloni



Svitozar Serkez



Takanori Tanikawa



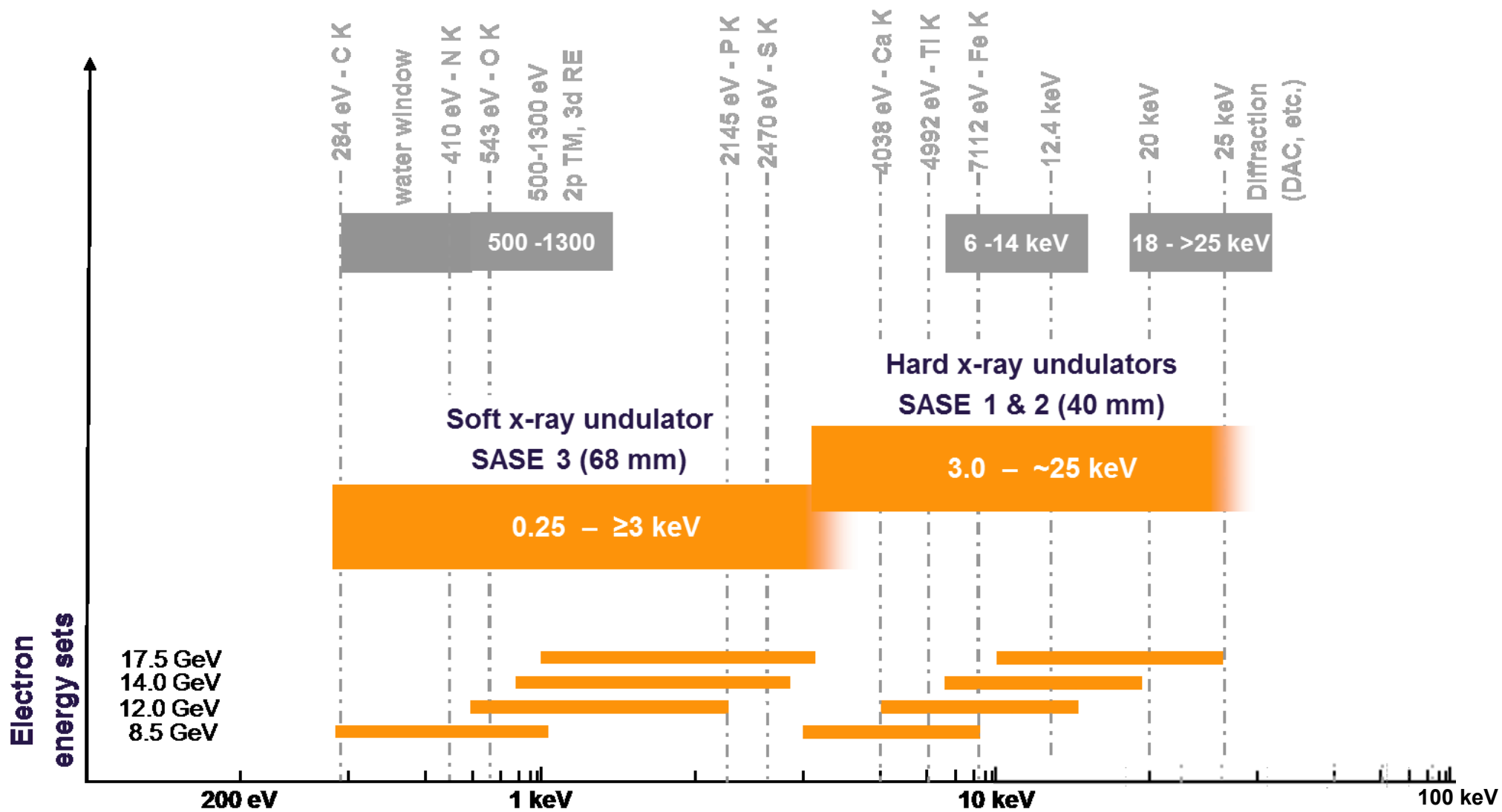
Sergey Tomin

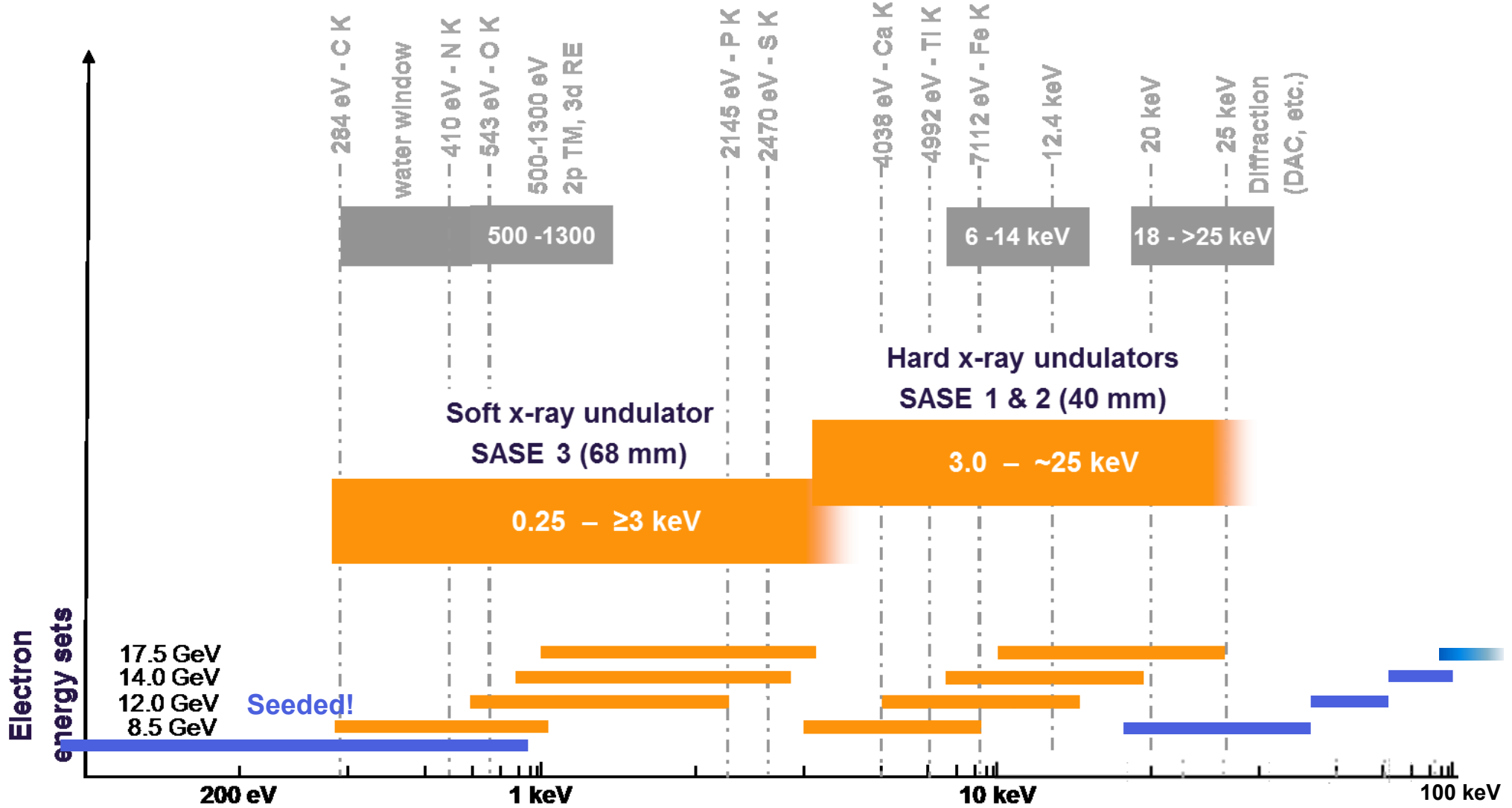
*“The **Simulation of Photon Fields (SPF)** Group devises and assesses novel advanced FEL schemes for improving the characteristics of the photon beams at the European XFEL.”*

This Workshop: three talks from my group [with substantial contribution and support from **Sara Casalbuoni (KIT), Michael Gensch (HZDR), Suren Karabekyan (EuXFEL), Vitali Kocharyan (DESY), Shan Liu (DESY), Evgeni Saldin (DESY), Nikola Stojanovic (DESY), Patrik Vagovic (EuXFEL), and many others...**]

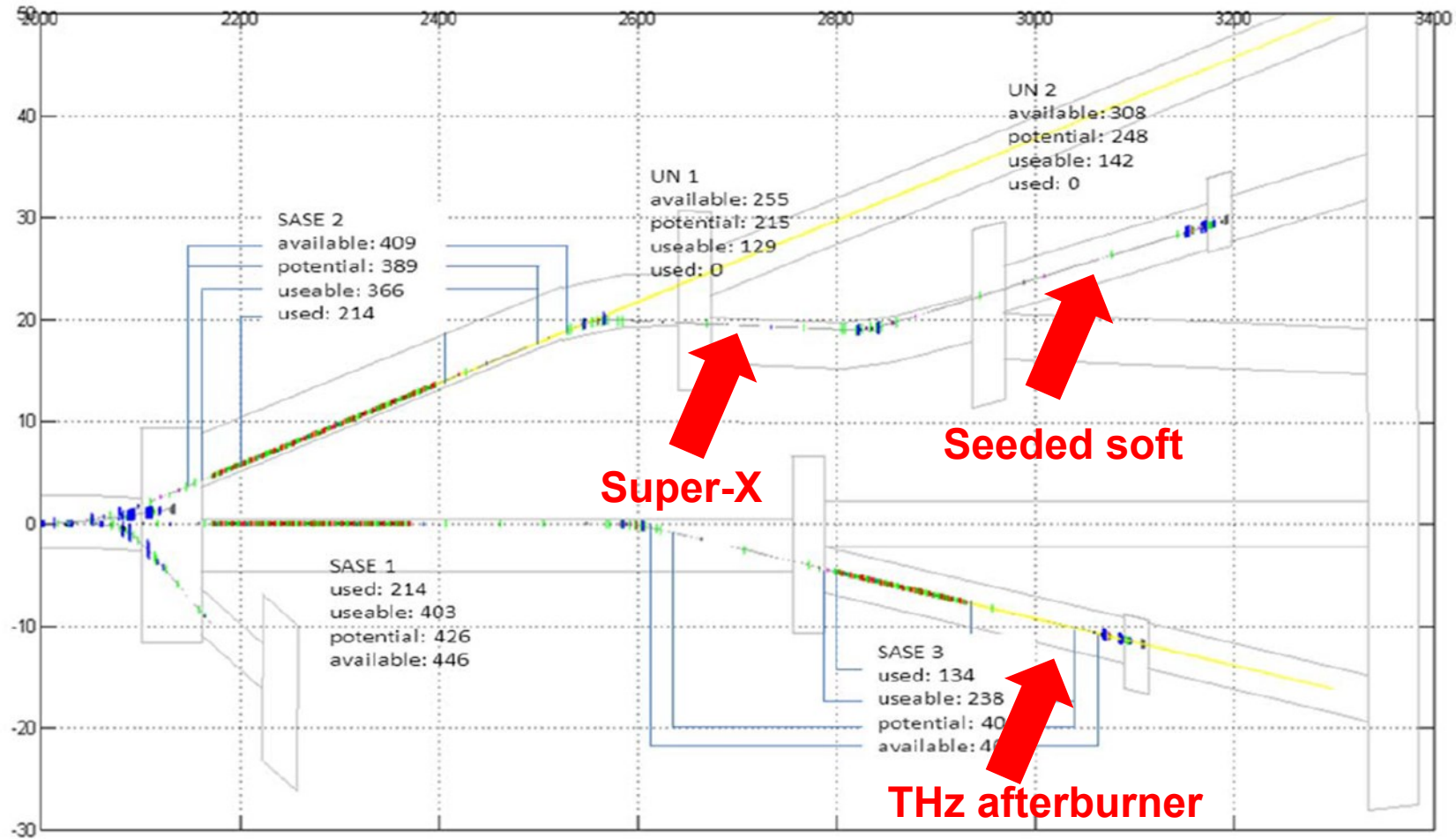
13:00 – 13:30	Svitozar Serkez, Gianluca Geloni (European XFEL) “Super-X: Simulations for the Super-Hard X-ray Generation with Short Period Undulators for the European XFEL”	■ Now
09:30 – 10:00	Takanori Tanikawa (European XFEL) “External Seeding Possibilities at the European XFEL (EEHG and HGHG) and THz Addition”	■ Tomorrow
13:30 – 14:00	Gianluca Geloni (European XFEL) “Self-seeding: Energy-Range Limits and Possibilities”	■ Tomorrow

There is a guiding idea linking these talks...





Plus THz Pump-probe possibilities between 3 THz and 40 THz



Fresh bunch needed...

- Many of the additions proposed require high-field and/or short period undulators
- One possibility: Superconducting Undulator Technology

Verbundprojekt FuE für
Erforschung der Materie an Großgeräten 2019-2022:
Supraleitende Undulatoren für die European XFEL

Vorhabenbeschreibung

Antragsteller:

Prof. Dr. Anke-Susanne Müller¹,
Prof. Dr.-Ing. Herbert De Gerssem²

*“Aim of this project is to explore the benefits of applying
superconducting undulators to the European XFEL”*

Proposed by KIT and TUD

Super-X: Simulations for super-hard X-ray generation with short period undulators for the European XFEL



Svitozar Serkez, Takanori Tanikawa, Sara Casalbuoni
Sergey Tomin, Suren Karabekyan, Gianluca Geloni

Outline

- Necessary assumptions
 - Electron beam
 - Space available
 - Undulator technology
- Analytical estimations
- Quantum fluctuations
- Comparison with harmonic lasing
- Period doubling
- CW operation
- Magnetic field tolerances
- Spread of SASE spectrum
- Radiation spatial coherence
- E-beam quality revisited
- 100keV numerical case study (incl. all detrimental effects)
- Conclusions

■ *Analytical estimation and post-processing of numerical simulations done with OCELOT <https://github.com/ocelot-collab/ocelot>

E-beam assumptions

- $I_{\text{peak}} = 5 \text{ kA}$
- $E = 17.5 \text{ GeV}$
- $dE = 1 \text{ MeV}$ ($d\gamma = 1.9$)
- Emittance = 0.4 mm mrad

Summary

■ Slice emittance in x/y plane, μm

Position	500 pC, 5kA	500 pC, 10 kA	250 pC, 5 kA	100 pC, 5 kA
after injector booster	0.50	0.50	0.36	0.18
after collimator	0.57	0.57 / 0.75	0.40	0.24 / 0.30
after T1 arc (before SASE2)	0.57	0.57 / 0.75	0.40	0.24 / 0.30

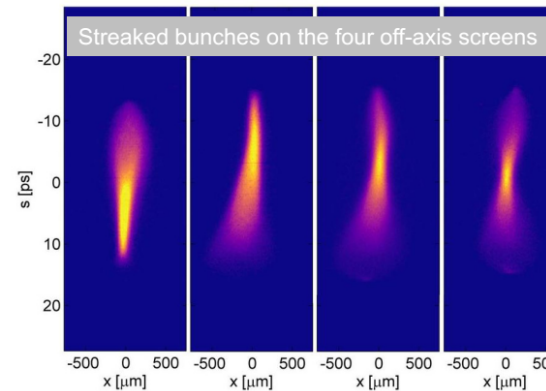
■ Projected emittance in x/y plane, μm

Position	500 pC, 5kA	500 pC, 10 kA	250 pC, 5 kA	100 pC, 5 kA
after injector booster	0.84	0.84	0.67	0.30
after collimator	1.15 / 1.21	1.10 / 2.93	0.80 / 1.37	0.30 / 0.82
after T1 arc (before SASE2)	1.35 / 1.16	2.64 / 2.52	1.34 / 1.26	0.83 / 0.73

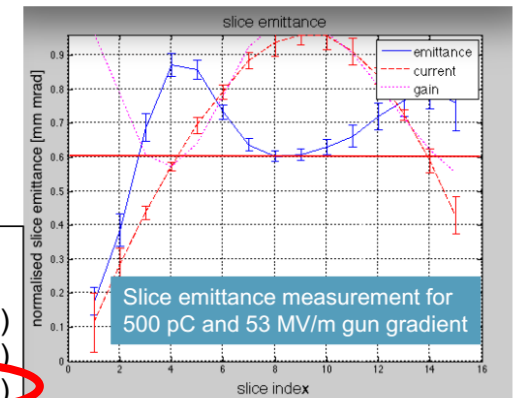
■ In the simulations we have used the laser heater in the injector to provide 1 MeV slice energy spread after BC2

■ Talk by Igor Zagorodnov

Slice Emittance Measurements



We are able to match single slices of the bunch. One matching iteration takes about 2 minutes including the magnet cycling.

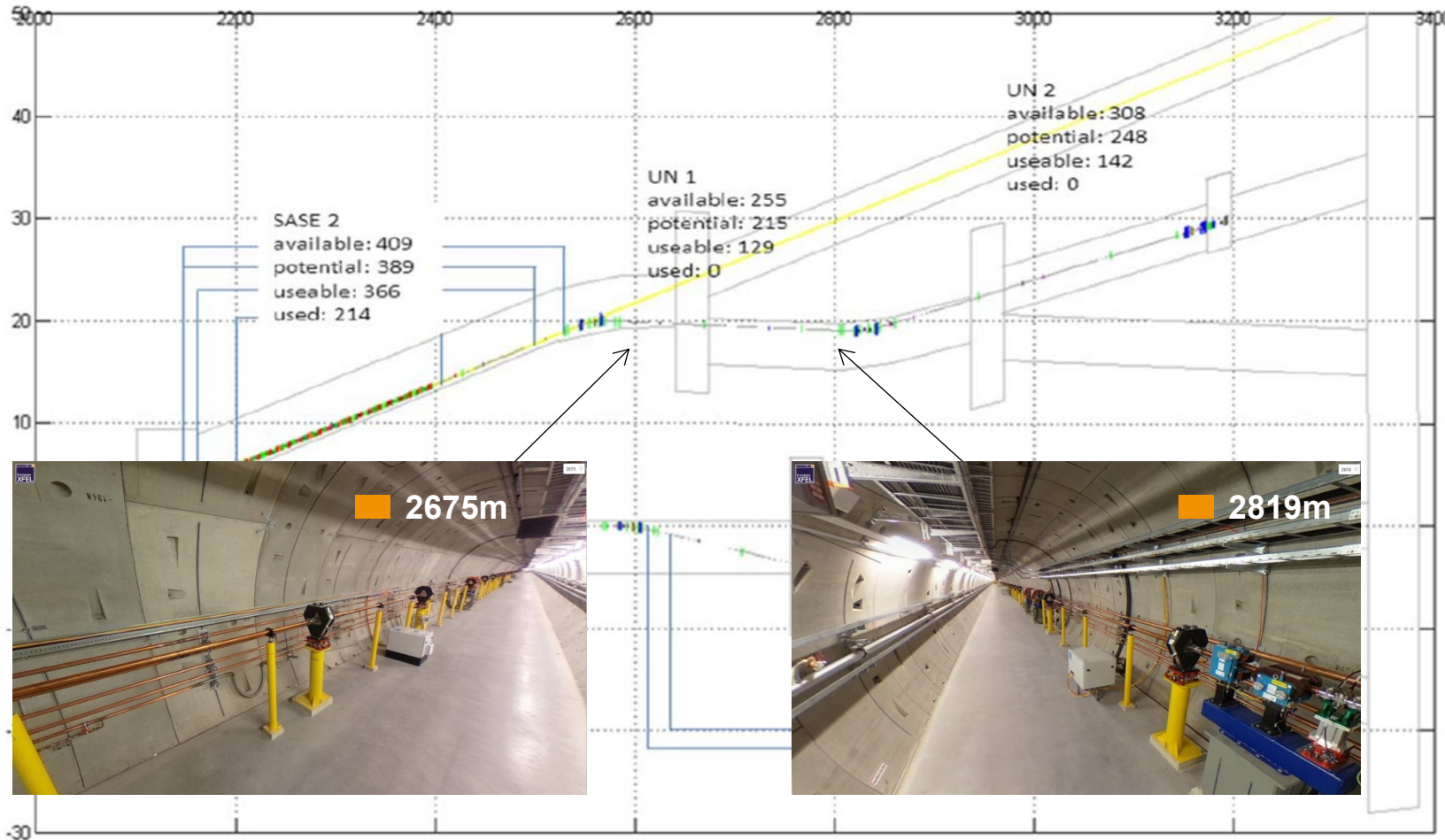


The smallest slice emittances achieved so far (four-screen method):

- 0.6 μm rad with 53 MV/m gun gradient (500 pC)
- 0.5 μm rad with 60 MV/m gun gradient (500 pC)
- 0.4 μm rad with 60 MV/m gun gradient (400 pC)

■ B. Beutner *European XFEL Injector Commissioning Results*, talk at International FEL Conference, Santa Fe (2017), slide of M.Scholz

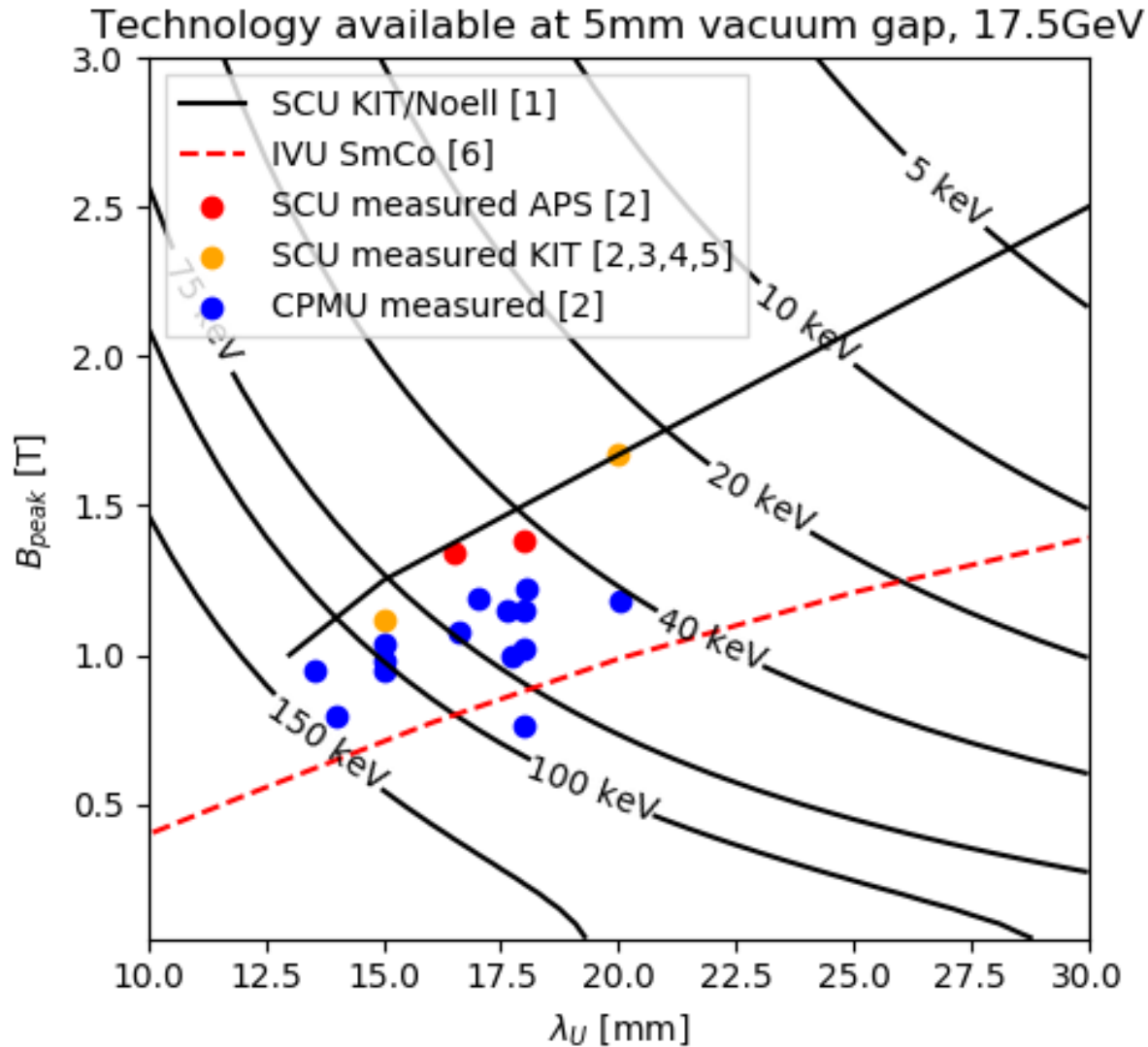
Tunnel location and length (XTD3/SASE4)



Assume:

- SASE2 open or bypassed
- 150m undulator
- 79% filling factor

Undulator technologies



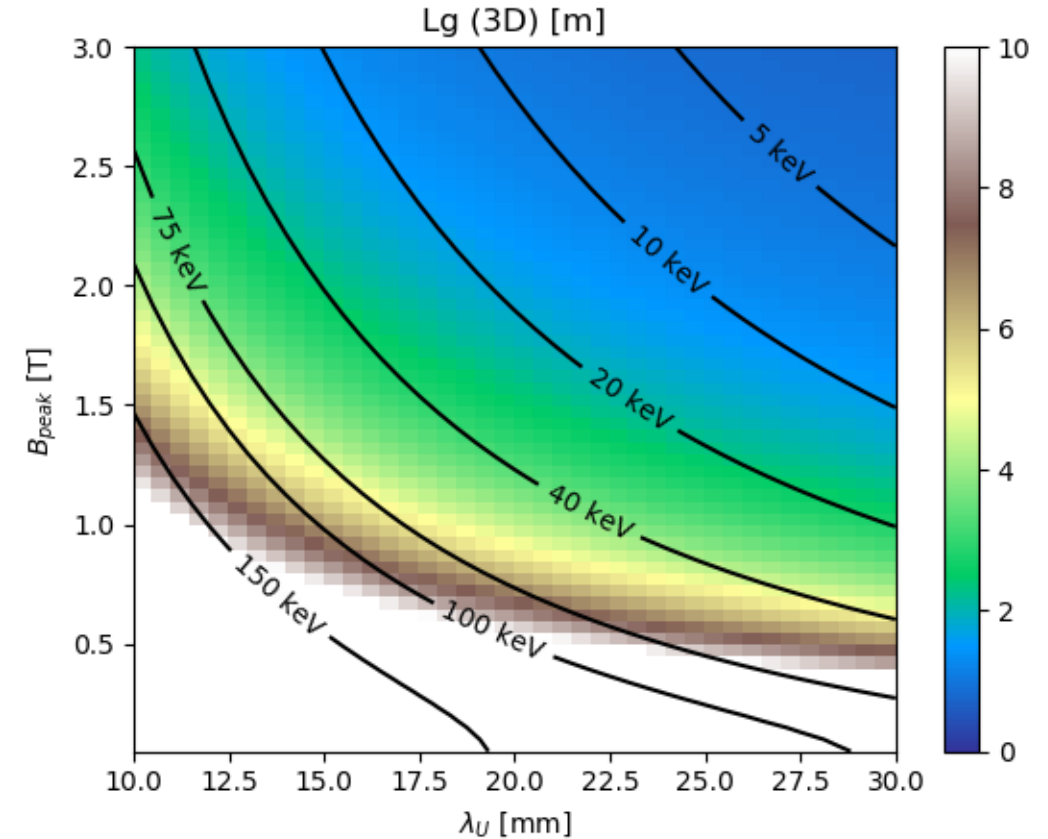
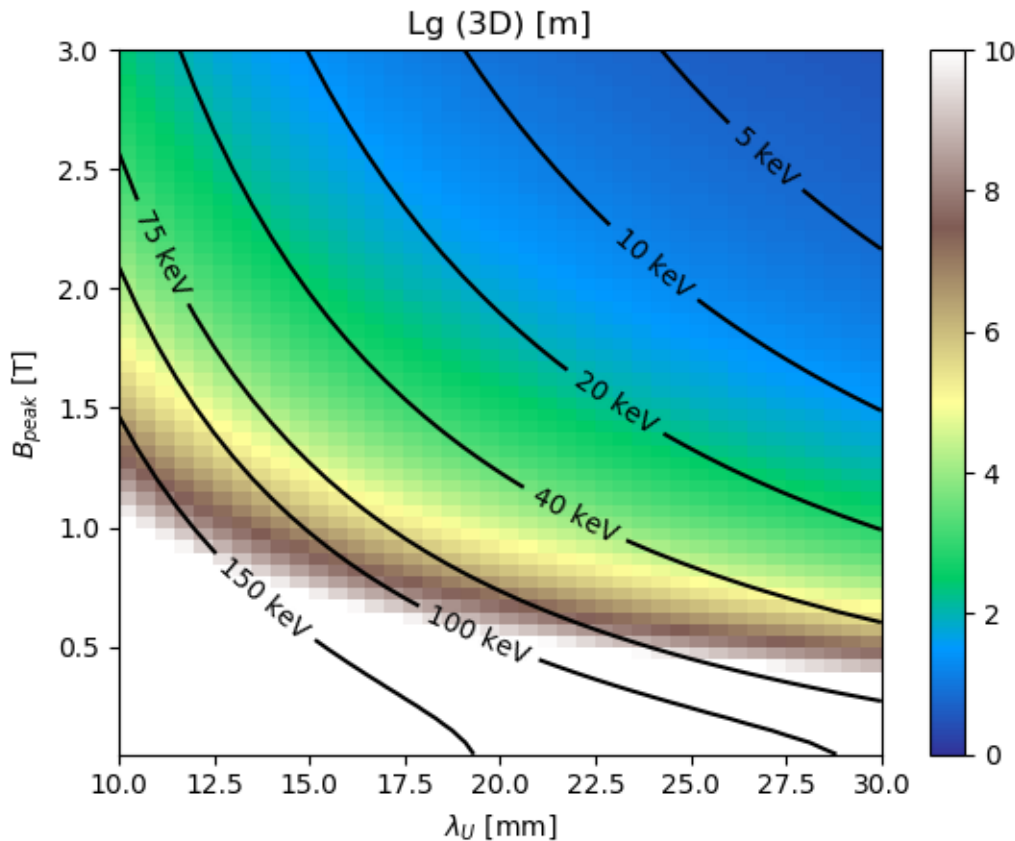
- [1] M. Turenne, C. Boffo, S. Casalbuoni, private communication
- [2] J. Bahrtdt and E. Gluskin, "Cryogenic permanent magnet and superconducting undulators," Nucl. Instruments Methods Phys. Res. Sect. A Accel. Spectrometers, Detect. Assoc. Equip., vol. 907, no. March, pp. 149–168, Nov. 2018.
- [3] S. Casalbuoni, et. al., "Magnetic Field Measurements of Full-Scale Conduction-Cooled Superconducting-Undulator-Coils," IEEE Trans. Appl. Supercond., vol. 28, no. 3, pp. 3–6, 2018.
- [4] S. Casalbuoni, et.al., "Characterization and long term operation of a novel superconducting undulator with 15 mm period length in a synchrotron light source," Phys. Rev. Accel. Beams, vol. 19, no. 11, p. 110702, Nov. 2016.
- [5] S. Casalbuoni, et.al., "Superconducting Undulators: From Development towards a Commercial Product," *Synchrotron Radiat. News*, vol. 31, no. 3, pp. 24–28, May 2018.
- [6] R. Dejus, M. Jaski, and S. H. Kim, "On-axis brilliance and power of in-vacuum undulators for the Advanced Photon Source.," Argonne, IL (United States), Nov. 2009.

Methods to estimate FEL performance (3D gain length)

$$L_g^{3d} = L_g^{1d}(1 + \delta)$$

■ Saldin, Schneidmiller, Yurkov

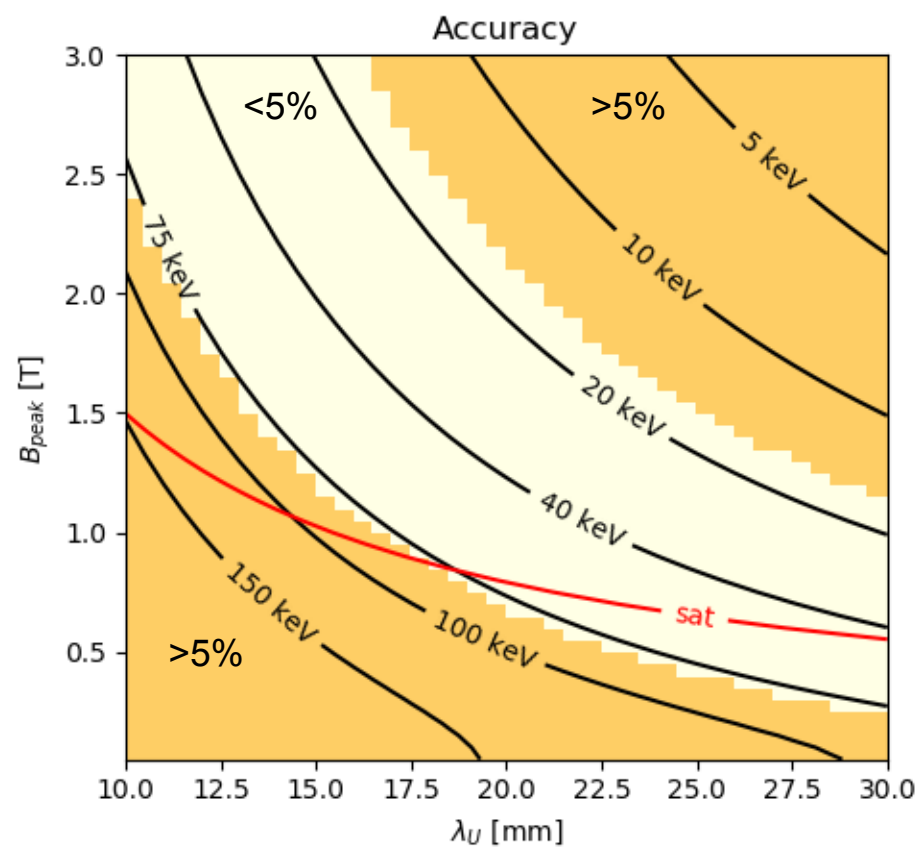
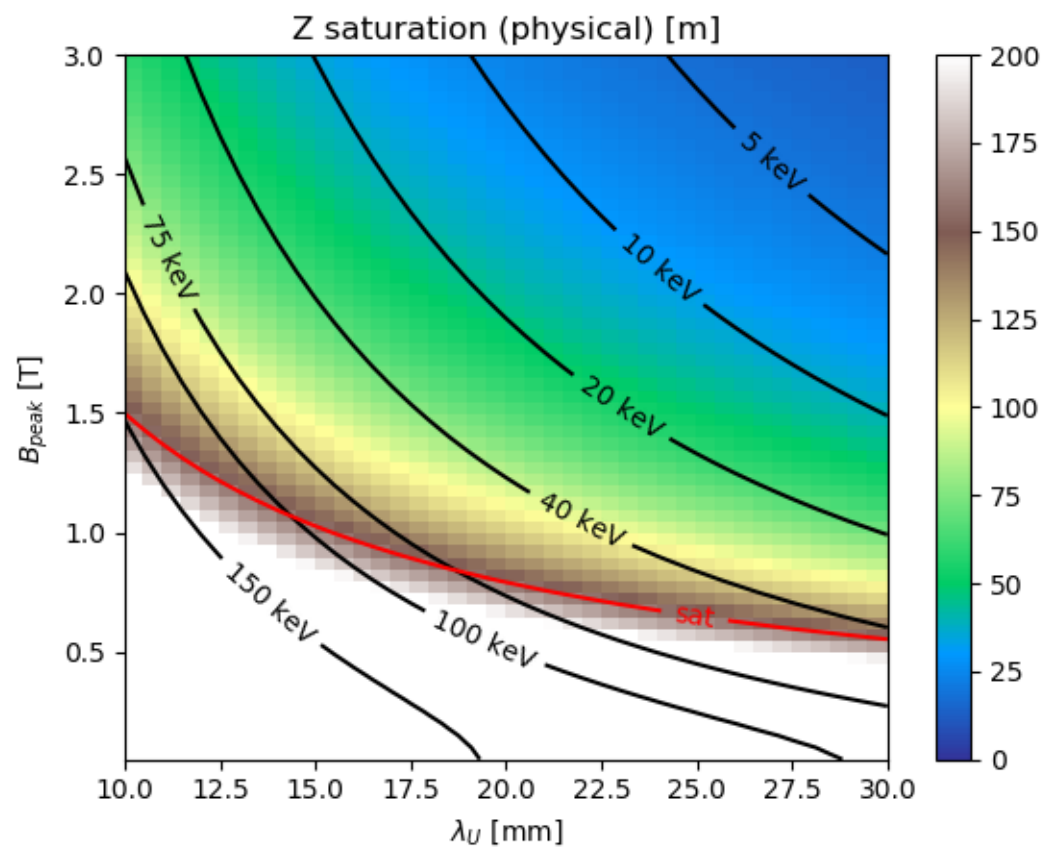
■ Xie



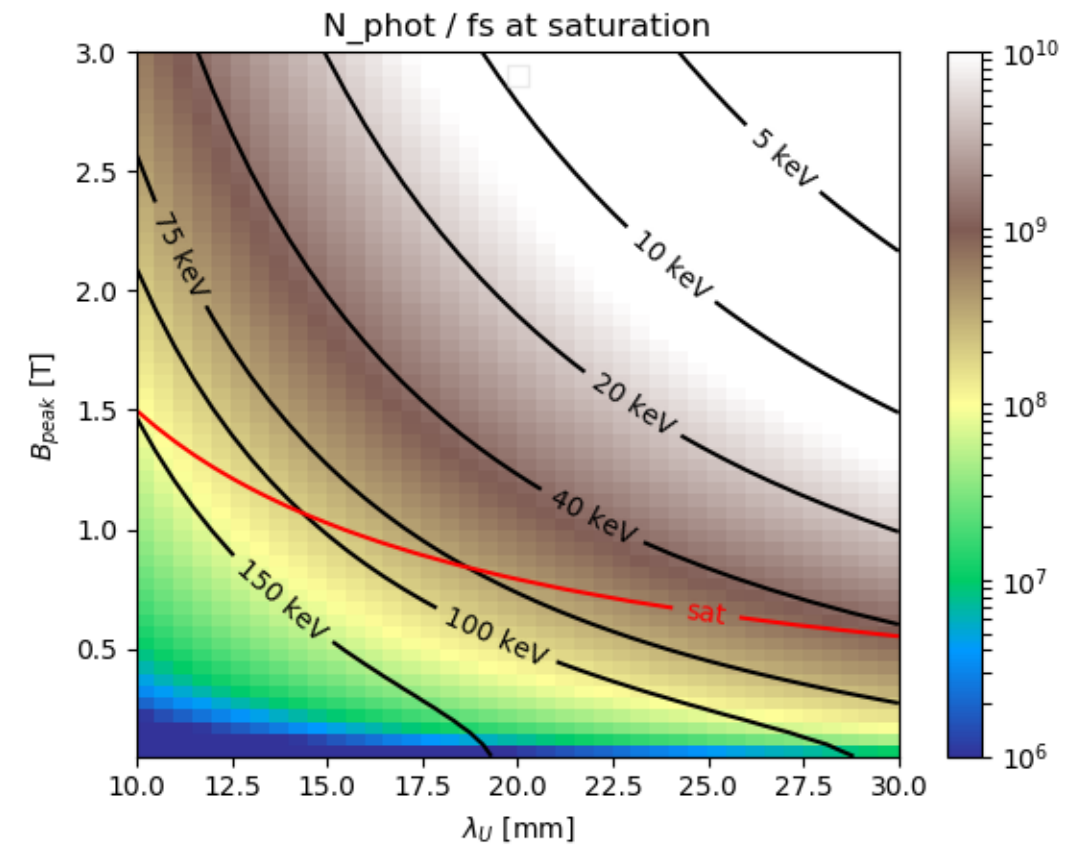
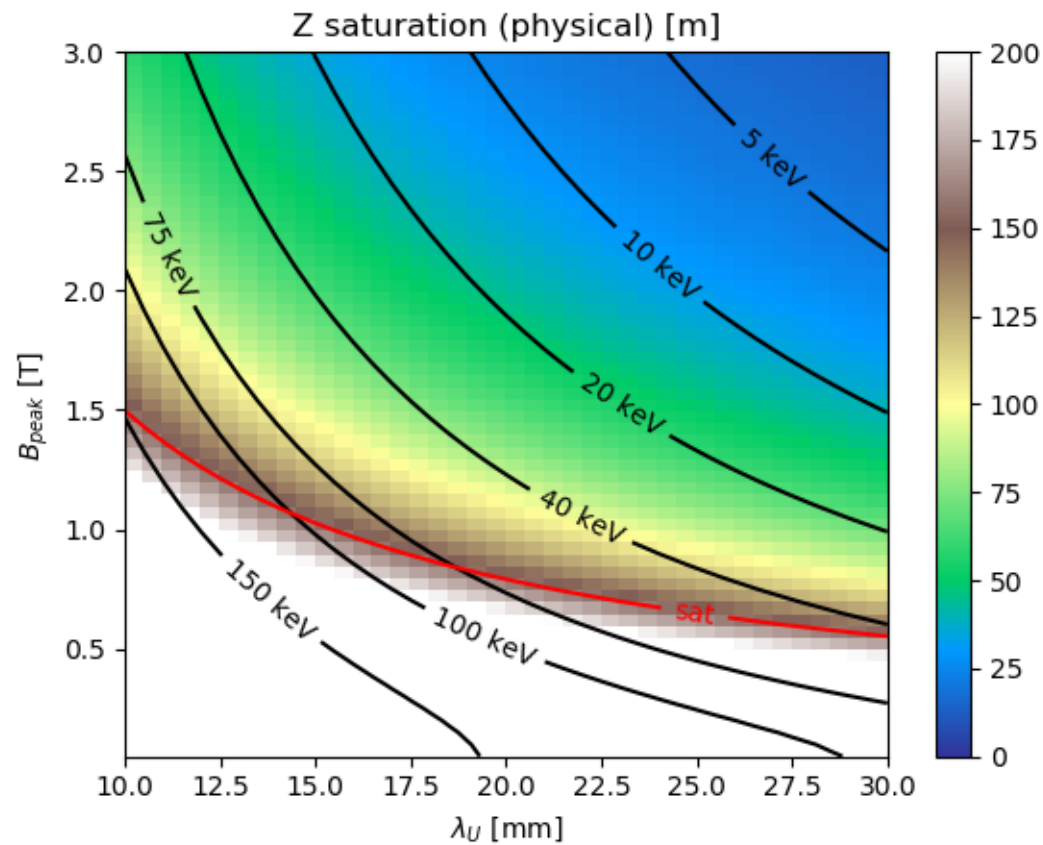
E. L. Saldin, E. A. Schneidmiller, and M. V. Yurkov, "Design formulas for short-wavelength FELs," *Opt. Commun.*, vol. 235, no. 4–6, pp. 415–420, May 2004.

M. Xie, "Exact and variational solutions of 3D eigenmodes in high gain FELs," *Nucl. Instruments Methods Phys. Res. Sect. A Accel. Spectrometers, Detect. Assoc. Equip.*, vol. 445, no. 1–3, pp. 59–66, 2000.

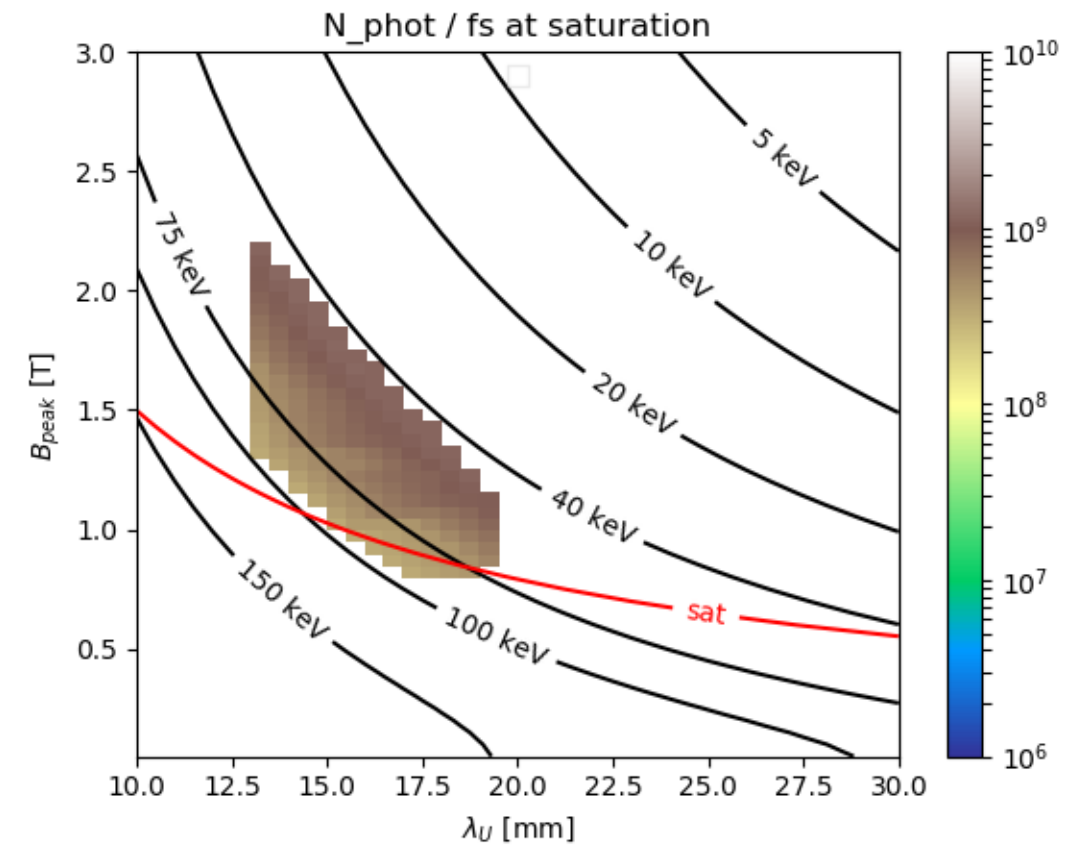
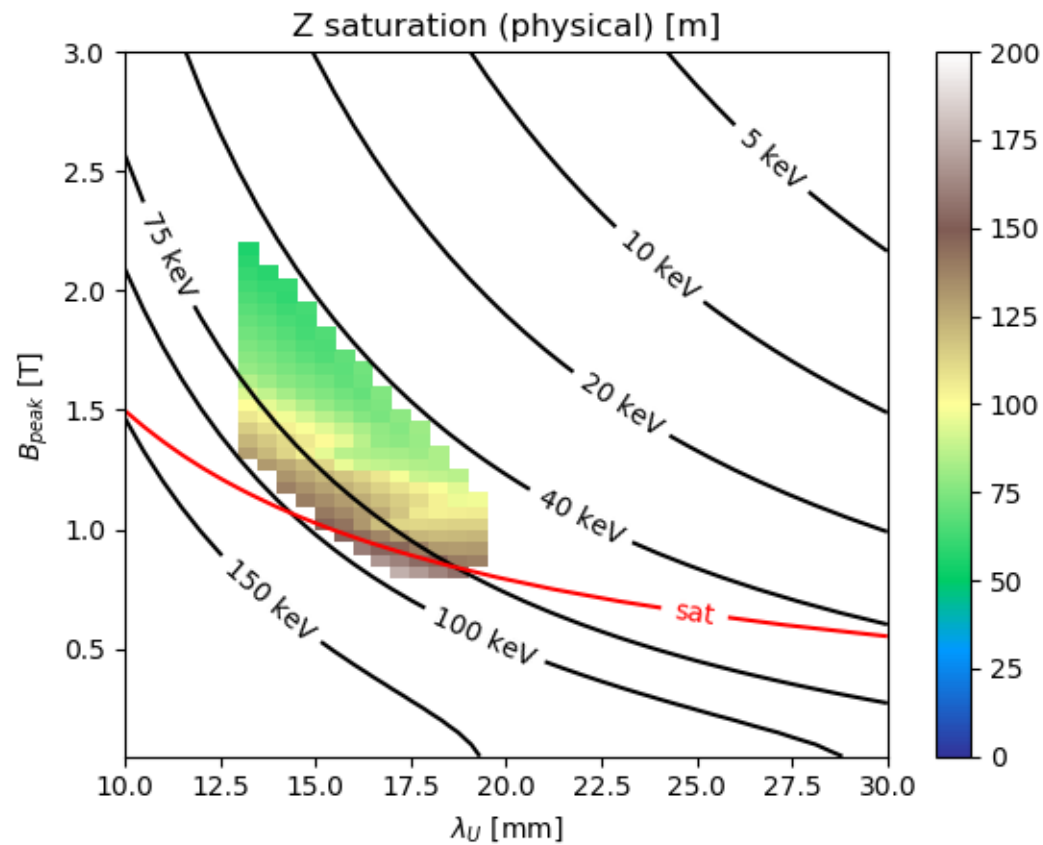
Saturation length and Accuracy



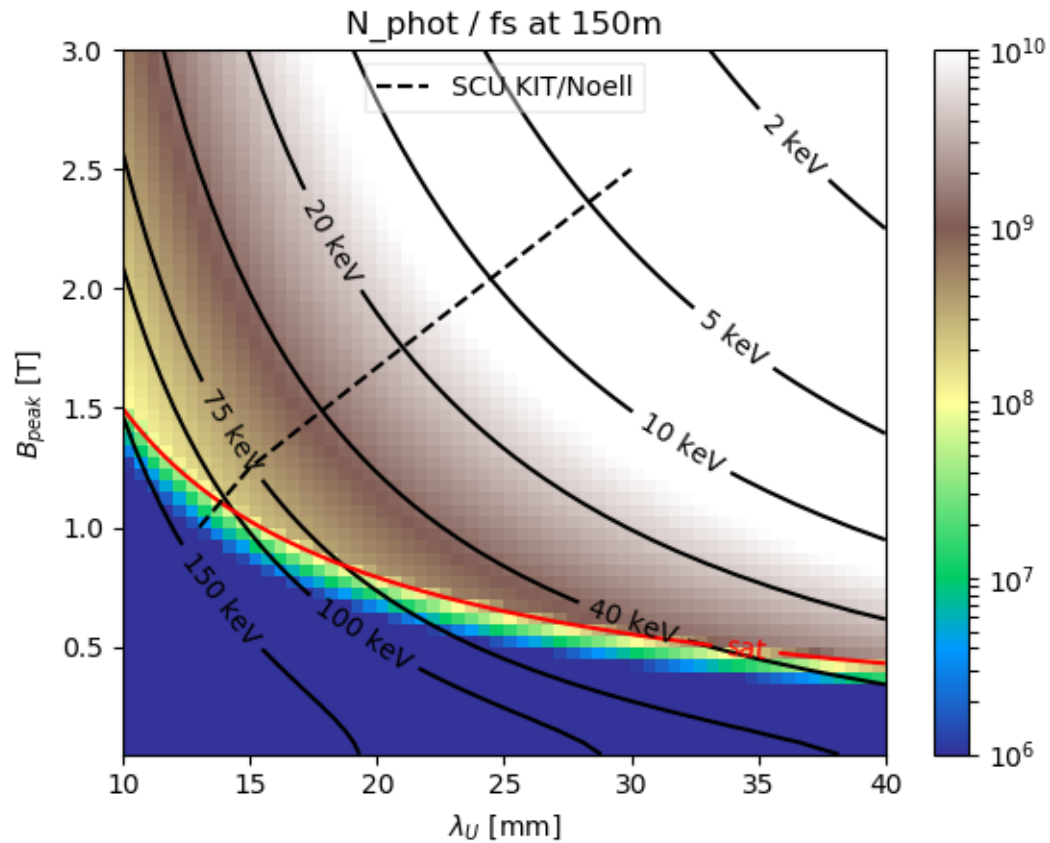
Saturation length and number of photons/femtosecond at saturation



Results of numerical simulation (Genesis v2)

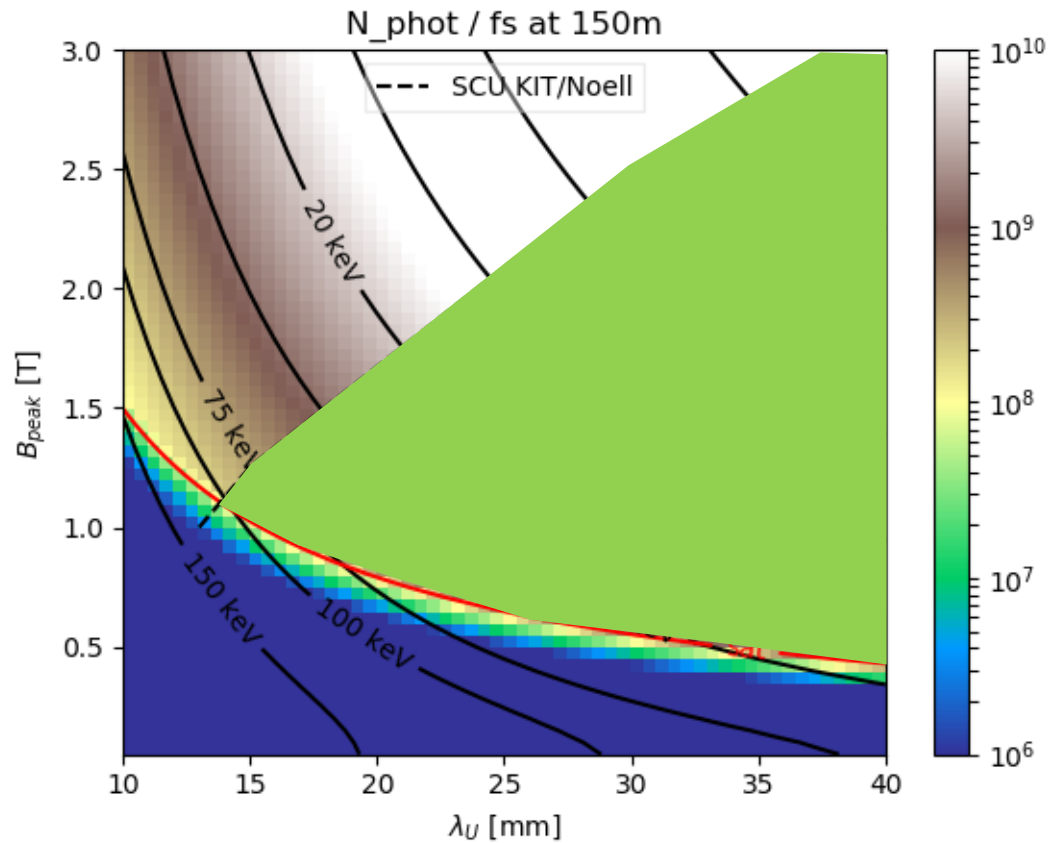


Estimated number of photons at the end of undulator

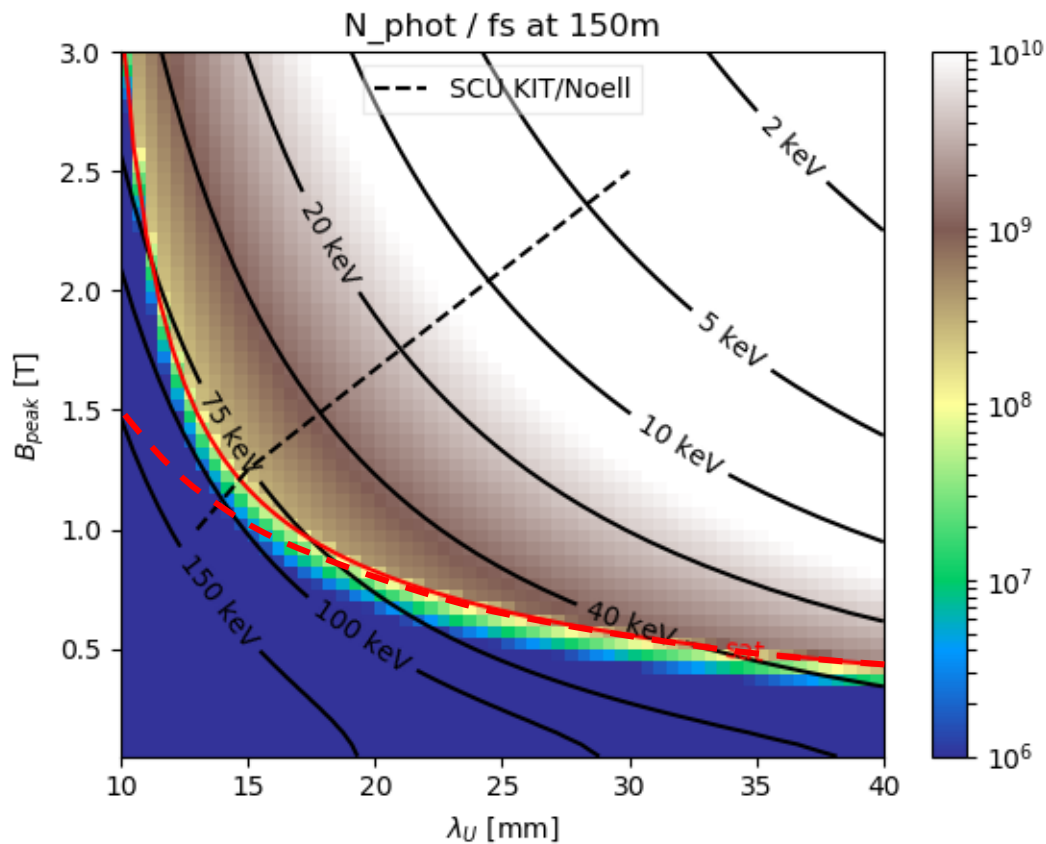


- Rough estimation, assuming no growth after- and exponential growth before saturation

Estimated number of photons at the end of undulator



Effect of Quantum fluctuations at 17.5 GeV



$$\frac{d\sigma_\gamma^2}{dz} = \frac{14}{15} \lambda_c r_e \gamma^4 \kappa_w^3 K^2 F(K)$$

■ FEL Gain at photon energies beyond 75keV is affected

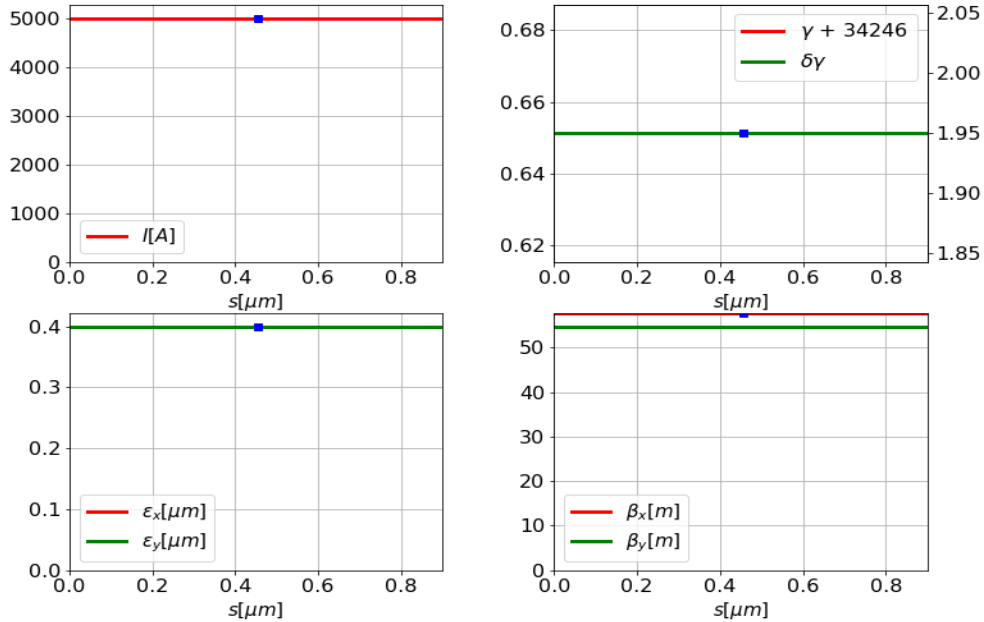
$$\delta_q = 5.5 \times 10^4 \left(\frac{I_A}{I}\right)^{3/2} \frac{\lambda_c r_e \epsilon_n^2}{\lambda_r^{11/4} \lambda_w^{5/4}} \frac{(1 + K^2)^{9/4} F(K)}{KA_{JJh}^3 h^{5/3}} \quad \delta_{\text{eff}} = \frac{\delta + \delta_q}{1 - \delta_q}$$

[1] J. Rossbach, E. L. Saldin, E. A. Schneidmiller, and M. V. Yurkov, "Fundamental limitations of an X-ray FEL operation due to quantum fluctuations of undulator radiation," *Nucl. Instruments Methods Phys. Res. Sect. A Accel. Spectrometers, Detect. Assoc. Equip.*, vol. 393, no. 1–3, pp. 152–156, 1997.

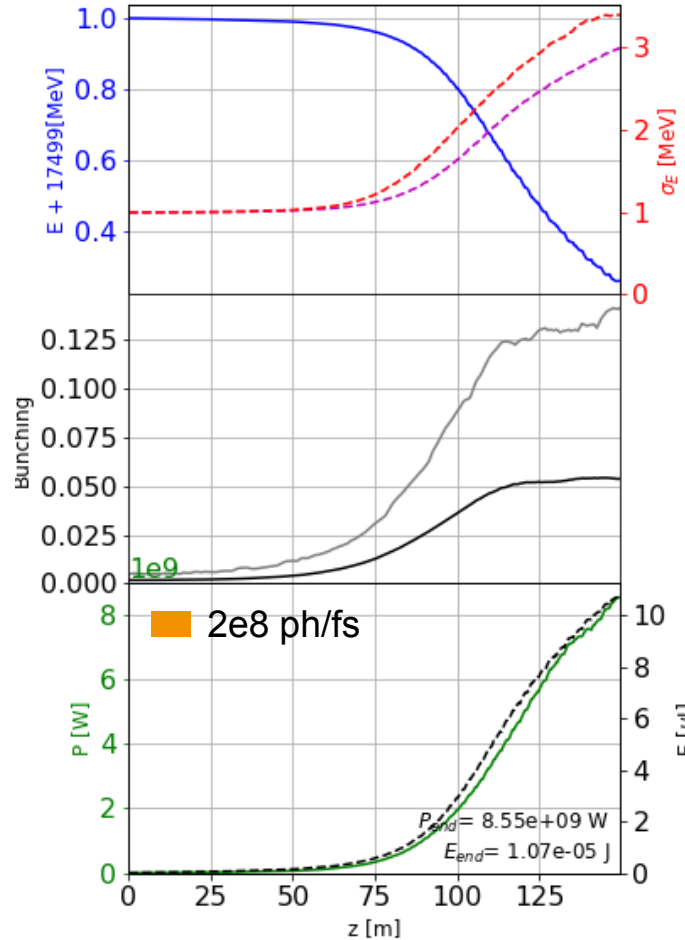
[2] E. L. Saldin, E. A. Schneidmiller, and M. V. Yurkov, "Design formulas for short-wavelength FELs," *Opt. Commun.*, vol. 235, no. 4–6, pp. 415–420, May 2004.

Effect of Quantum fluctuations at 17.5 GeV, 100keV

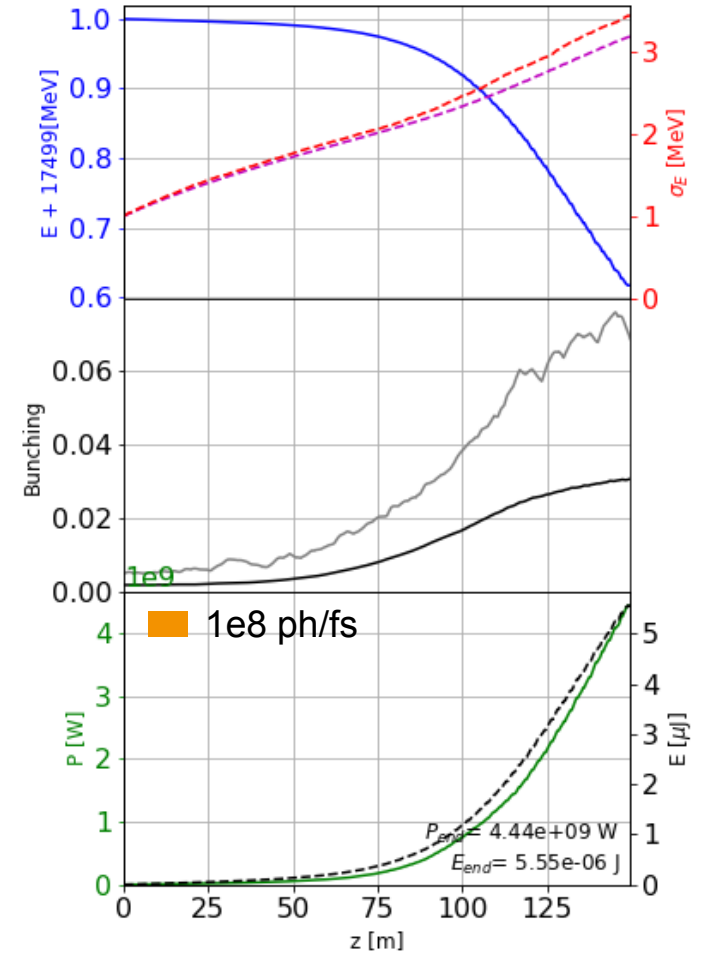
Model beam



no QF



with QF



Time-dependent Genesis simulation with model electron beam

Undulator period doubling

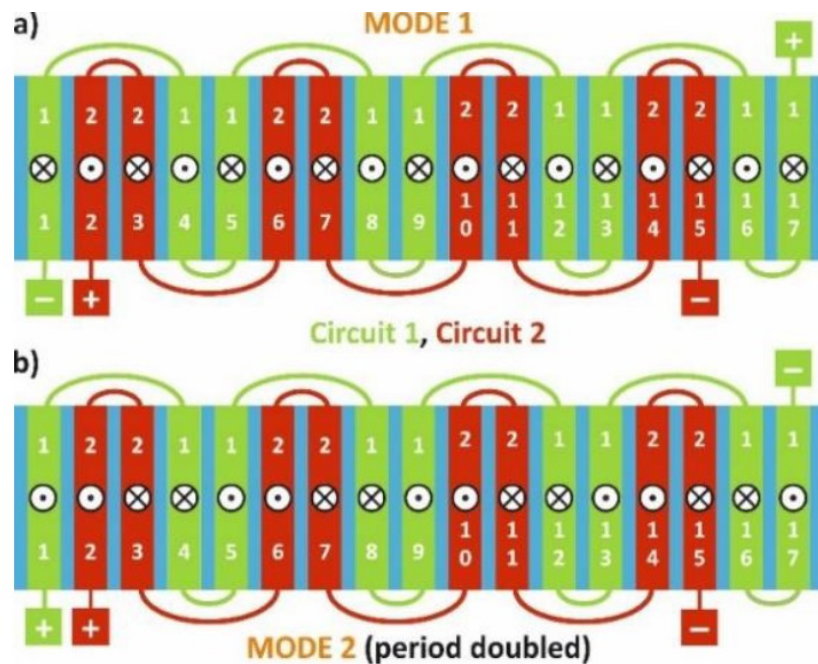


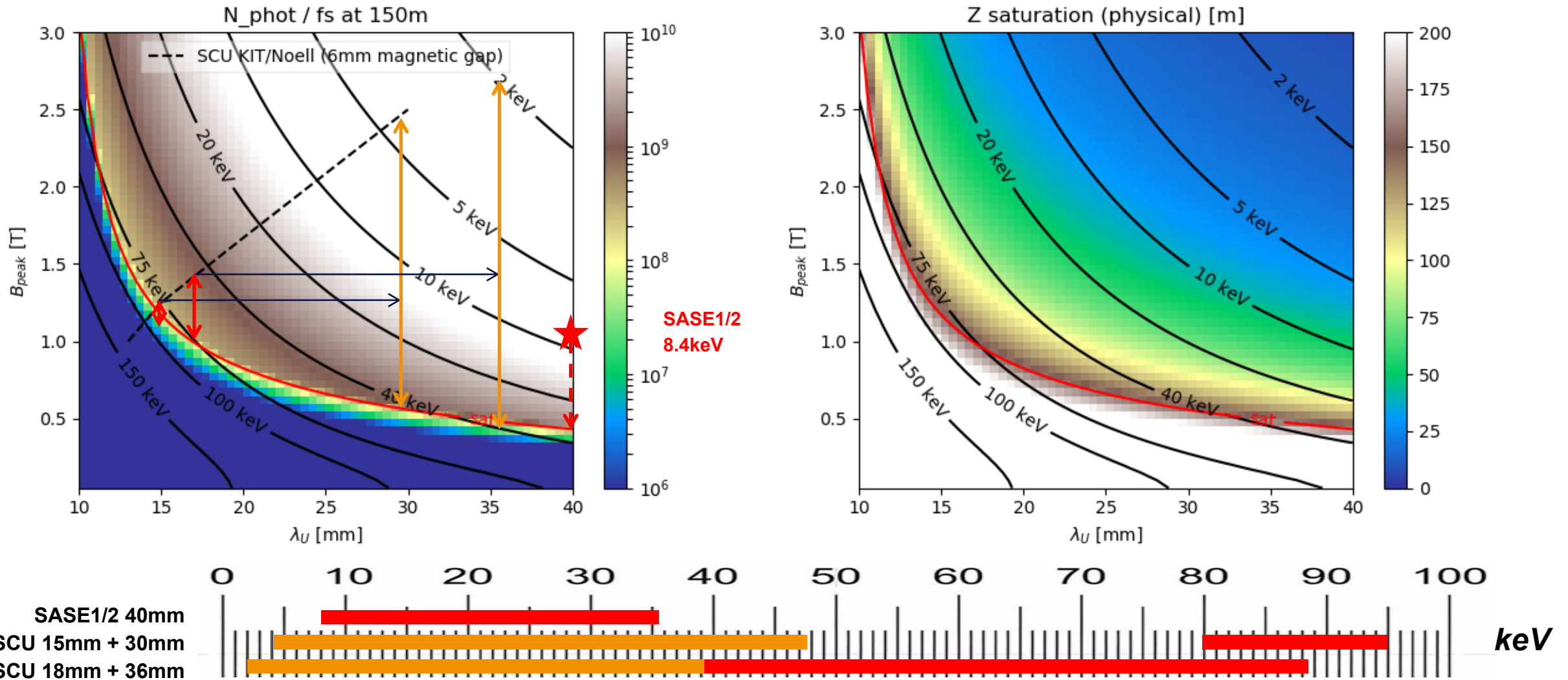
Figure 1: Sketch of period length doubling for superconducting undulators by changing the current direction in one subset of windings.

$$\lambda_r = \frac{\lambda_u[m] + (93B_{rms}[T])^2 \lambda_u^3[m]}{2\gamma^2}$$

- Increasing undulator period allows to significantly reduce resonant photon energy

T. Holubek, S. Casalbuoni, S. Gerstl, N. Glamann, A. Grau, C. Meuter, and D. S. de Jauregui, "Design and Tests of Switchable Period Length Superconducting Undulator Coils," in IPAC, 2018, pp. 4226–4228.


Undulator period doubling (17.5GeV)



CW operation (7.8 GeV)

TABLE VI. Beam energy and DF estimated for the upgraded XFEL accelerator.

Operation mode	E_{beam} [GeV]	E_{acc} in ML [MV/m]	Beam-on DF [%]
sp (nominal)	19.8	23.4	0.6
cw	7.8	7.3	100
lp	10	10	53
lp	14	15	23

$$\lambda_r = \frac{\lambda_u [m] + (93 B_{rms} [T])^2 \lambda_u^3 [m]}{2\gamma^2}$$


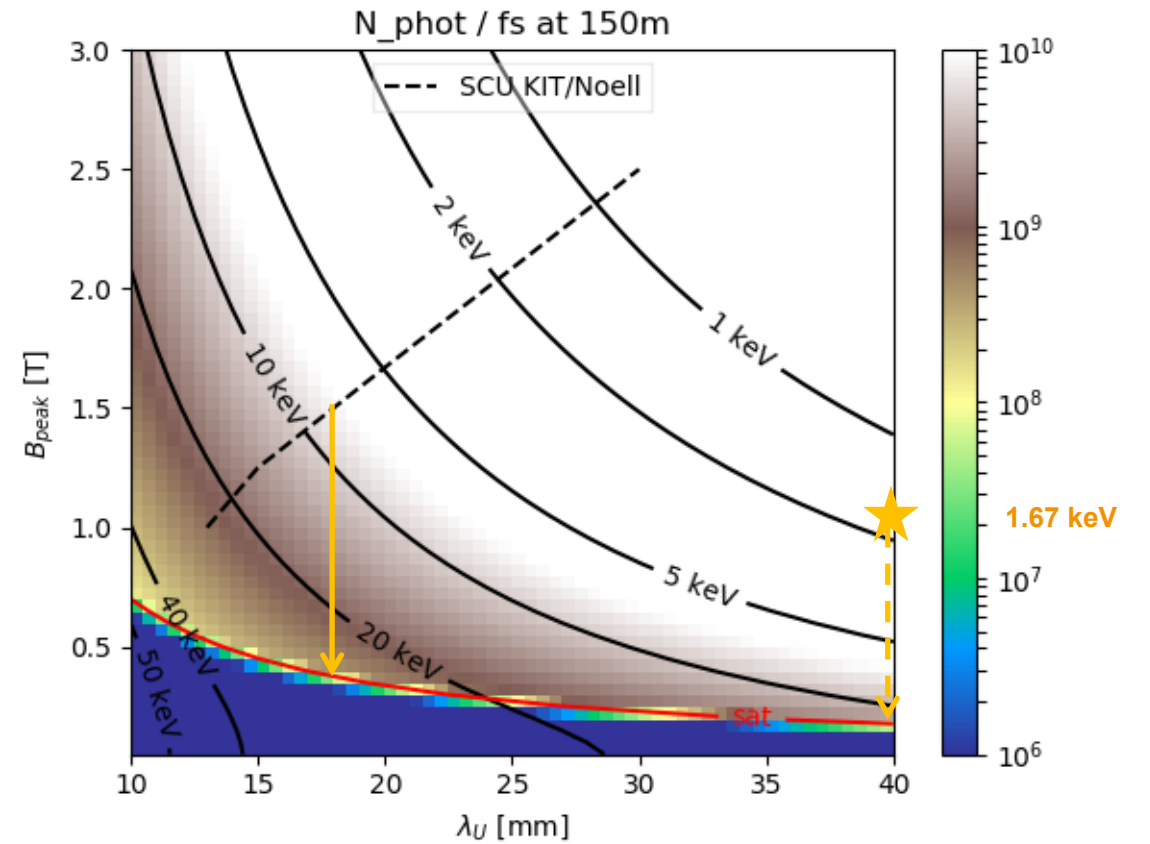
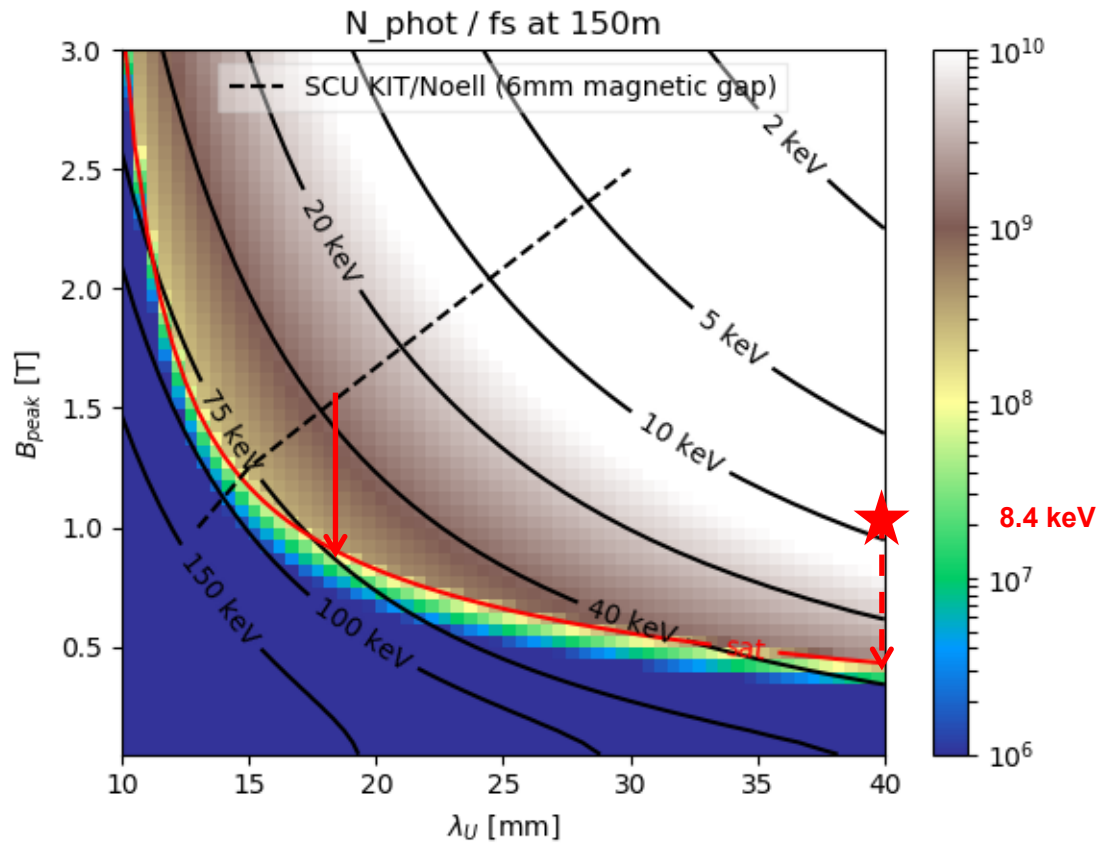
[1] J. Sekutowicz, V. Ayvazyan, M. Barlak, J. Branlard, W. Cichalewski, W. Grabowski, D. Kostin, J. Lorkiewicz, W. Merz, R. Nietubyc, R. Onken, A. Piotrowski, K. Przygoda, E. Schneidmiller, and M. Yurkov, "Research and development towards duty factor upgrade of the European X-Ray Free Electron Laser linac," *Phys. Rev. Spec. Top. - Accel. Beams*, vol. 18, no. 5, pp. 1–9, 2015.

[2] R. Brinkmann, E. A. Schneidmiller, J. Sekutowicz, and M. V. Yurkov, "Prospects for CW and LP operation of the European XFEL in hard X-ray regime," *Nucl. Instruments Methods Phys. Res. Sect. A Accel. Spectrometers, Detect. Assoc. Equip.*, vol. 768, pp. 20–25, Mar. 2014.

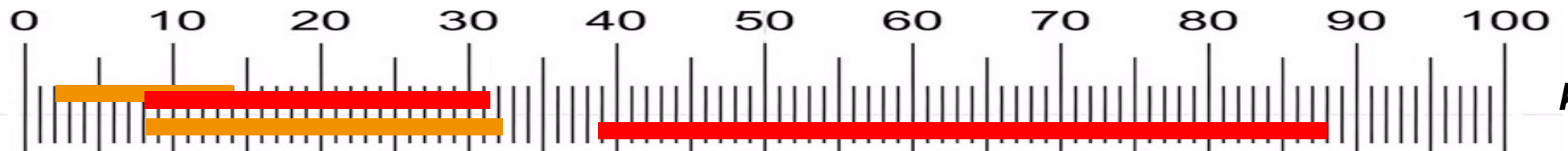
CW operation (7.8 GeV)

17.5 GeV

7.8 GeV



SASE1/2 8.5+17.5
18mm SCU 8.5+17.5



keV

Comparison with harmonic lasing

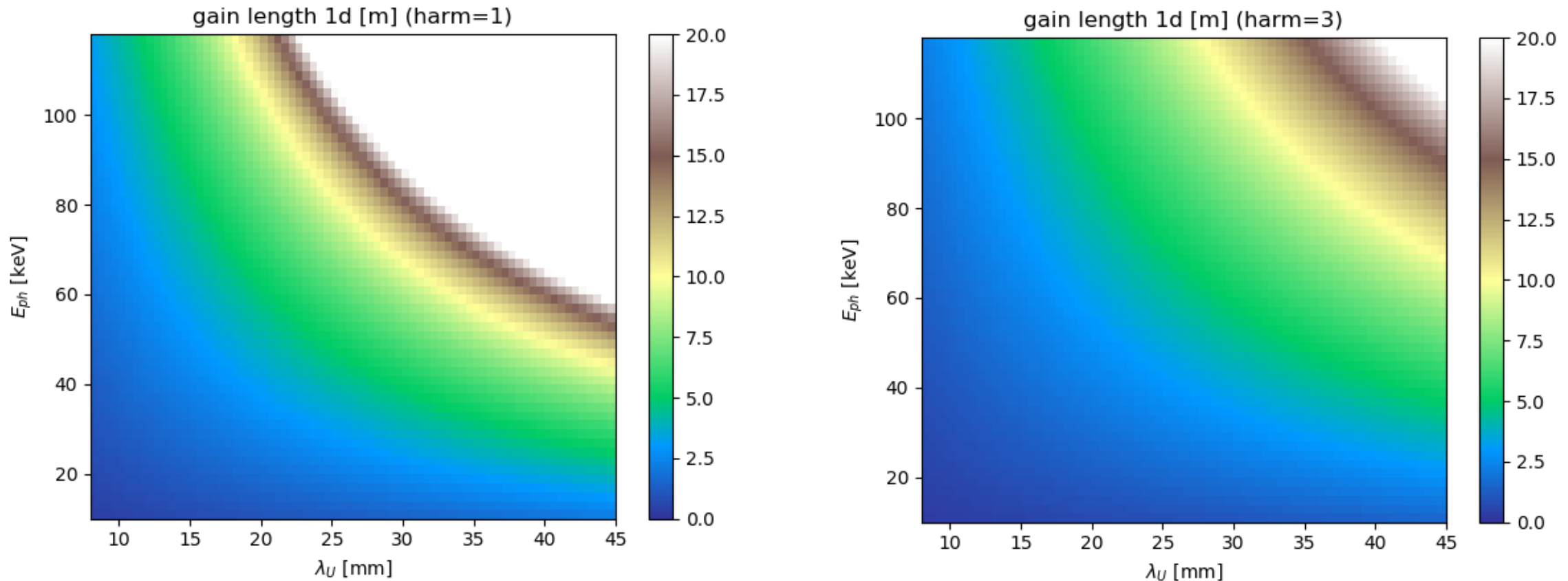
$$h\lambda_{wh}(1 + K_h^2) = \lambda_{wSC}(1 + K_{SC}^2)$$

$$L_{g0SC} = 1.67 \left(\frac{I_A}{I} \right)^{1/2} \frac{(\epsilon_n \lambda_{wSC})^{5/6} (1 + K_{SC}^2)^{1/3}}{\lambda_t^{2/3} K A_{JJSC}}$$

$$L_{g0h} = 1.67 \left(\frac{I_A}{I} \right)^{1/2} \frac{(\epsilon_n \lambda_{wh})^{5/6} (1 + K_h^2)^{1/3}}{\lambda_t^{2/3} h^{5/6} K A_{JJh}}$$

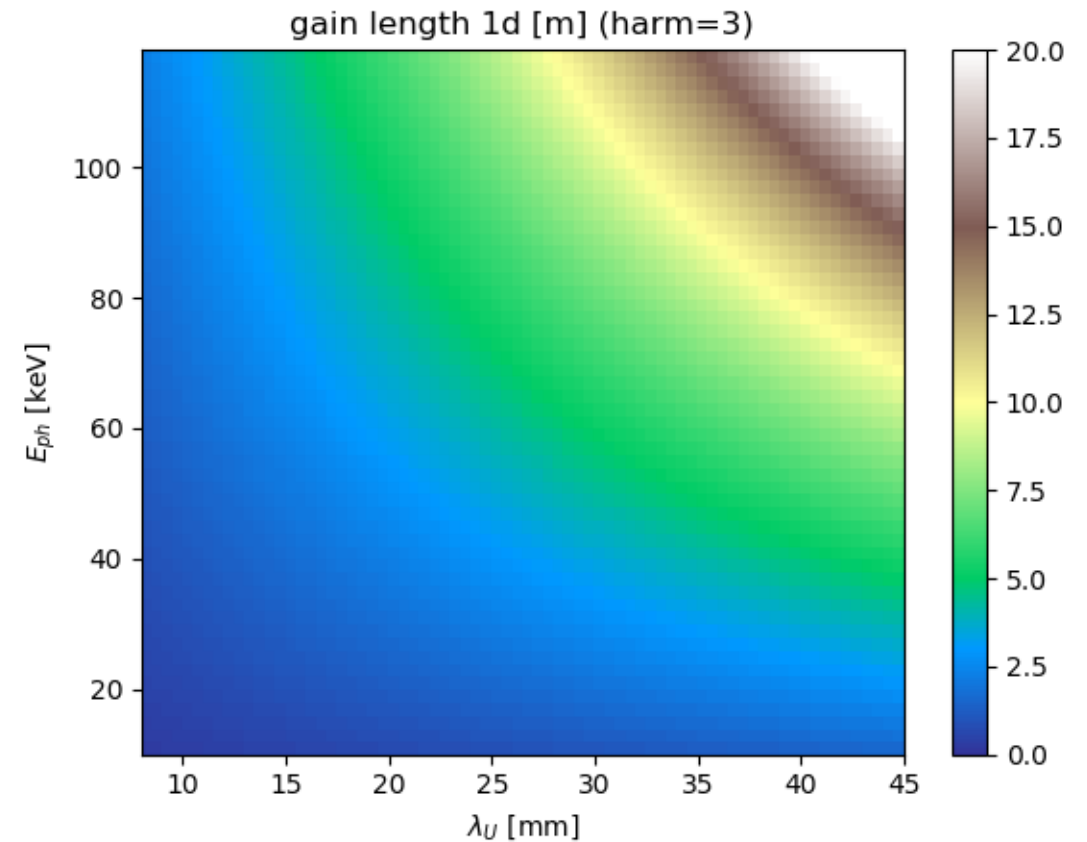
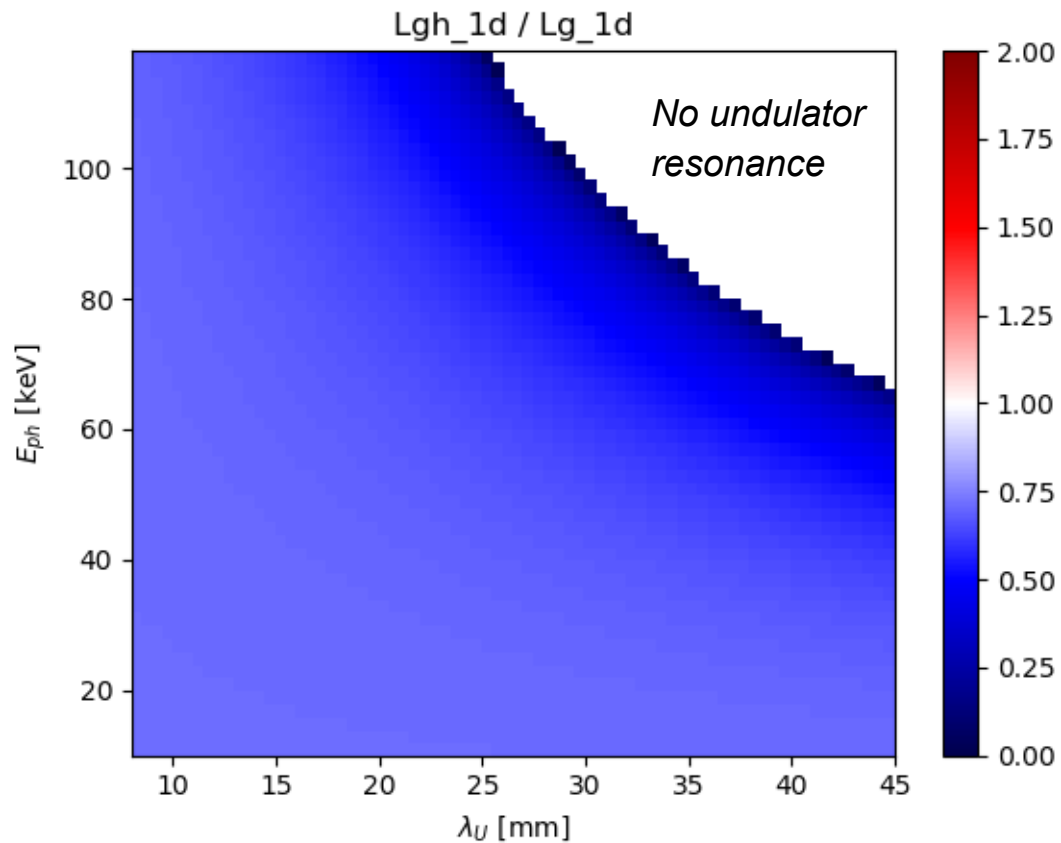
E. A. Schneidmiller and M. V. Yurkov, "Harmonic lasing in x-ray free electron lasers," Phys. Rev. Spec. Top. - Accel. Beams, vol. 15, no. 8, p. 080702, Aug. 2012.

Comparison with harmonic lasing



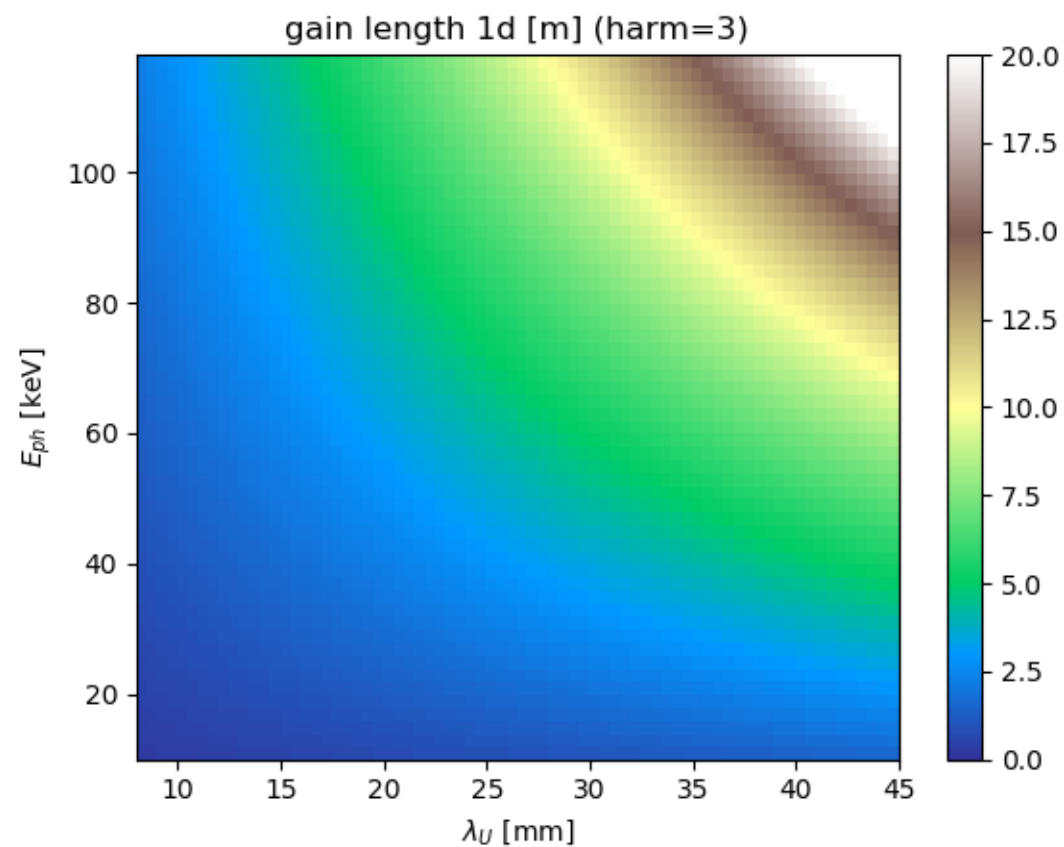
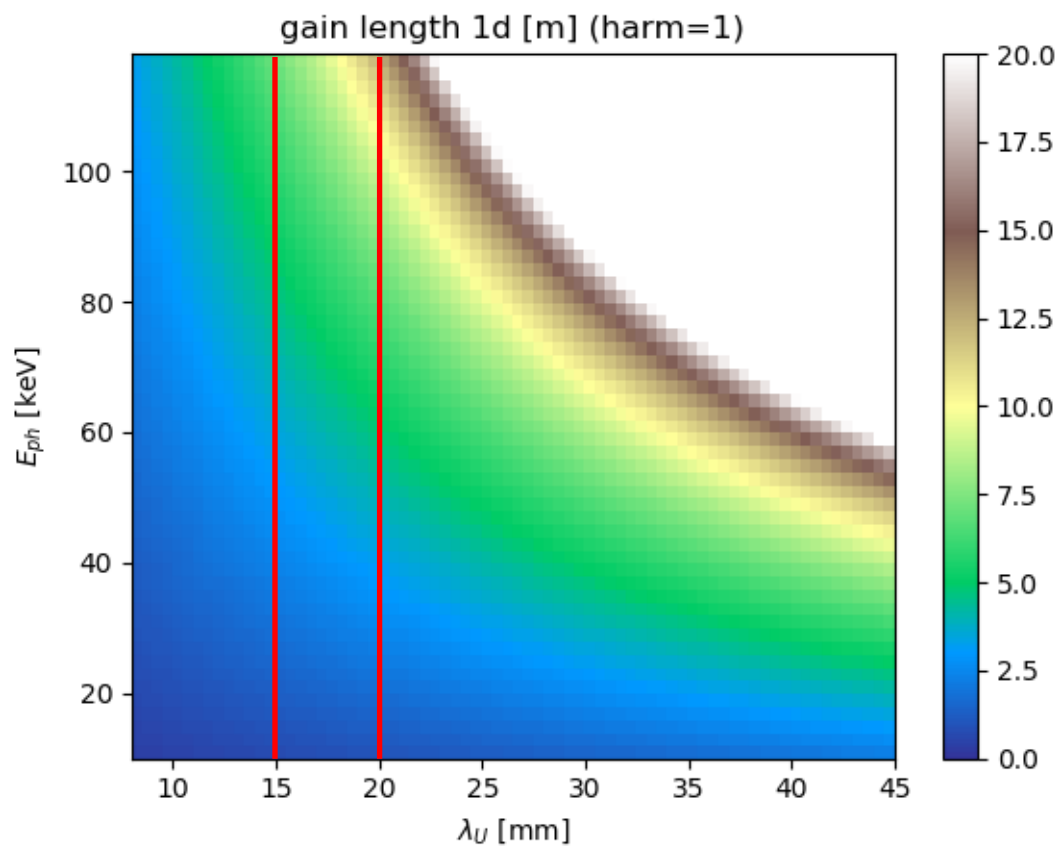
Harmonic lasing is superior for the same combination of λ_U and E_{photon}

Comparison with harmonic lasing

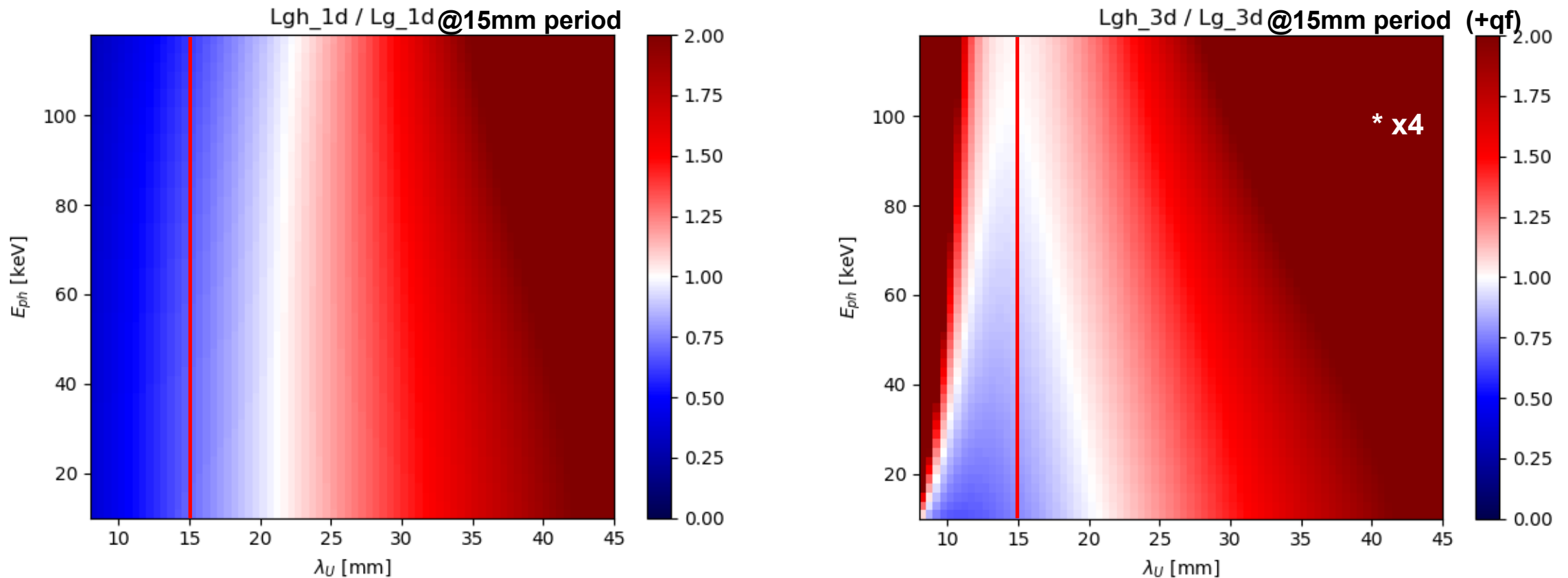


Harmonic lasing is superior for the same combination of λ_U and E_{photon}

Comparison with harmonic lasing

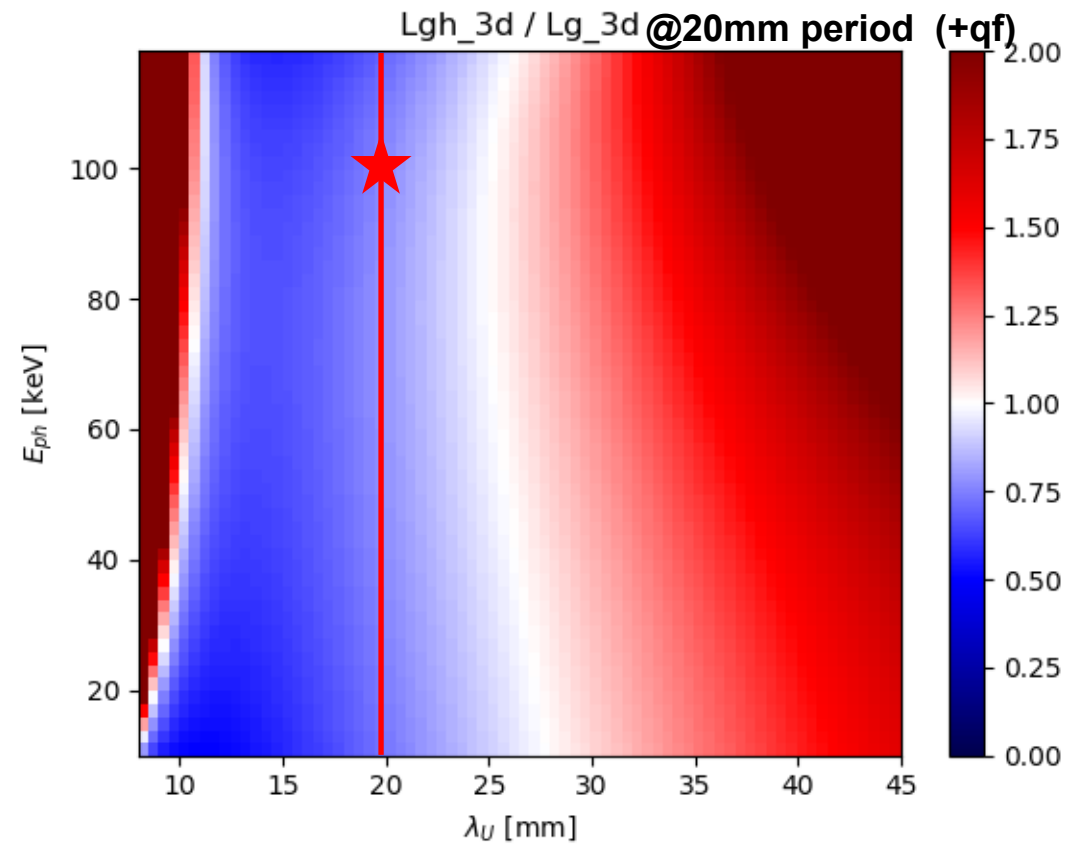
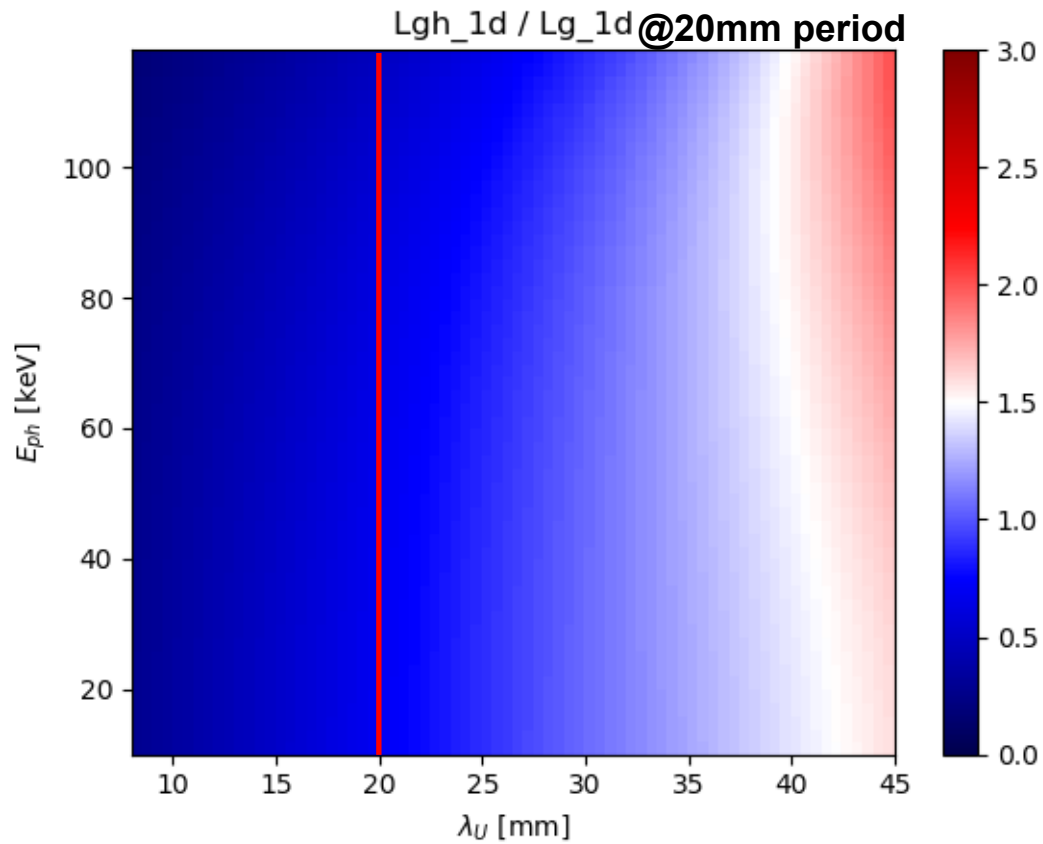


Comparison with harmonic lasing



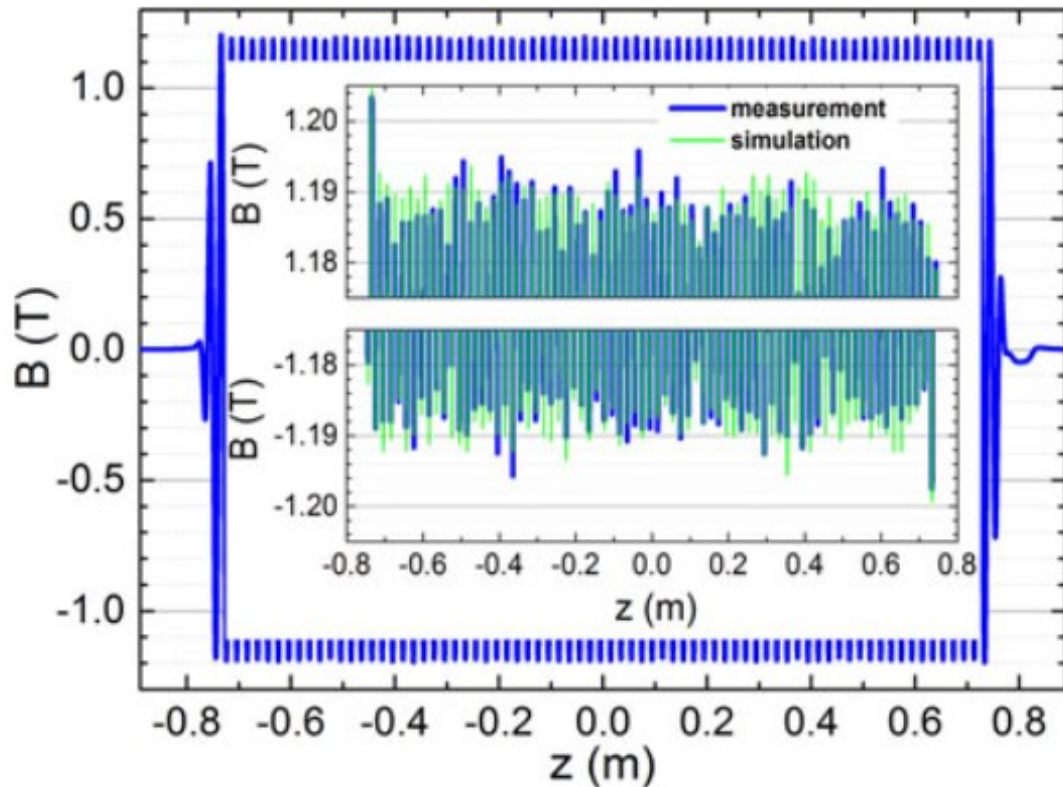
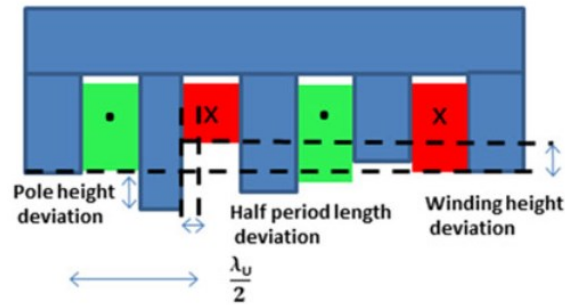
Comparison with $\lambda_U=15$ mm at fundamental

Comparison with harmonic lasing

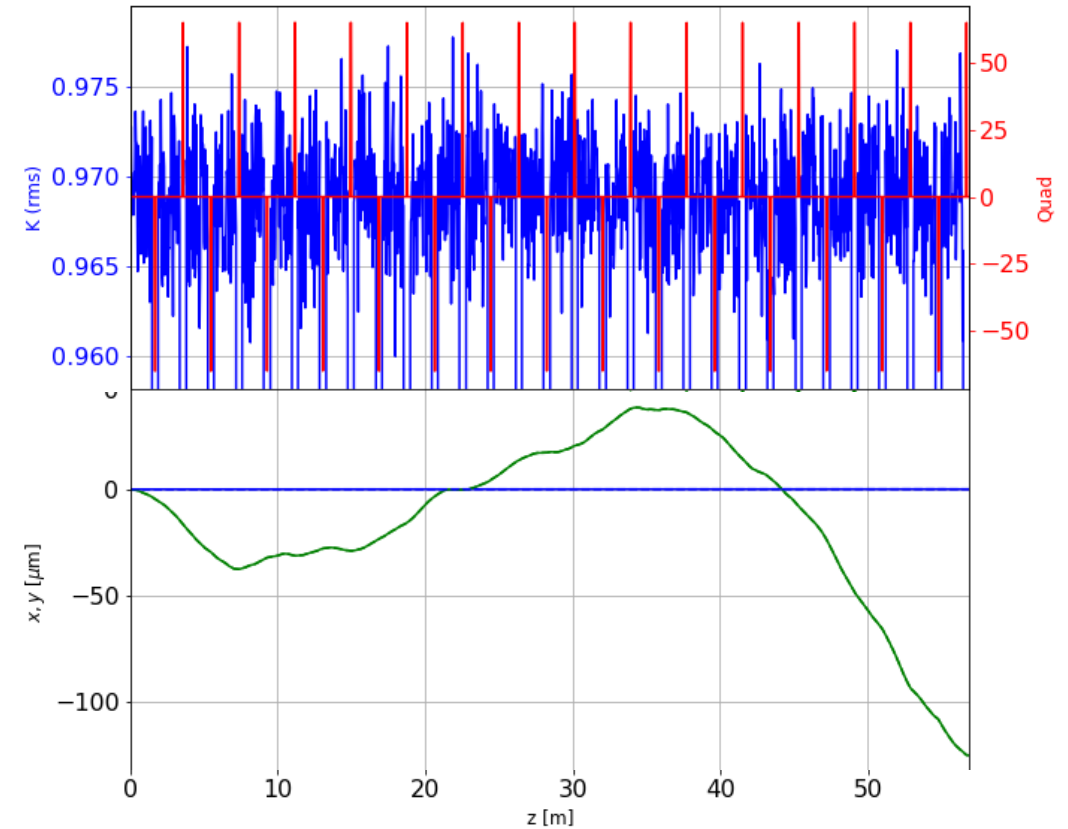


Comparison with $\lambda_U=20$ mm at fundamental

Effect of undulator field errors



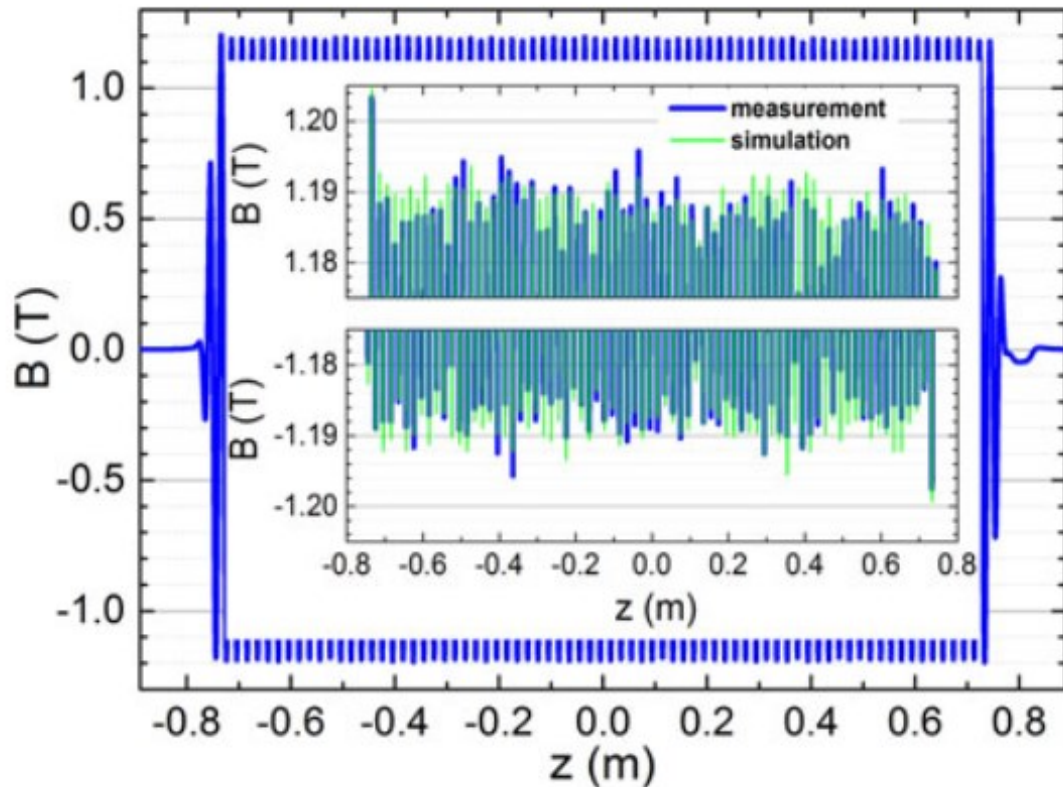
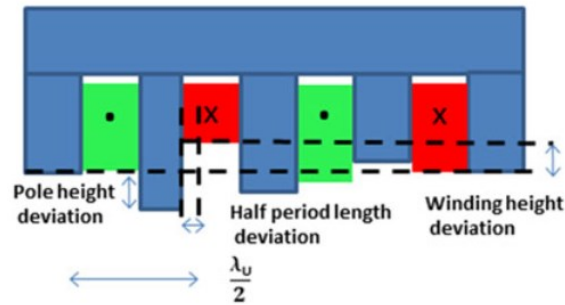
■ $\sigma_K/K=0.3\%$ period-wise field error (rms)



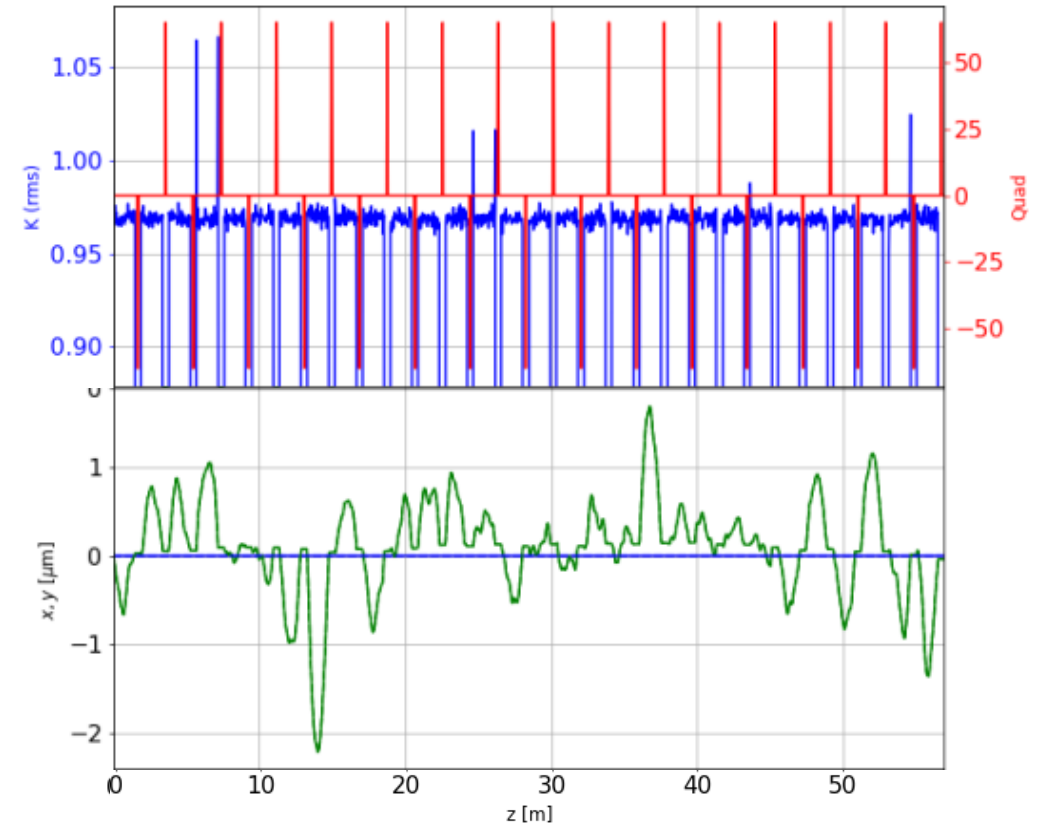
S. Casalbuoni, N. Glamann, A. Grau, T. Holubek, D. S. de Jauregui, C. Boffo, T. Gerhard, M. Turenne, and W. Walter, "Magnetic Field Measurements of Full-Scale Conduction-Cooled Superconducting-Undulator-Coils," *IEEE Trans. Appl. Supercond.*, vol. 28, no. 3, pp. 1–4, Apr. 2018.

Y. Li, B. Faatz, and J. Pflueger, "Study of undulator tolerances for the European XFEL," *29th Int. Free Electron Laser Conf. FEL 2007*, pp. 330–333, 2007.

Effect of undulator field errors



- $\sigma_K/K=0.3\%$ period-wise field error (rms)
- Corrected field integrals



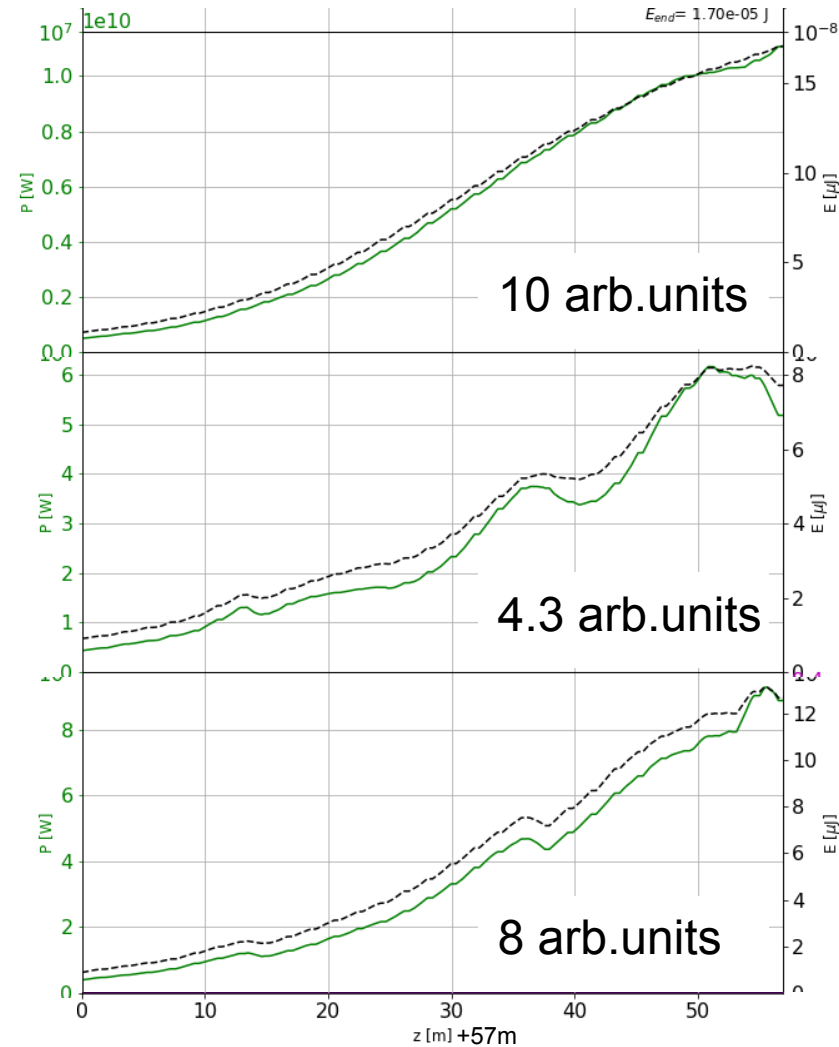
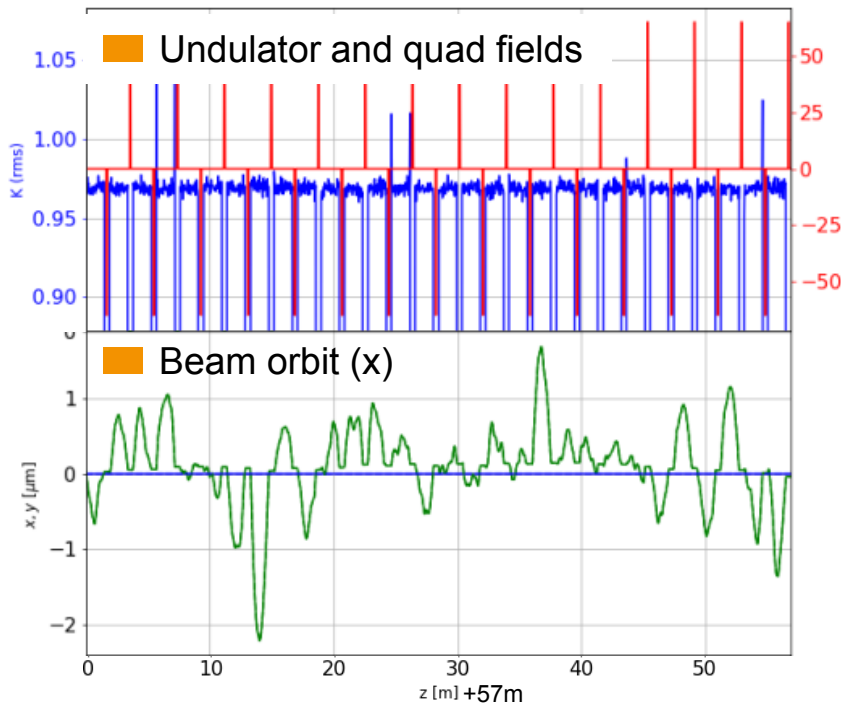
S. Casalbuoni, N. Glamann, A. Grau, T. Holubek, D. S. de Jauregui, C. Boffo, T. Gerhard, M. Turenne, and W. Walter, "Magnetic Field Measurements of Full-Scale Conduction-Cooled Superconducting-Undulator-Coils," *IEEE Trans. Appl. Supercond.*, vol. 28, no. 3, pp. 1–4, Apr. 2018.

Y. Li, B. Faatz, and J. Pflueger, "Study of undulator tolerances for the European XFEL," *29th Int. Free Electron Laser Conf. FEL 2007*, pp. 330–333, 2007.

Effect of undulator field errors

100keV = 0.12 Angstrom

- 100keV, 15mm period
- Phase-shake effect
- Added path was calculated and compensated with phase shifter

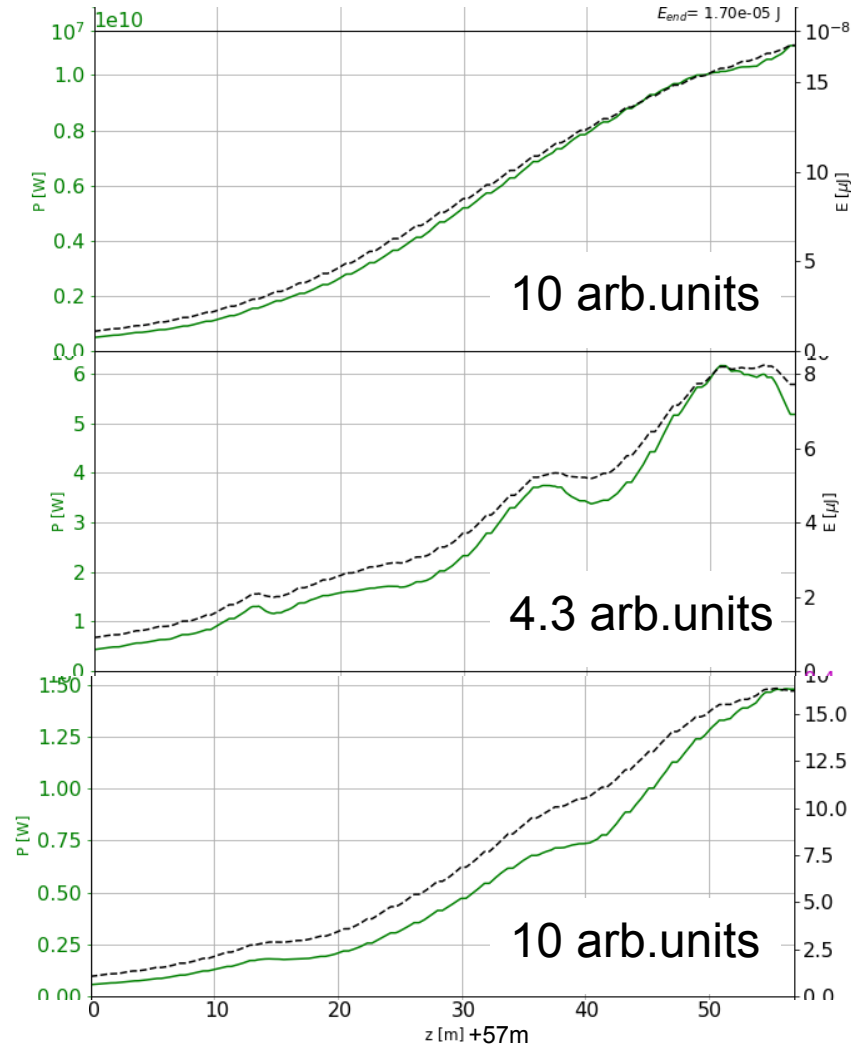
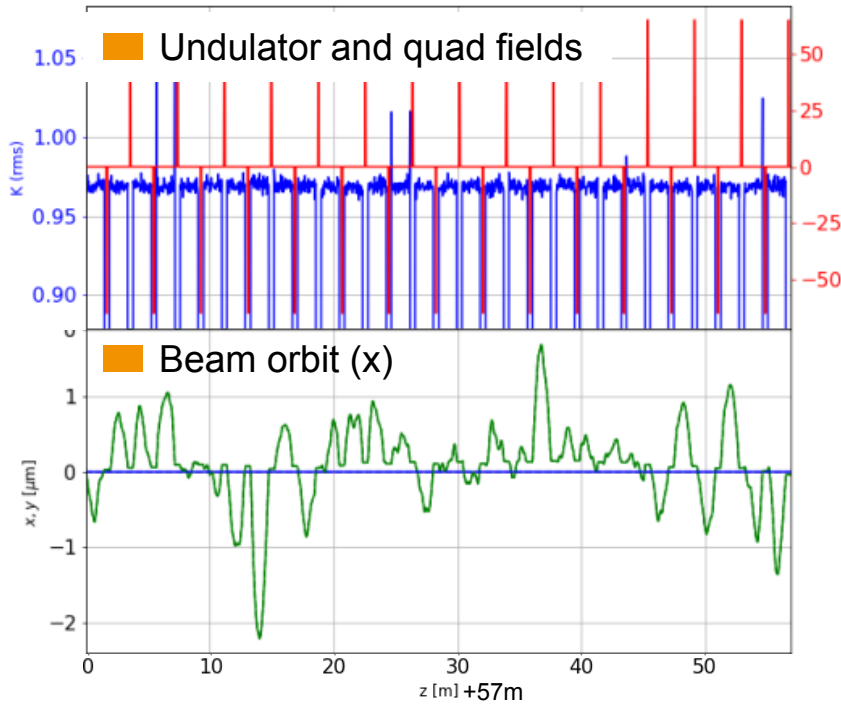


- No errors
- Corrected 1 and 2 field integrals
- Corrected 1 and 2 field integrals and phase shifters

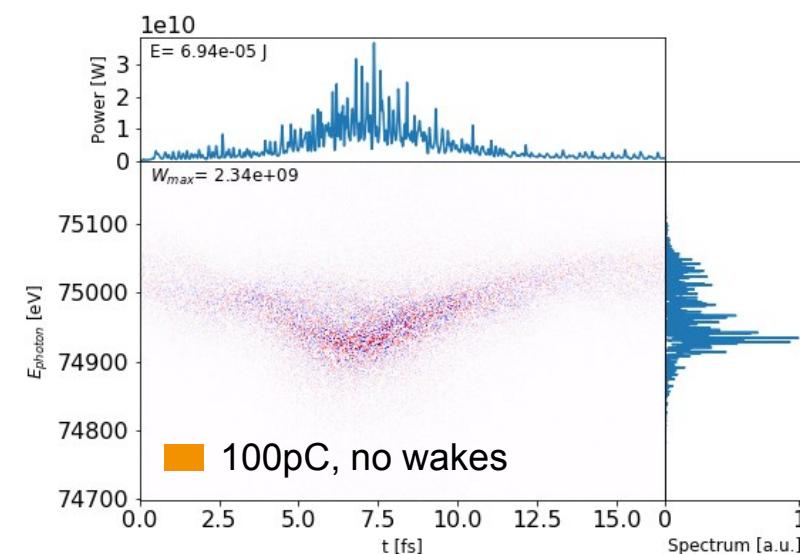
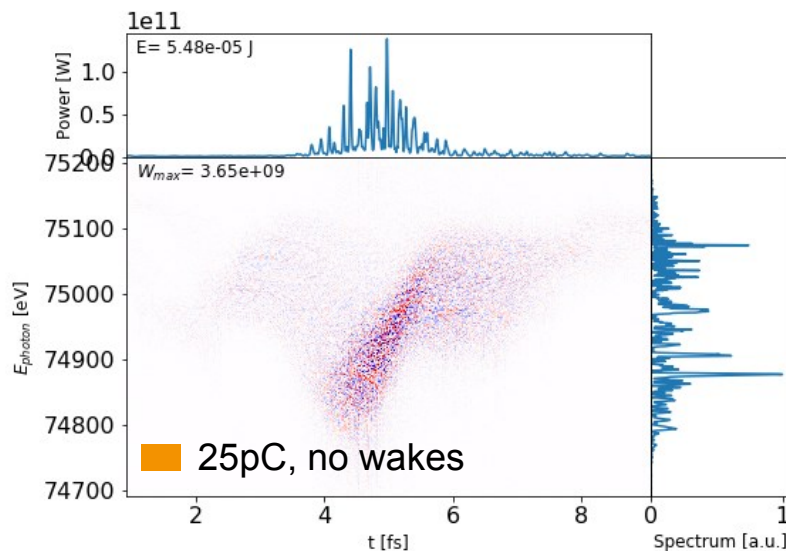
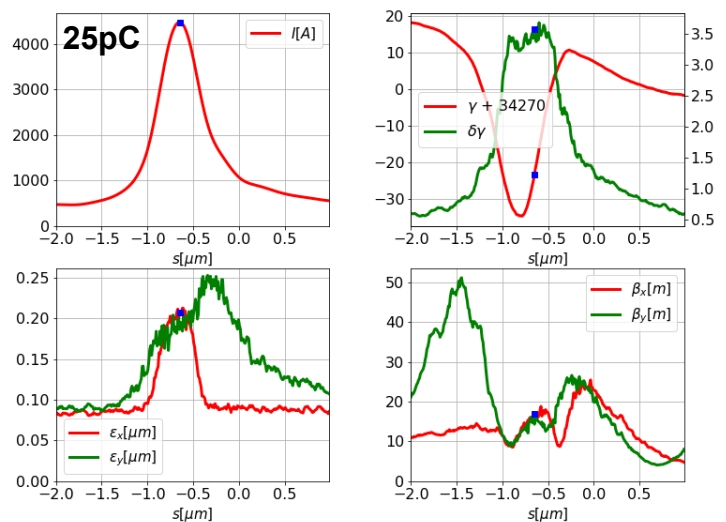
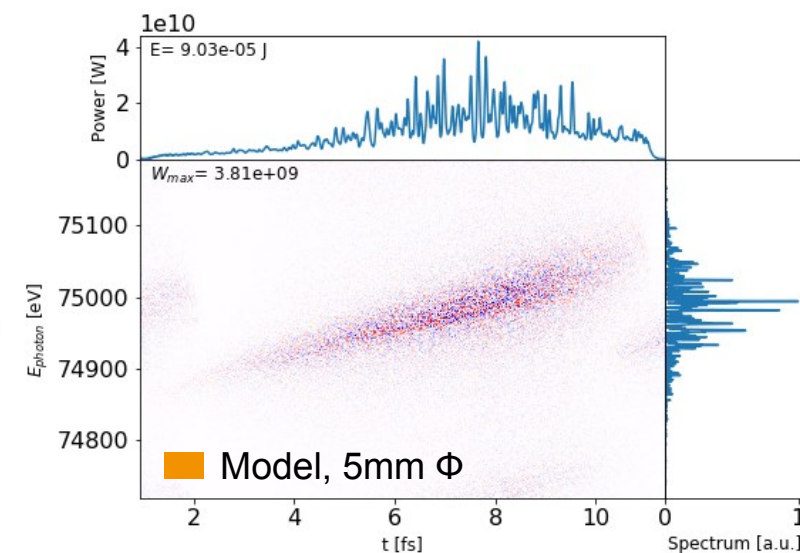
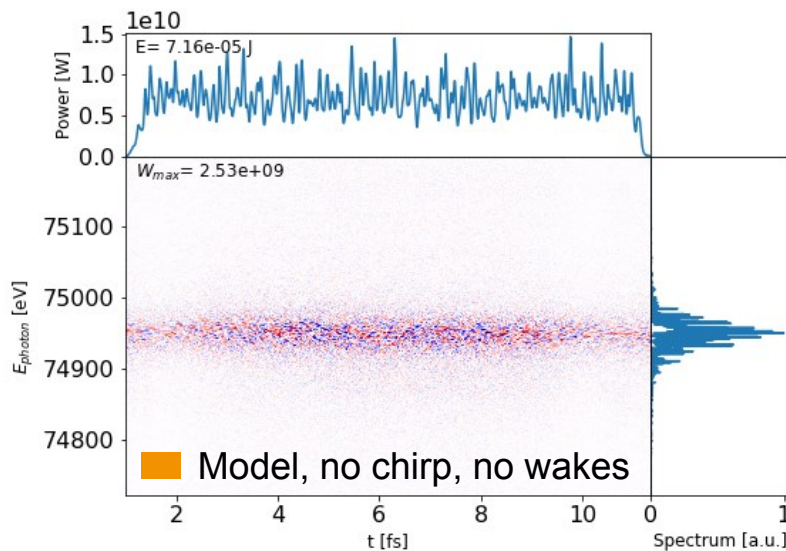
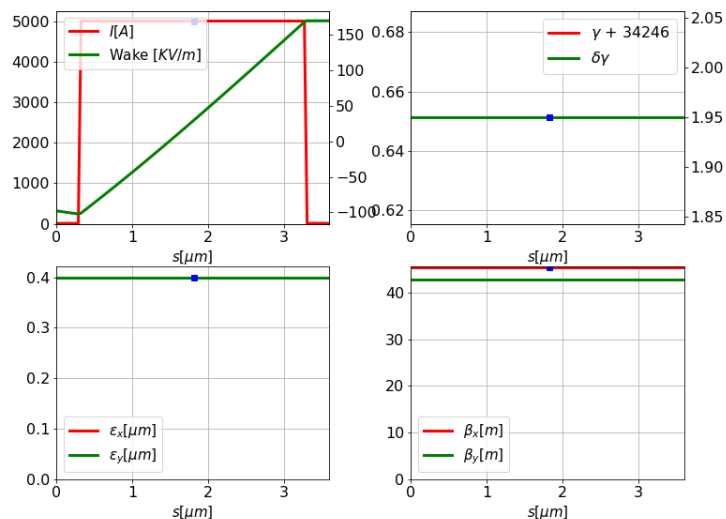
Effect of undulator field errors

100keV = 0.12 Angstrom

- 100keV, 15mm period
- Phase-shake effect
- Added path was calculated and compensated with phase shifter
- With 50% error magnitude effect negligible
 - Note: .15% errors > .01% rho



Spread of SASE spectrum (beam energy chirps & resistive wakefields)



Transverse coherence (17mm period)

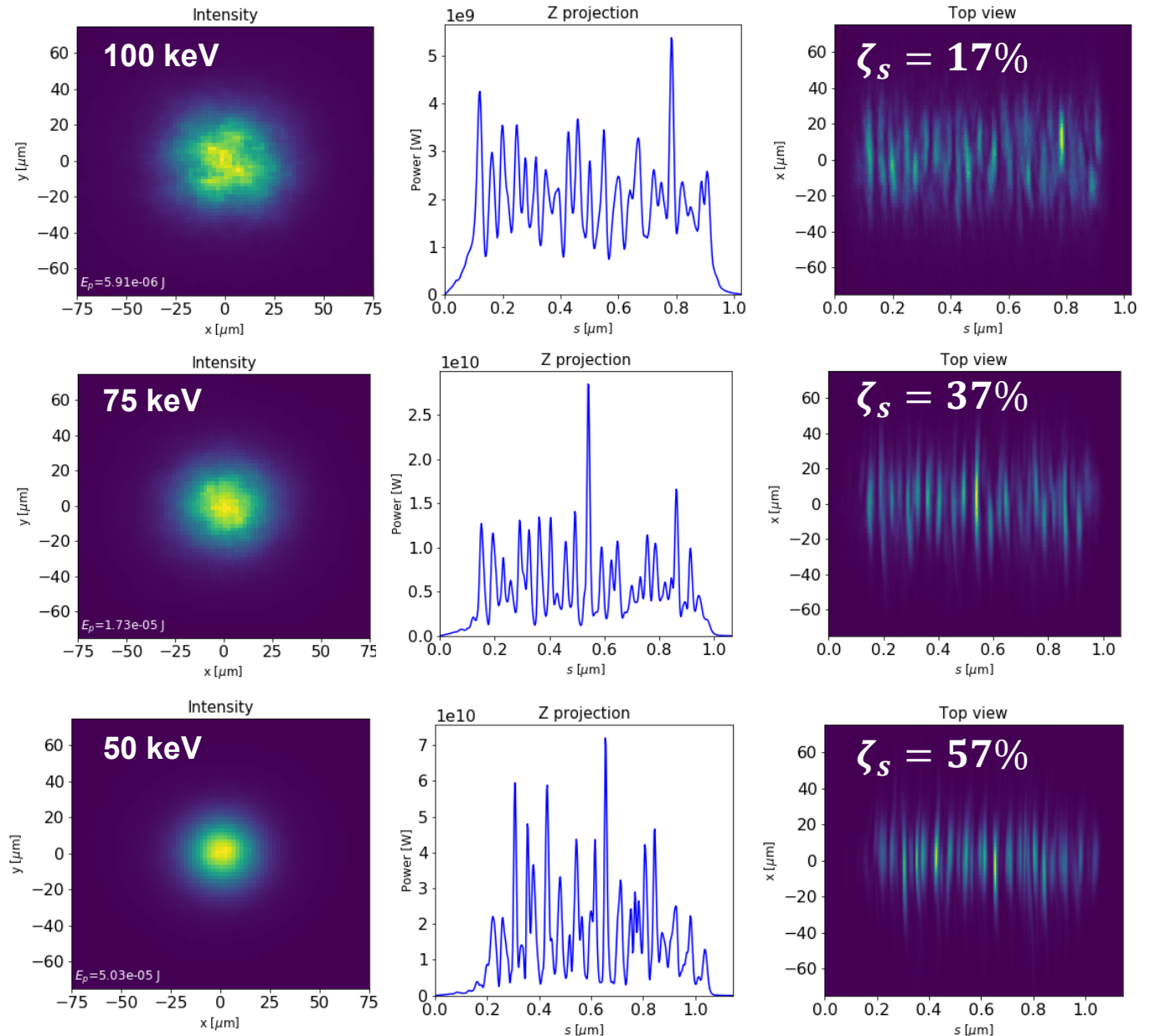
■ Radiation fields simulated with Genesis ($\epsilon_{xy}=0.4\mu\text{rad}$, $z=150\text{m}$)

■ $J(r_1, r_2, t) \equiv \langle E^*(r_1, t)E(r_2, t) \rangle$
Mutual intensity function

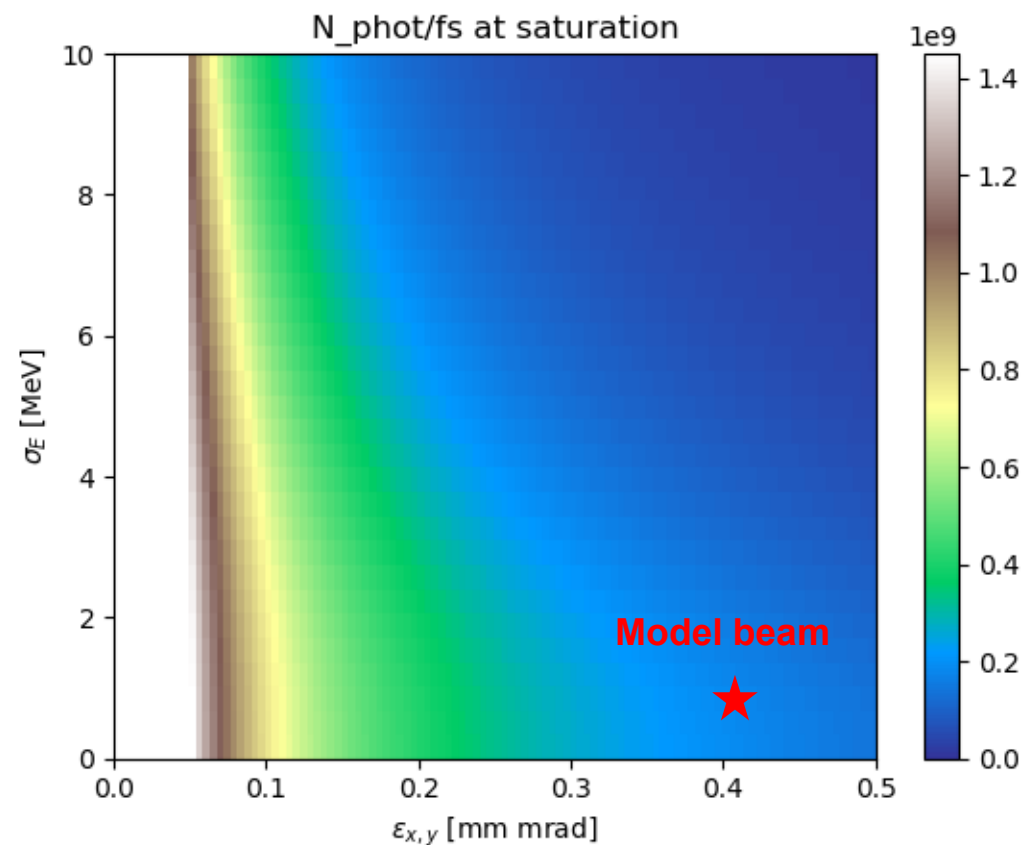
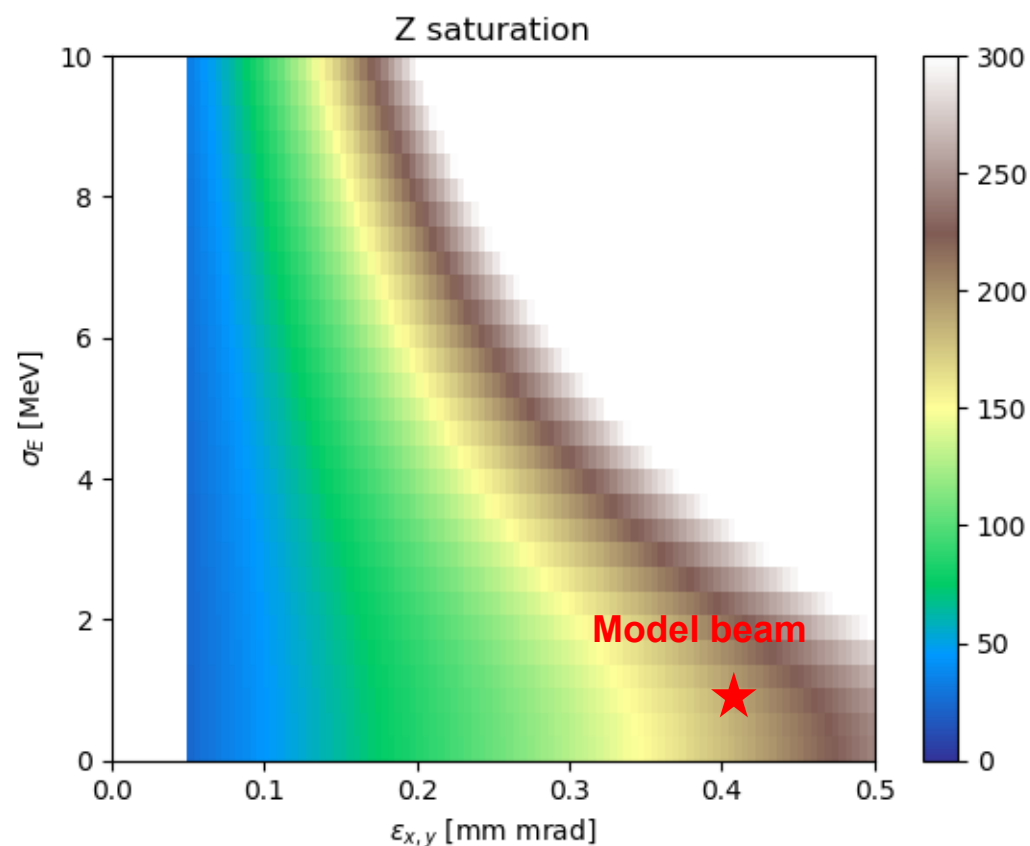
$$\zeta_s = \frac{\int |J(r_1, r_2)|^2 dr_1 dr_2}{(\int I(r) dr)^2}$$

Degree of spatial coherence

■ Also depends on electron beam quality

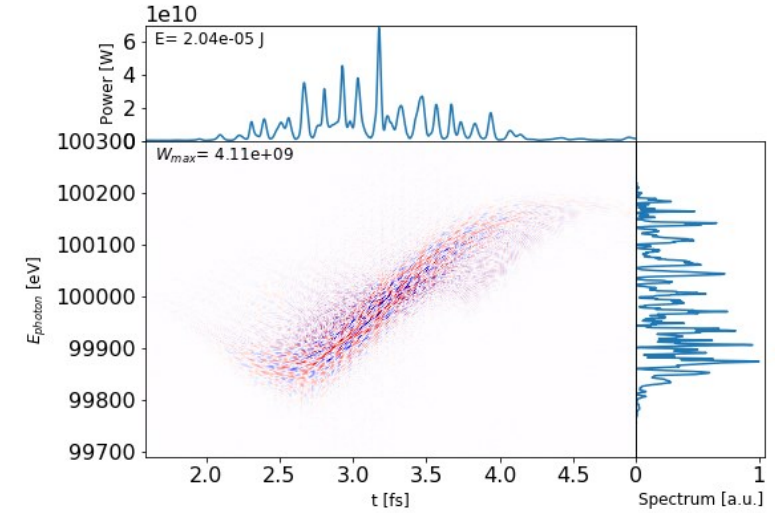
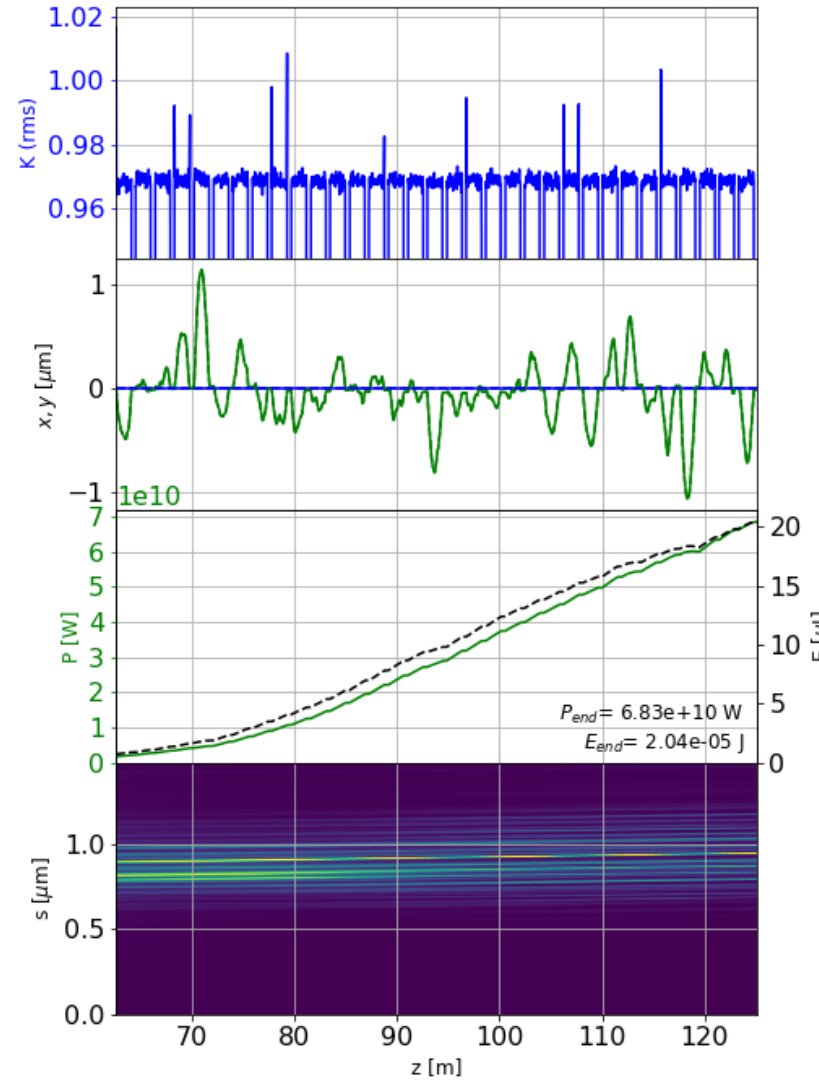
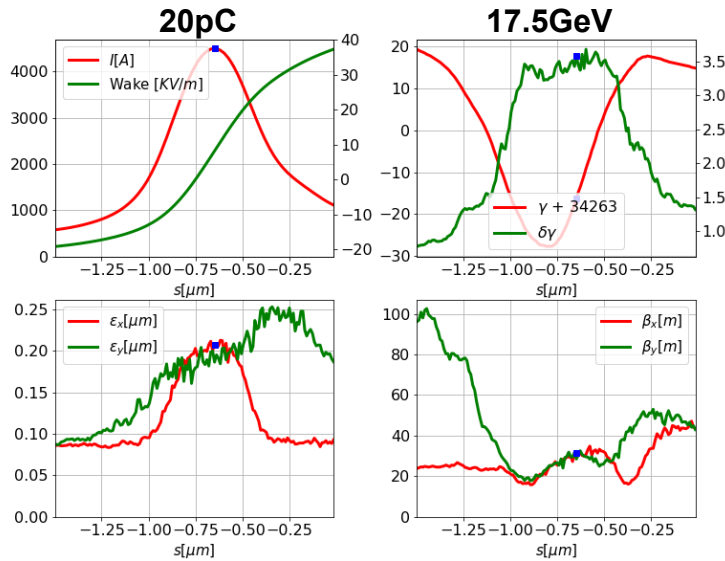


E-beam quality effect, 100keV, 15mm period



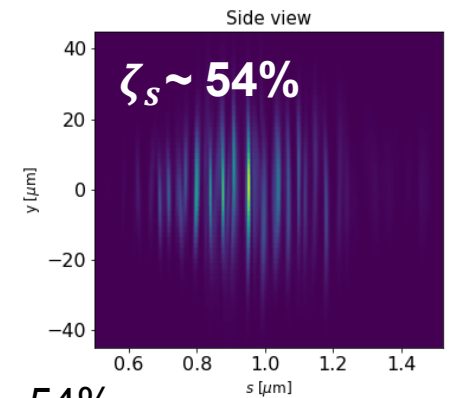
■ Emittance / 2 = Energy spread * 7

100keV S2E simulation:



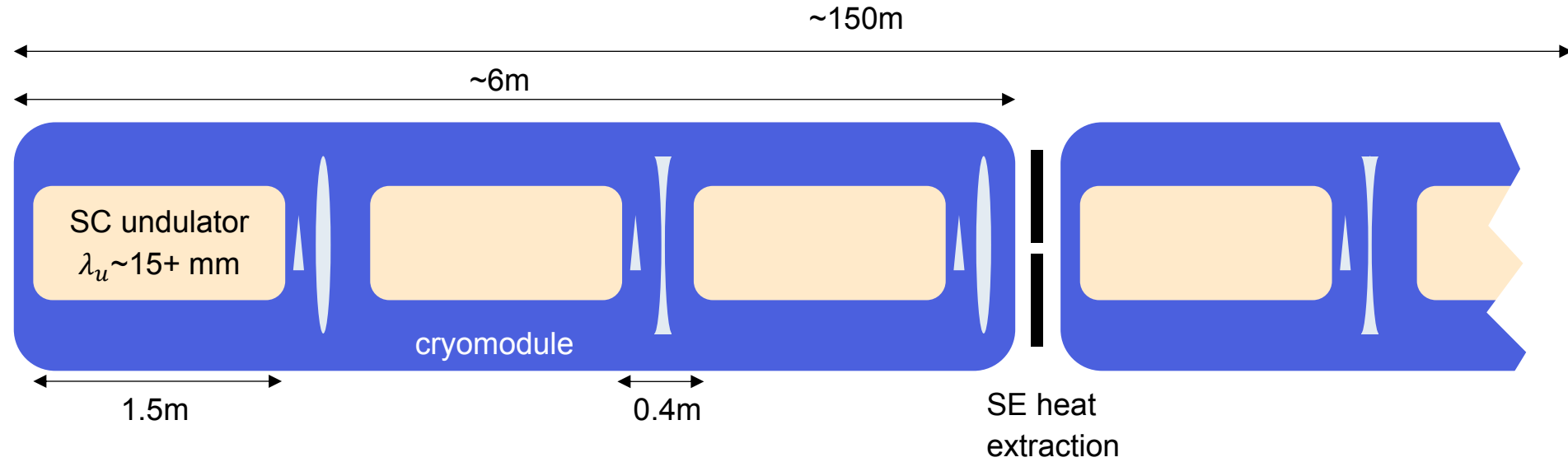
- Undulator:
- 125m
- 15mm period
- $\sigma_K/K=0.15\%$ (1/2 of measured)
- Wakefields for 5mm vacuum pipe
- No post-saturation tapering

- $E_{ph}=100\text{keV}$
- $dE/E_{ph}=3 \cdot 10^{-3}$
- $N_{ph} \sim 10^9$
- $T_{fwhm} \sim 1.5\text{fs}$
- Coherence: $\zeta_S \sim 54\%$



Summary 1: Undulator

- 25 cryomodules
- 79% filling factor



- SASE2 is best suited for SCU location
- Otherwise – SASE4 (provided SASE2 is open or bypassed)



Summary 2

- Our findings are based on two analytical approaches (SSY, Mxie) and two codes (Genesis, Simplex [T.Tanikawa])
- Potential detrimental effects on lasing:
 - E-beam quality is crucial (in particular: emittance $< 0.4\mu\text{rad}$); it affects choice of the period
 - Quantum fluctuations important beyond 75keV at 17.5GeV
 - Undulator errors $\gg \rho$ can be compensated
 - Resistive wakefields and energy chirps in e-beam increase radiation bandwidth
 - Radiation coherence rapidly drops with photon energy and beam emittance
- At CW operation 18mm SCU complements SASE1/2 undulator photon energy range
- Period doubling is possible and allows one to significantly increase photon energy range at given e-beam energy
- SCU radiation damage (probably) smaller compared to IVU/CPMU
- Harmonic lasing becomes beneficial with 20mm SCU

- But the most important...

Reaching 100keV in EuXFEL is possible!

/10keV used to be Sci-fi/

Thank you

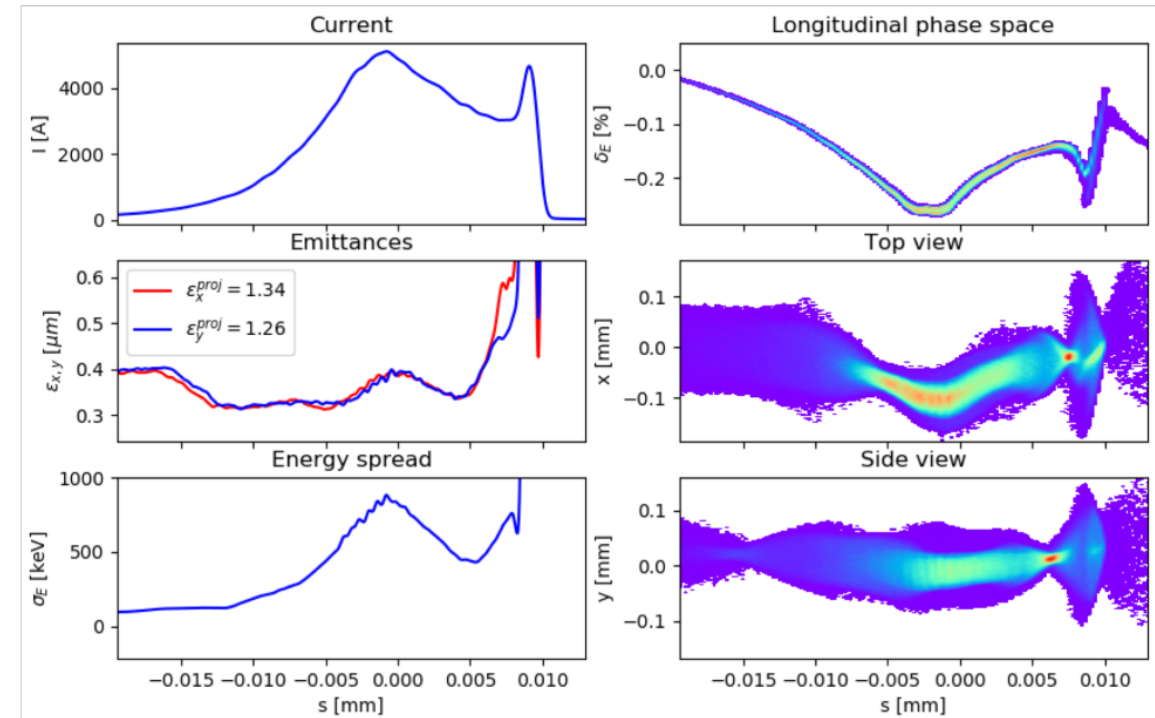
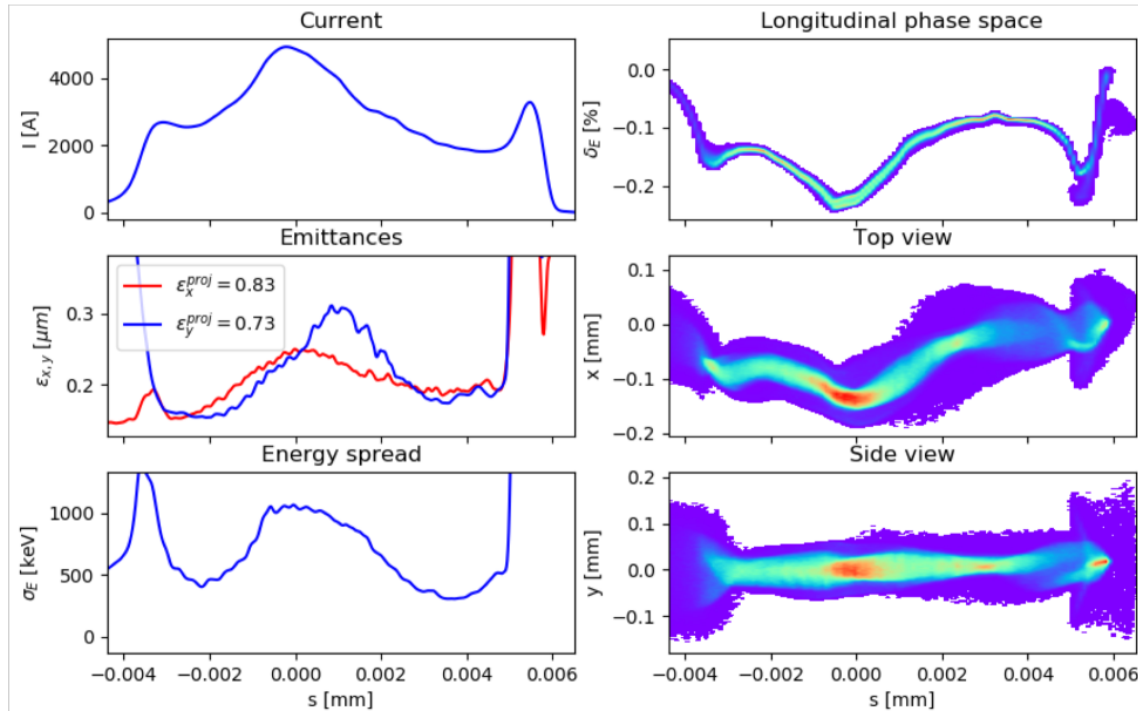
E-beam

Beam Dynamics at the European XFEL up to SASE4/5

Igor Zagorodnov, 06.12.2018

100pC

250pC



Methods to estimate FEL performance (3D gain length)

■ Saldin, Schneymiller, Yurkov

$$L_g \simeq L_{g0}(1 + \delta),$$

$$L_{g0} = 1.67 \left(\frac{I_A}{I} \right)^{1/2} \frac{(\epsilon_n \lambda_w)^{5/6} (1 + K^2)^{1/3}}{\lambda_h^{2/3} h^{5/6} K A_{JJh}},$$

$$\delta = 131 \frac{I_A}{I} \frac{\epsilon_n^{5/4}}{\lambda_h^{1/8} \lambda_w^{9/8}} \frac{h^{9/8} \sigma_\gamma^2}{(K A_{JJh})^2 (1 + K^2)^{1/8}}$$

$$A_{JJh}(K) = J_{(h-1)/2} \left(\frac{hK^2}{2(1 + K^2)} \right) - J_{(h+1)/2} \left(\frac{hK^2}{2(1 + K^2)} \right)$$

E. L. Saldin, E. A. Schneymiller, and M. V. Yurkov, "Design formulas for short-wavelength FELs," *Opt. Commun.*, vol. 235, no. 4–6, pp. 415–420, May 2004.

E. A. Schneymiller and M. V. Yurkov, "Harmonic lasing in x-ray free electron lasers," *Phys. Rev. Spec. Top. - Accel. Beams*, vol. 15, no. 8, p. 080702, Aug. 2012.

■ M.Xie

$$\frac{L_{1d}}{L_g} = \frac{1}{1 + \Lambda}$$

$$L_{1d} = 1/2 \sqrt{3} k_w \rho$$

$$\rho = \sqrt[3]{(I/I_A)(\lambda_w a_w f_B / 2\pi \sigma_x)^2 (1/2\gamma_0)^3}$$

$$\Lambda = a_1 \eta_d^{a_2} + a_3 \eta_\epsilon^{a_4} + a_5 \eta_\gamma^{a_6}$$

$$+ a_7 \eta_\epsilon^{a_8} \eta_\gamma^{a_9} + a_{10} \eta_d^{a_{11}} \eta_\gamma^{a_{12}} + a_{13} \eta_d^{a_{14}} \eta_\epsilon^{a_{15}}$$

$$+ a_{16} \eta_d^{a_{17}} \eta_\epsilon^{a_{18}} \eta_\gamma^{a_{19}}$$

$$\eta_d = 1/F_d$$

$$\eta_\epsilon = 4\pi(L_{1d}/\lambda_\beta)k_r \epsilon$$

$$\eta_\gamma = 4\pi(L_{1d}/\lambda_w)\sigma_\eta$$

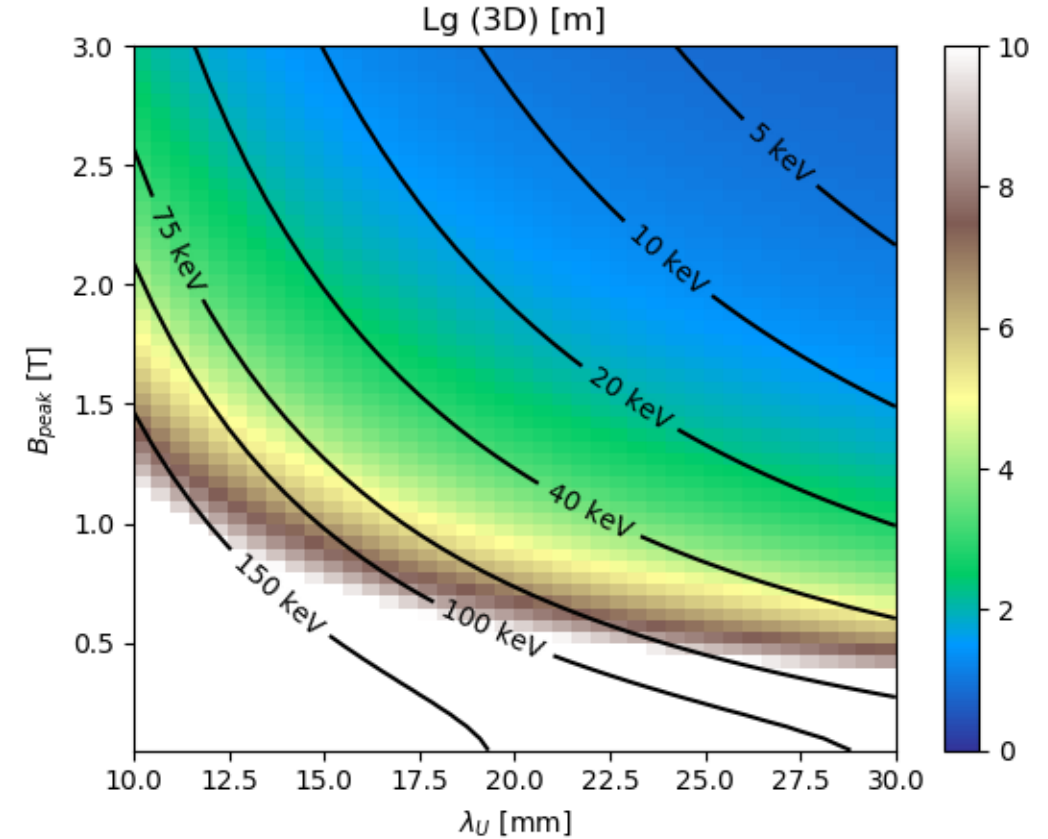
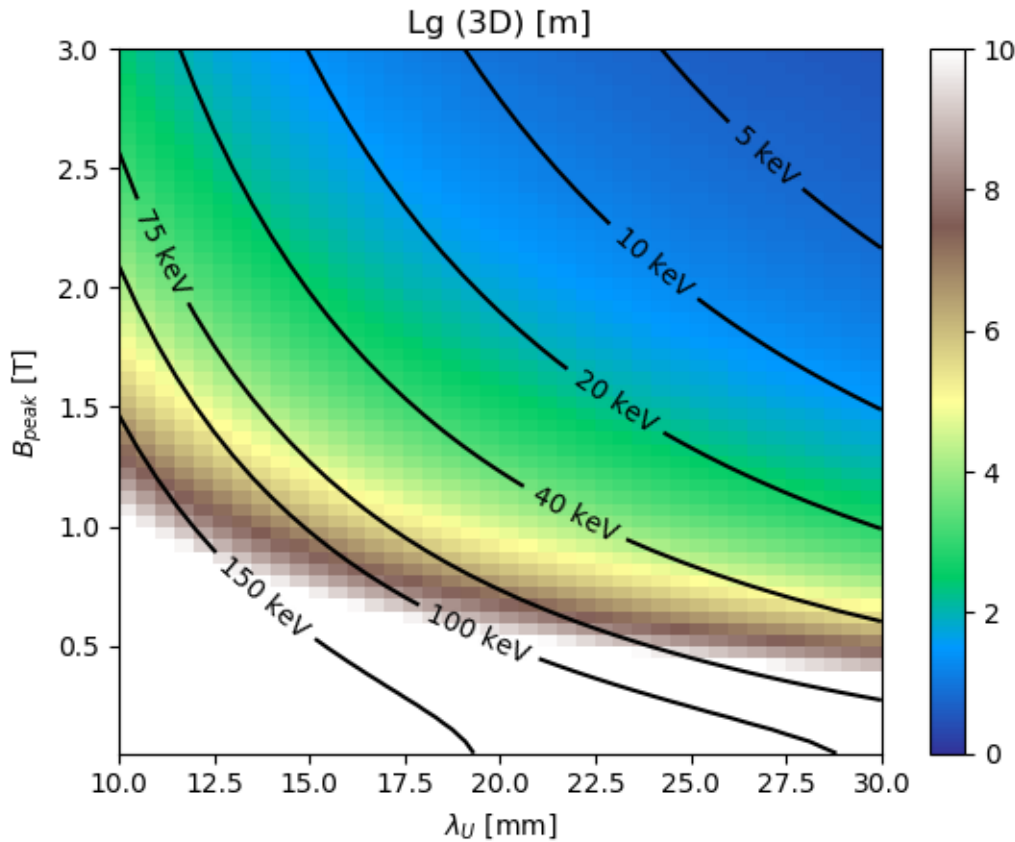
M. Xie, "Exact and variational solutions of 3D eigenmodes in high gain FELs," *Nucl. Instruments Methods Phys. Res. Sect. A Accel. Spectrometers, Detect. Assoc. Equip.*, vol. 445, no. 1–3, pp. 59–66, 2000.

Methods to estimate FEL performance (3D gain length)

$$L_g^{3d} = L_g^{1d}(1 + \delta)$$

■ Saldin, Schneidmiller, Yurkov

■ M.Xie



E. L. Saldin, E. A. Schneidmiller, and M. V. Yurkov, "Design formulas for short-wavelength FELs," *Opt. Commun.*, vol. 235, no. 4–6, pp. 415–420, May 2004.

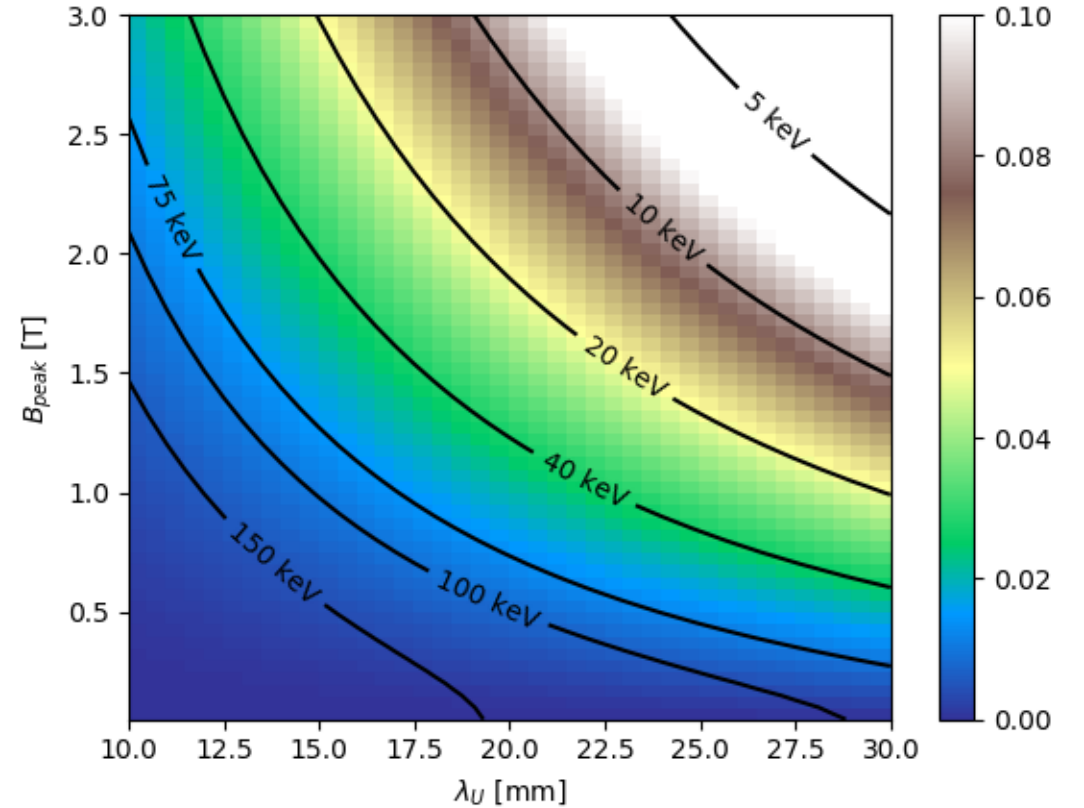
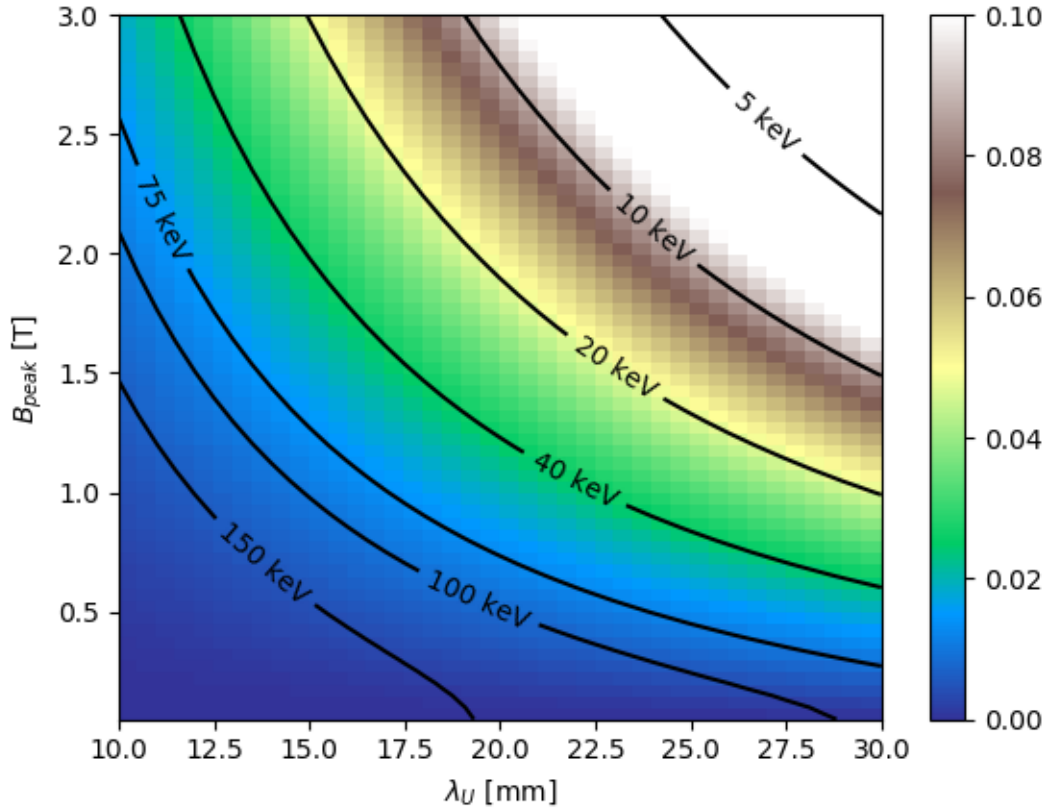
M. Xie, "Exact and variational solutions of 3D eigenmodes in high gain FELs," *Nucl. Instruments Methods Phys. Res. Sect. A Accel. Spectrometers, Detect. Assoc. Equip.*, vol. 445, no. 1–3, pp. 59–66, 2000.

Methods to estimate FEL performance (~3D efficiency)

$$\frac{\lambda_u}{4\pi\sqrt{3}L_g^{3d}} * 100\%$$

■ Saldin, Schneidmiller, Yurkov

■ M.Xie



E. L. Saldin, E. A. Schneidmiller, and M. V. Yurkov, "Design formulas for short-wavelength FELs," Opt. Commun., vol. 235, no. 4–6, pp. 415–420, May 2004.

M. Xie, "Exact and variational solutions of 3D eigenmodes in high gain FELs," Nucl. Instruments Methods Phys. Res. Sect. A Accel. Spectrometers, Detect. Assoc. Equip., vol. 445, no. 1–3, pp. 59–66, 2000.

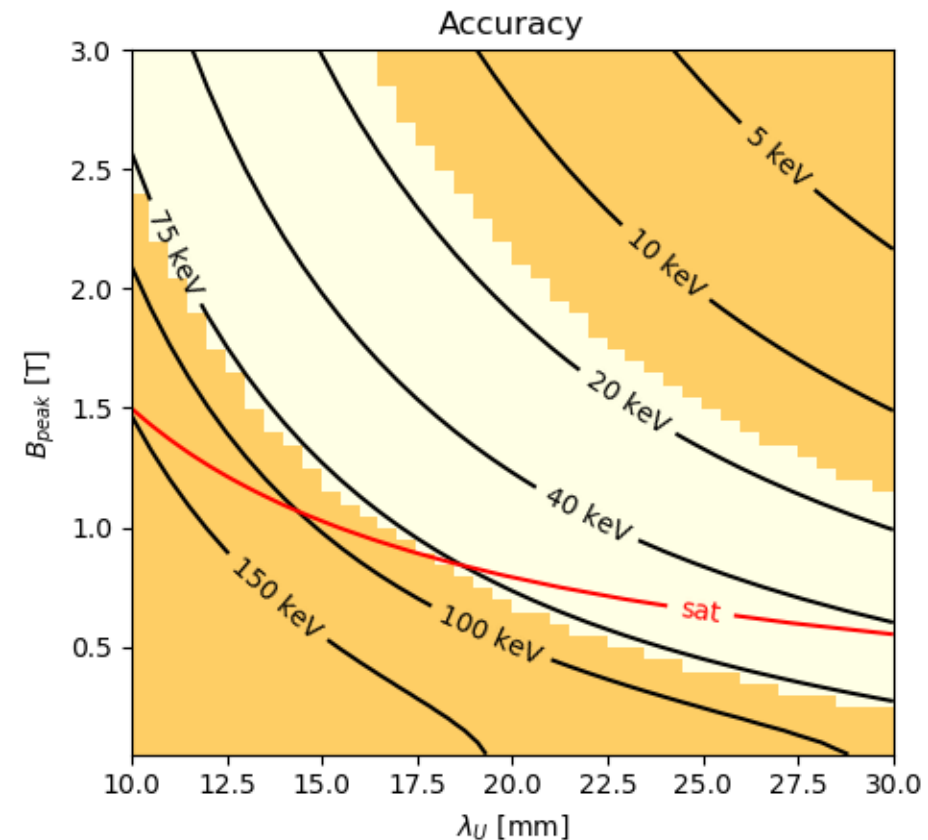
Accuracy

The formulas (3)–(5) provide an accuracy better than 5% in the range of parameters

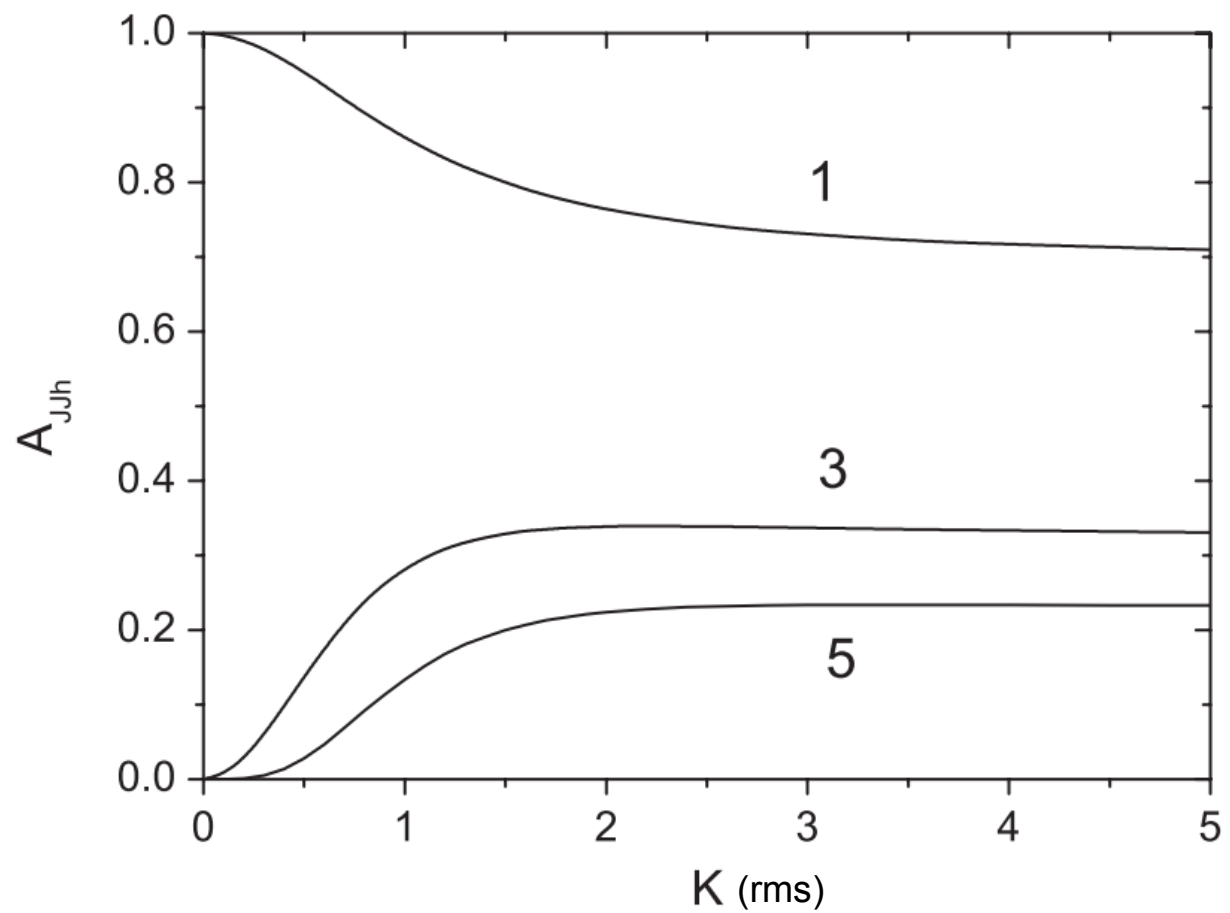
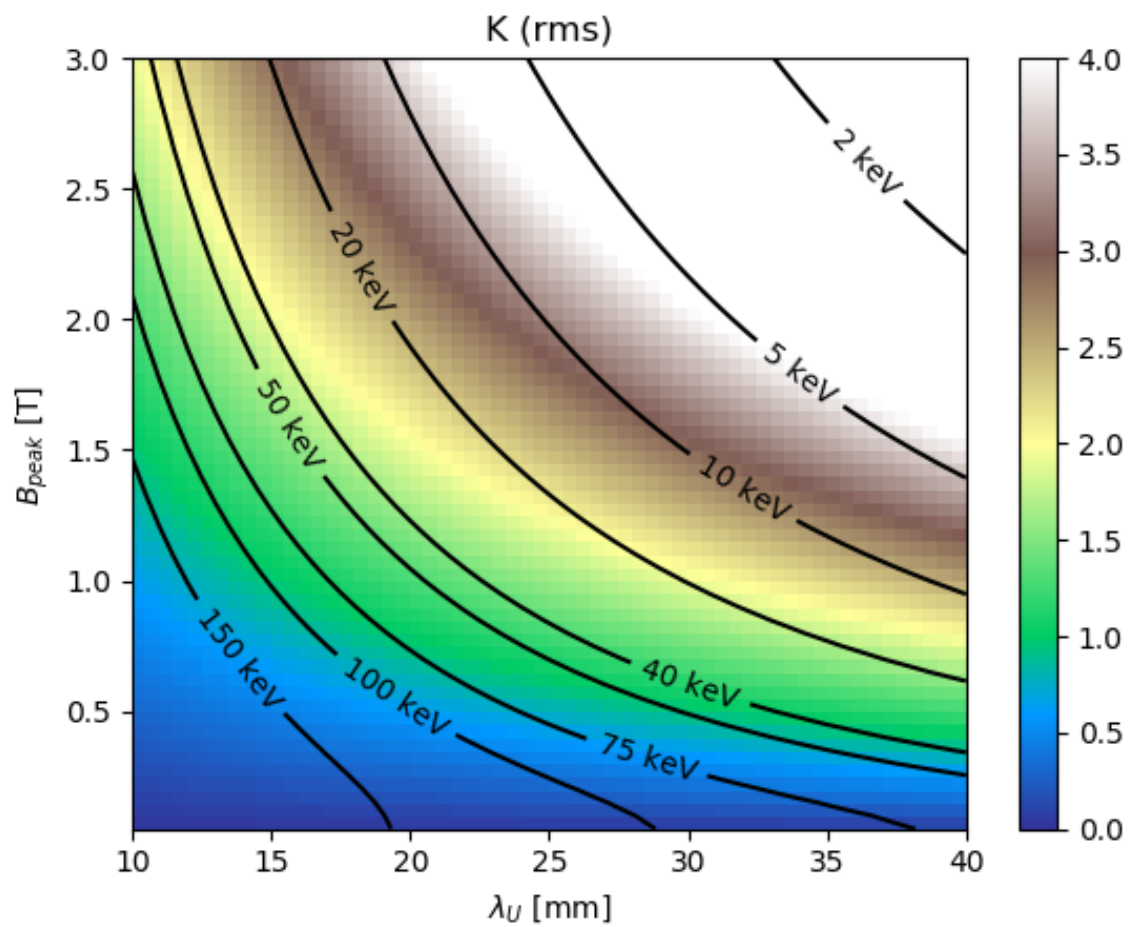
$$1 < \frac{2\pi\epsilon}{\lambda_h} < 5, \quad (6)$$

$$\delta < 2.5 \left\{ 1 - \exp \left[-\frac{1}{2} \left(\frac{2\pi\epsilon}{\lambda_h} \right)^2 \right] \right\}. \quad (7)$$

In fact, the formulas (3)–(5) can also be used well beyond this range, but the above-mentioned accuracy is not guaranteed.



E. A. Schneidmiller and M. V. Yurkov, "Harmonic lasing in x-ray free electron lasers," *Phys. Rev. Spec. Top. - Accel. Beams*, vol. 15, no. 8, p. 080702, Aug. 2012.



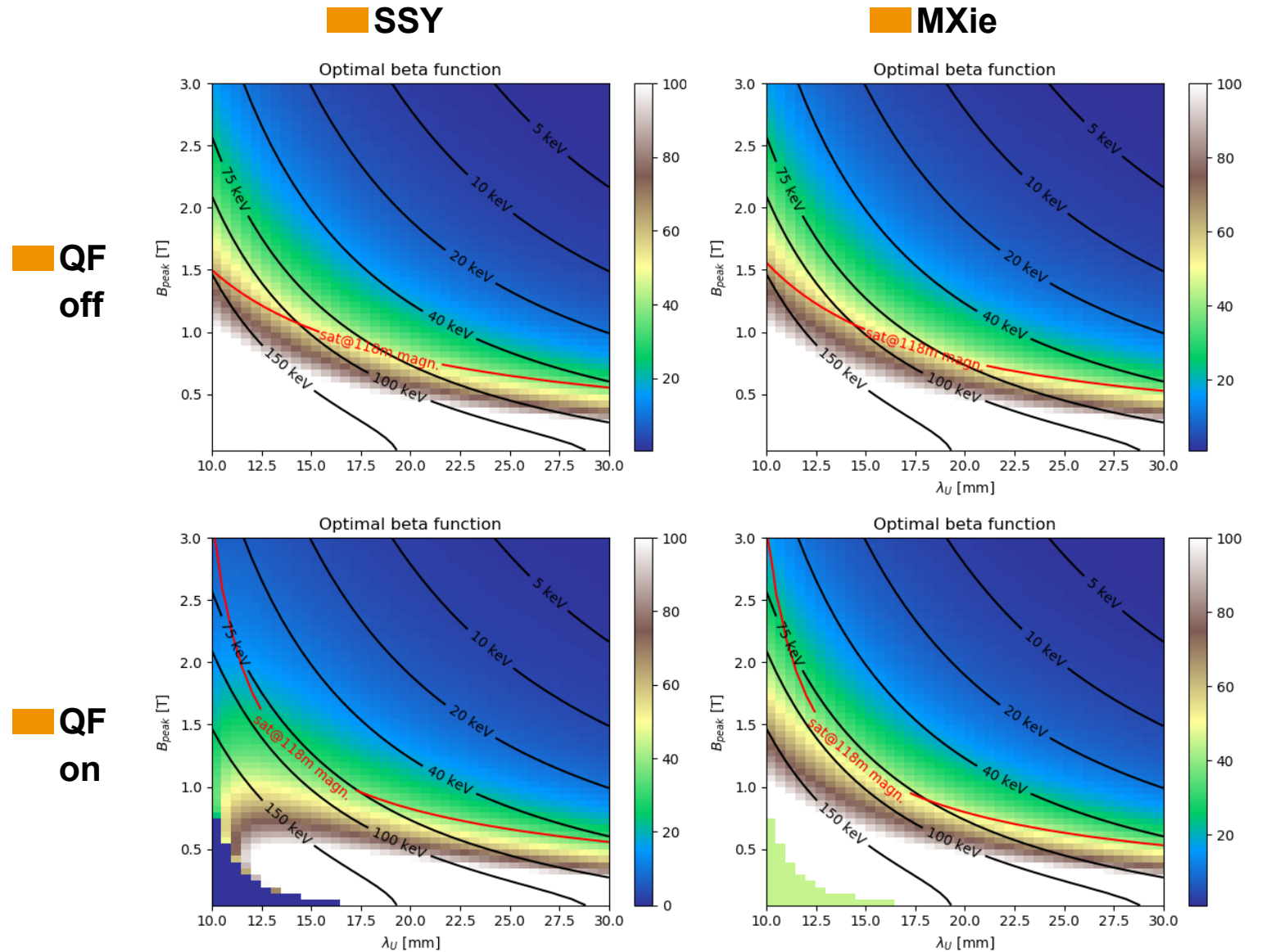
Effect of beam energy chirps & resistive wakefields

Wakefield calculated with OCELOT assuming:

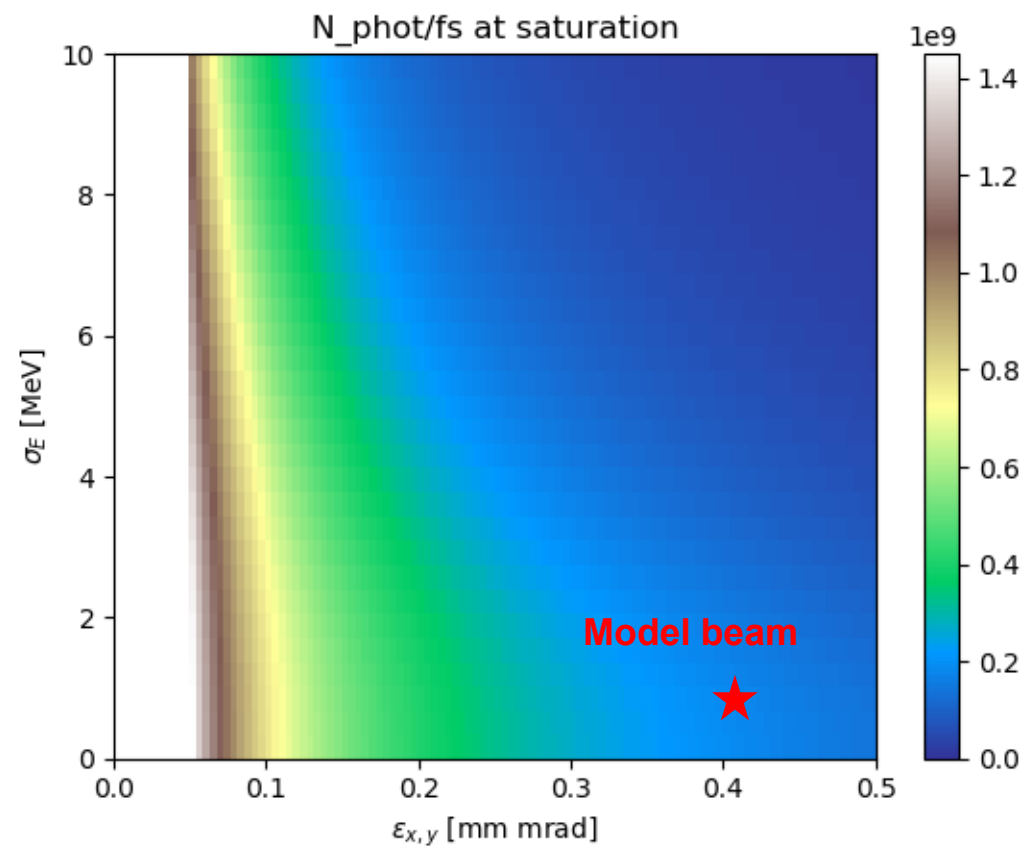
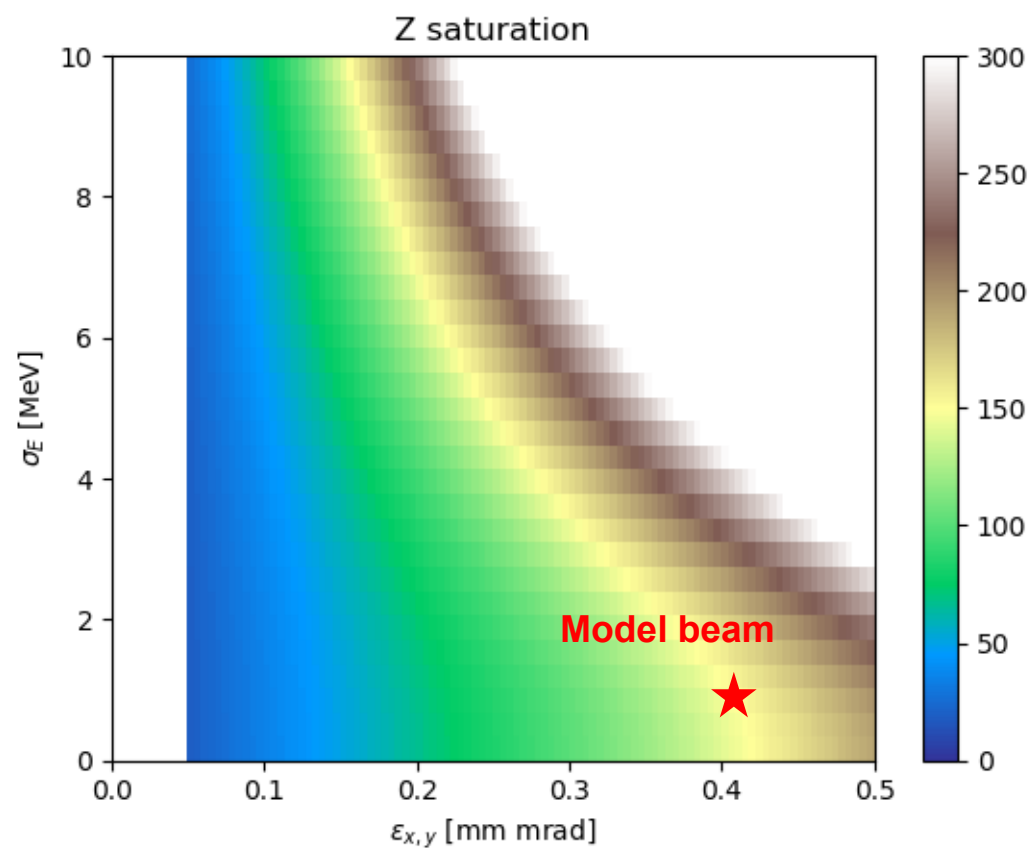
- tube_radius=2.5e-3,
- tube_len=1,
- conductivity=3.66e+7,
- tau=7.1e-15,
- roughness=600e-9,
- d_oxid=5e-9

```
self.eloss = pipe_wake(self.s, self.l, tube_radius, tube_len,  
conductivity, tau, roughness, d_oxid)[1][1][::-1]
```

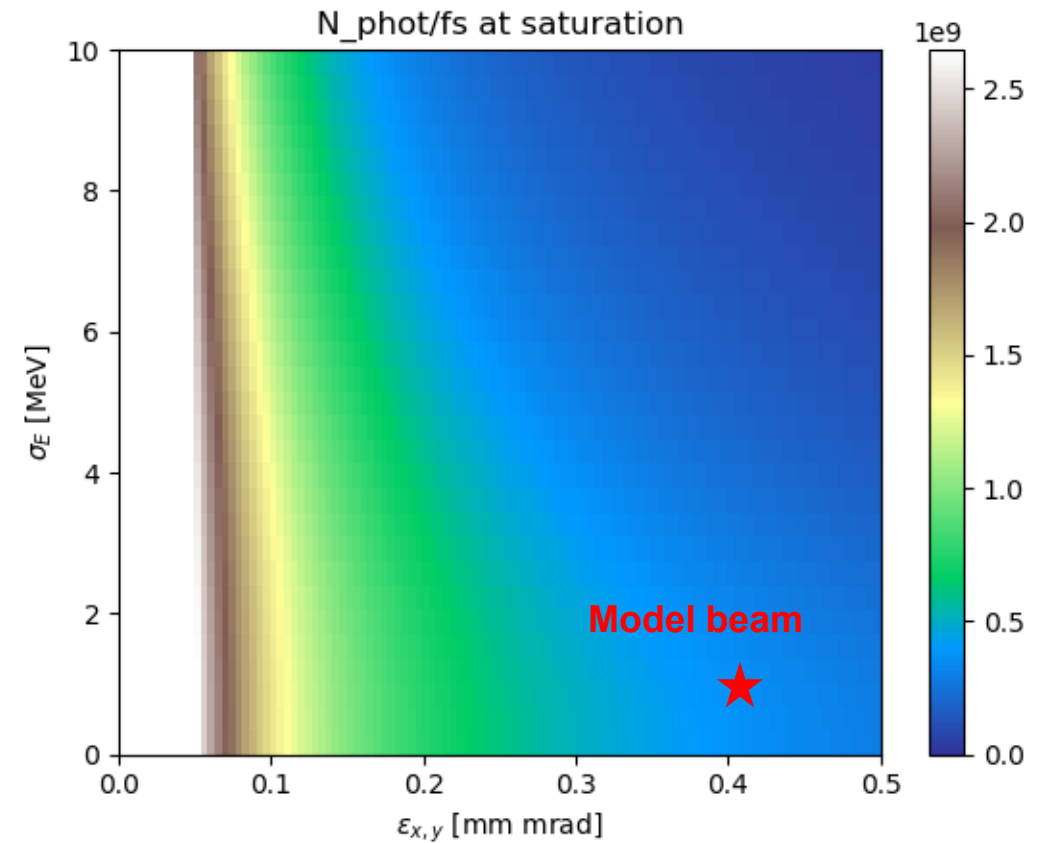
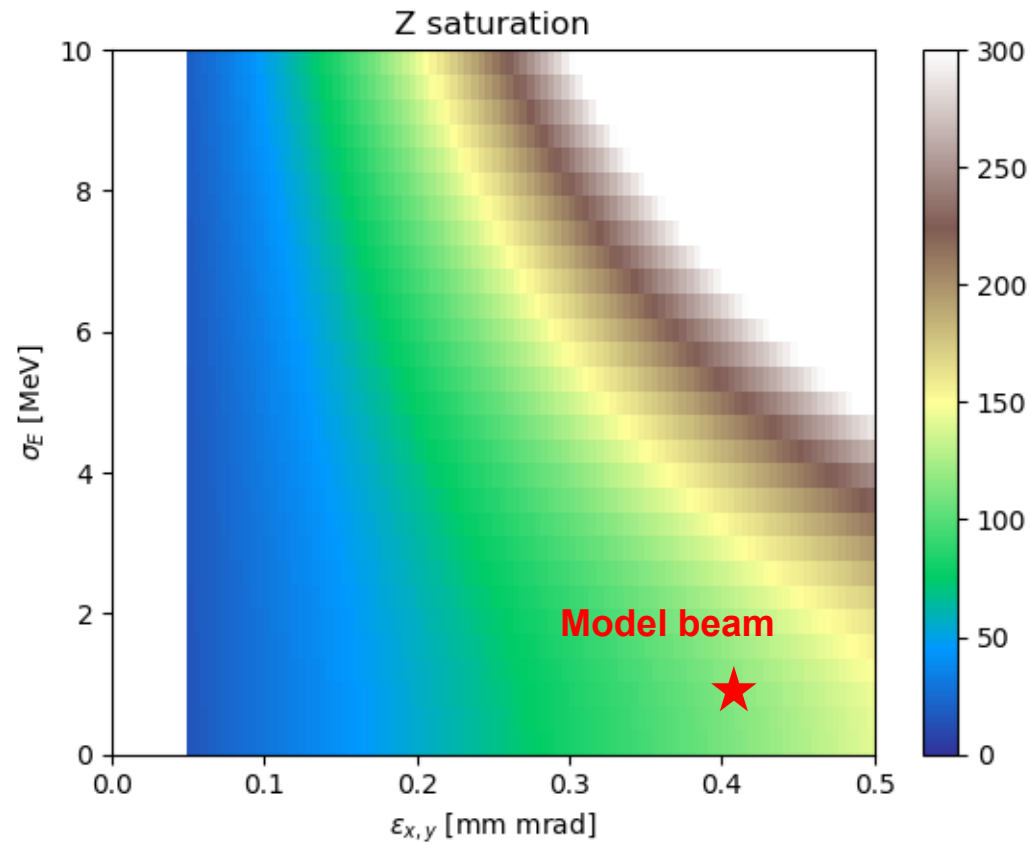
Optimal Beta Functions



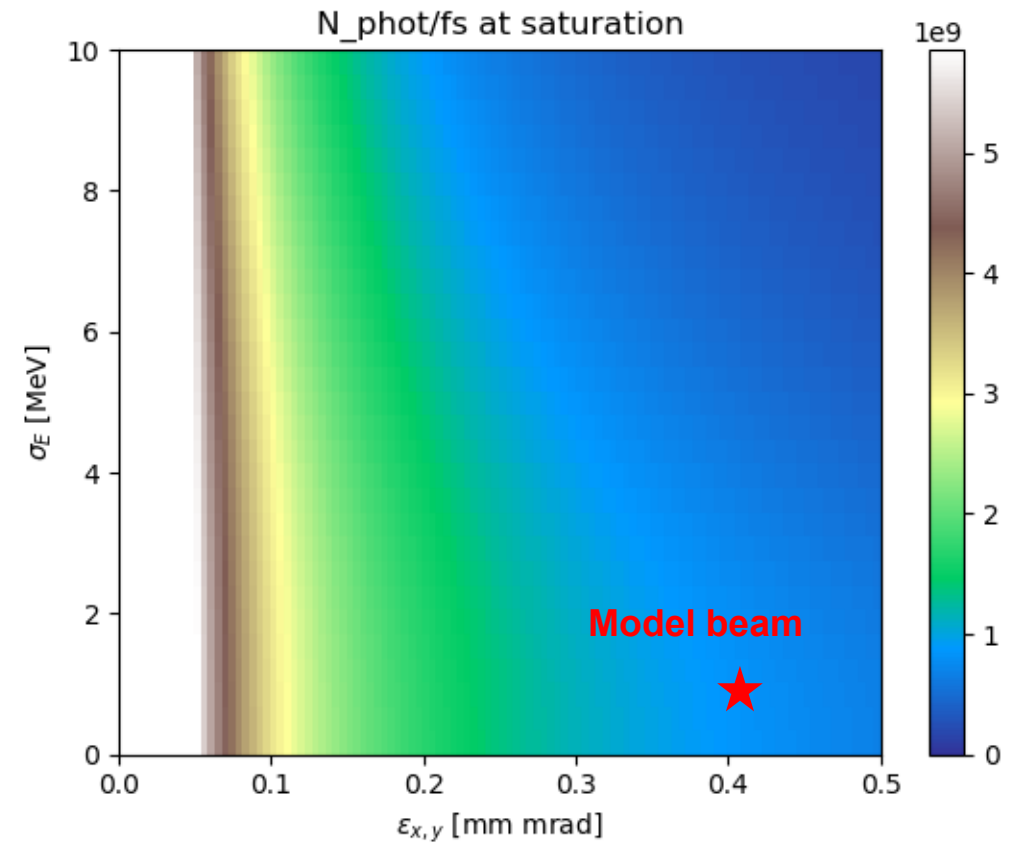
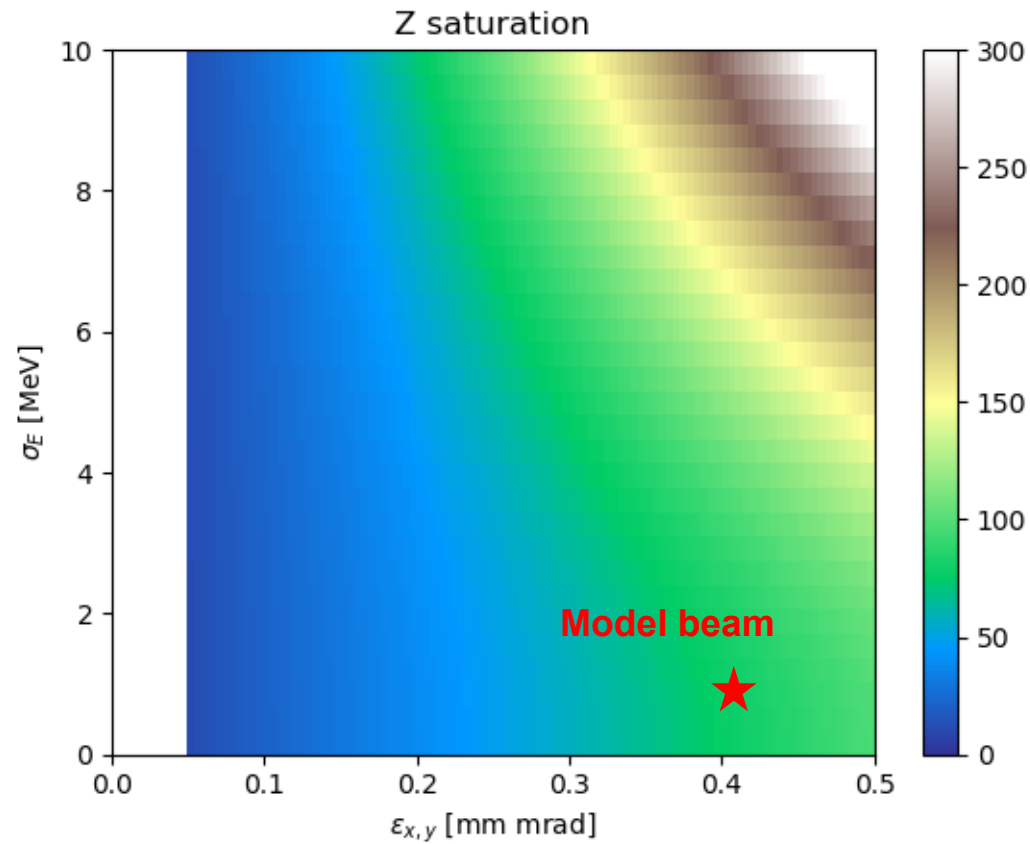
E-beam quality effect, 100keV, 15mm period



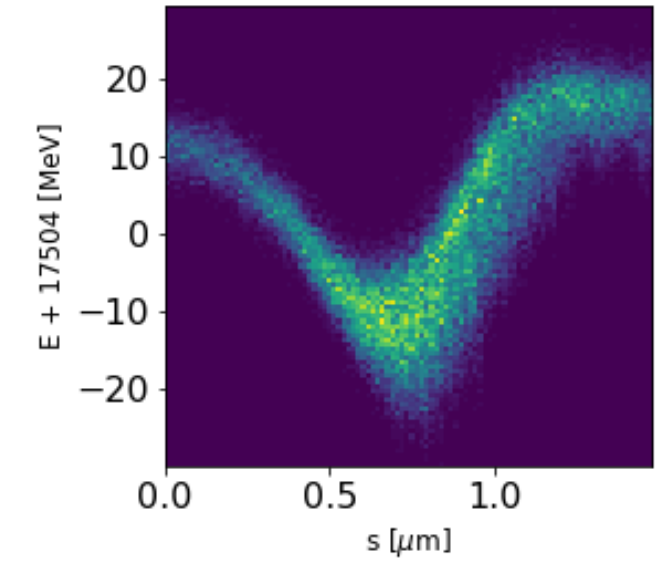
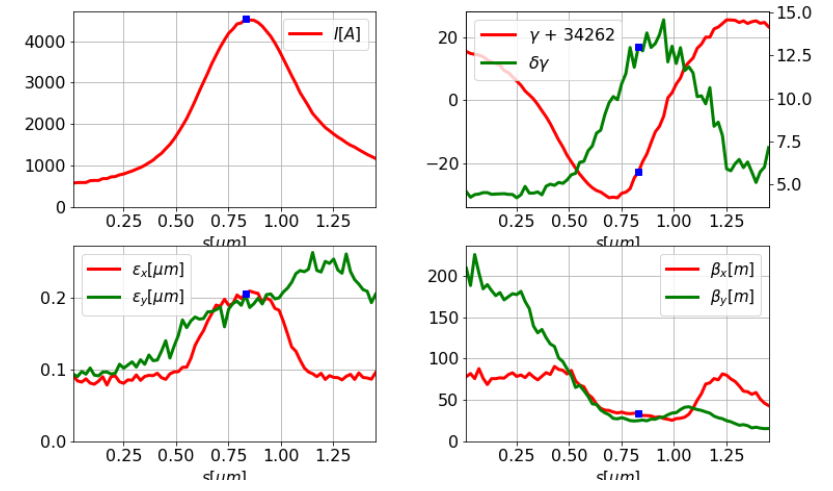
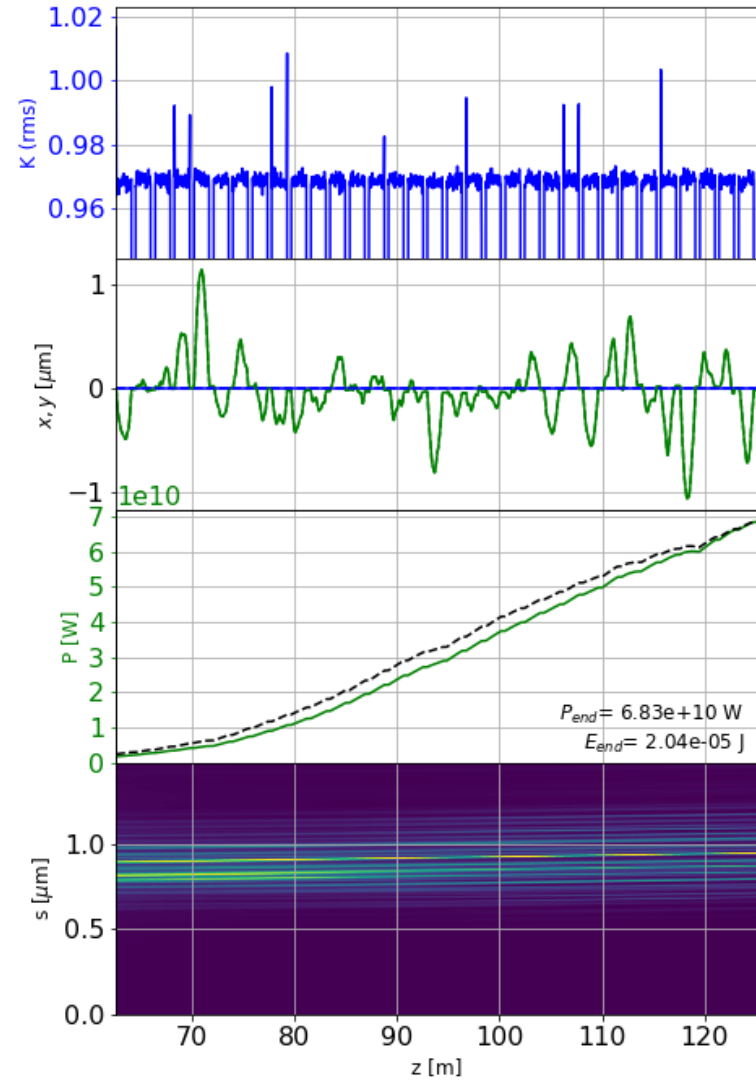
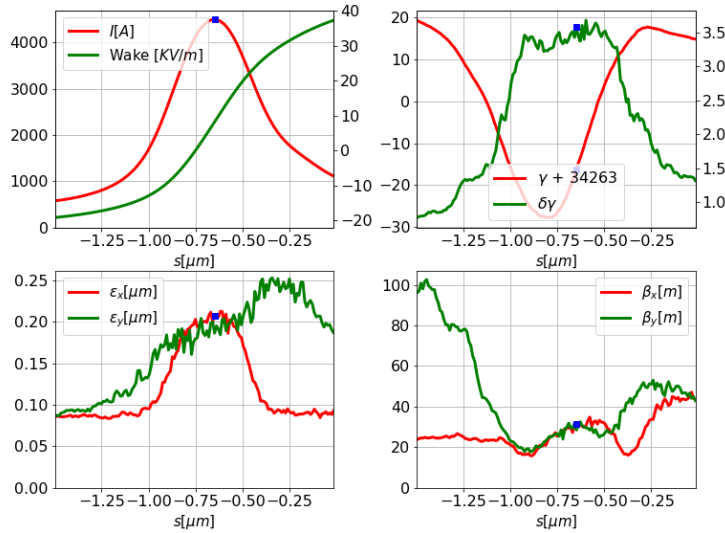
E-beam quality effect, 75keV, 17mm period



E-beam quality effect, 50keV, 18mm period



Beam after SASE4:



Optimistic scenario (SP mode, 19.8 GeV, 0.2mm*mrad beam)

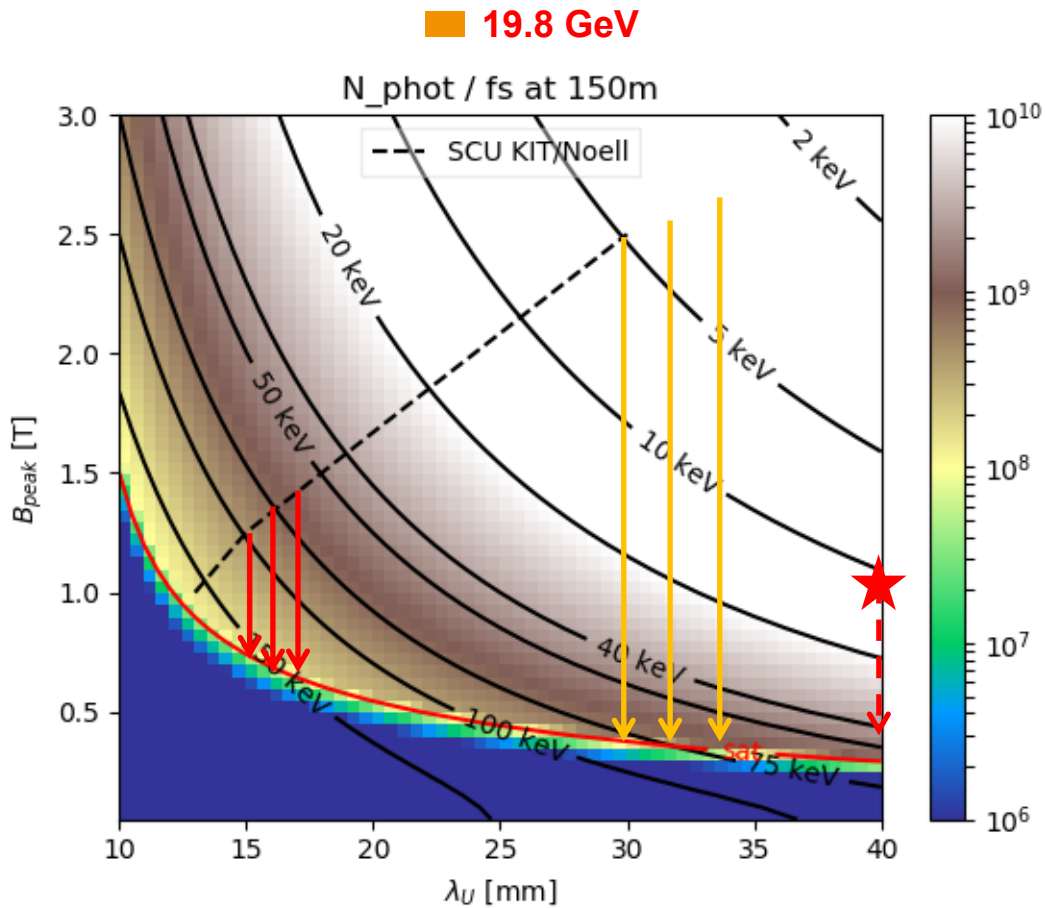
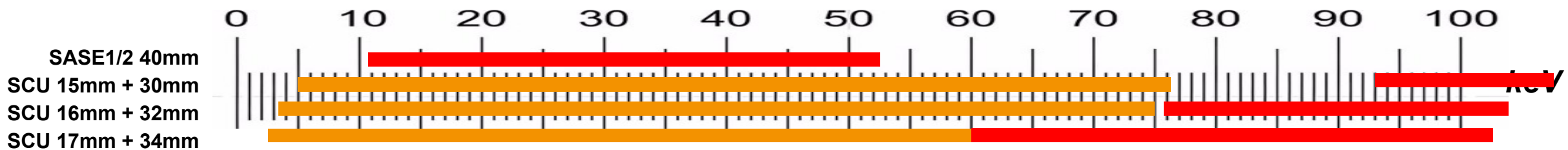


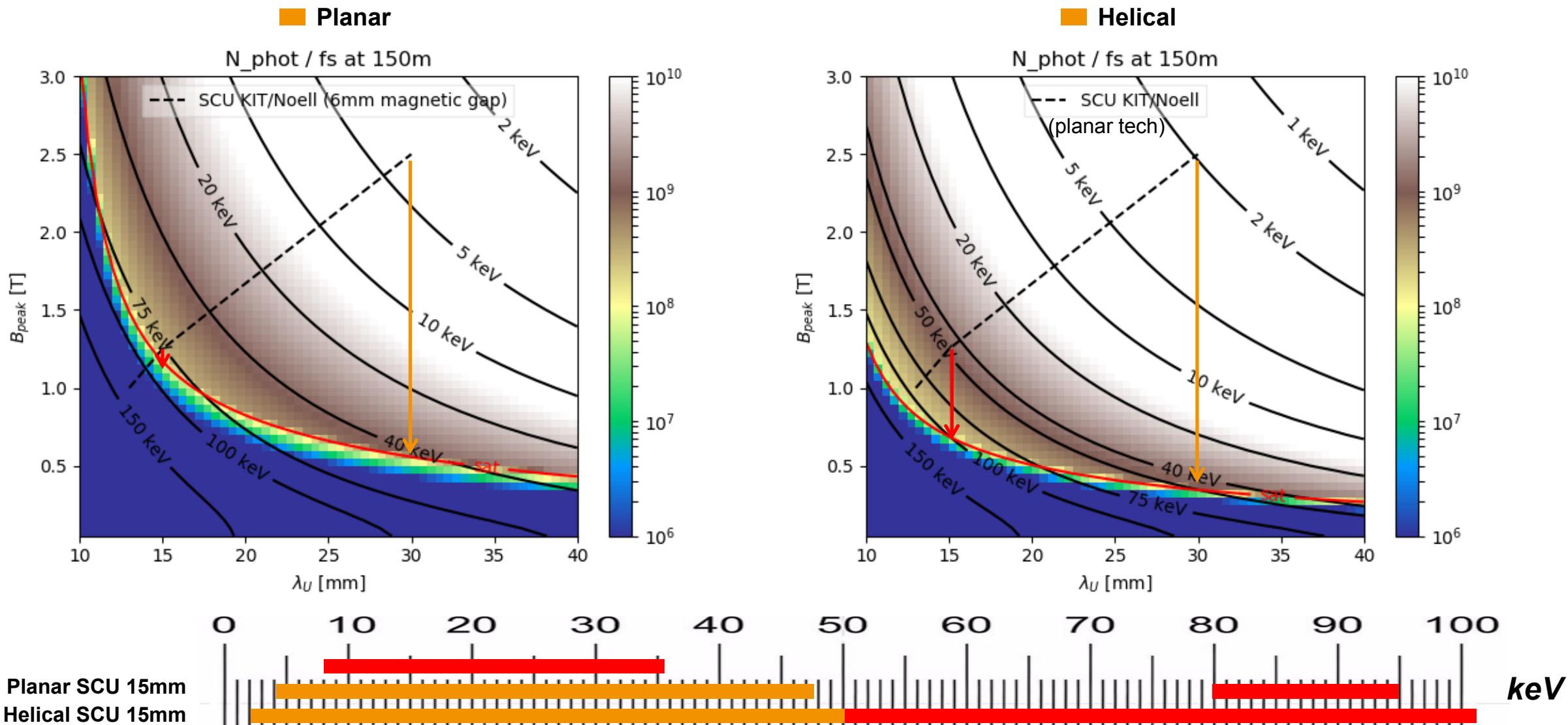
TABLE VI. Beam energy and DF estimated for the upgraded XFEL accelerator.

Operation mode	E_{beam} [GeV]	E_{acc} in ML [MV/m]	Beam-on DF [%]
sp (nominal)	19.8	23.4	0.6
cw	7.8	7.3	100
lp	10	10	53
lp	14	15	23

At optimistic electron energy and emittance parameters one can expect to reach beyond 100keV



Planar vs Helical undulator



Optimistic scenario (SP mode, 19.8 GeV, 0.2mm*mrad beam)

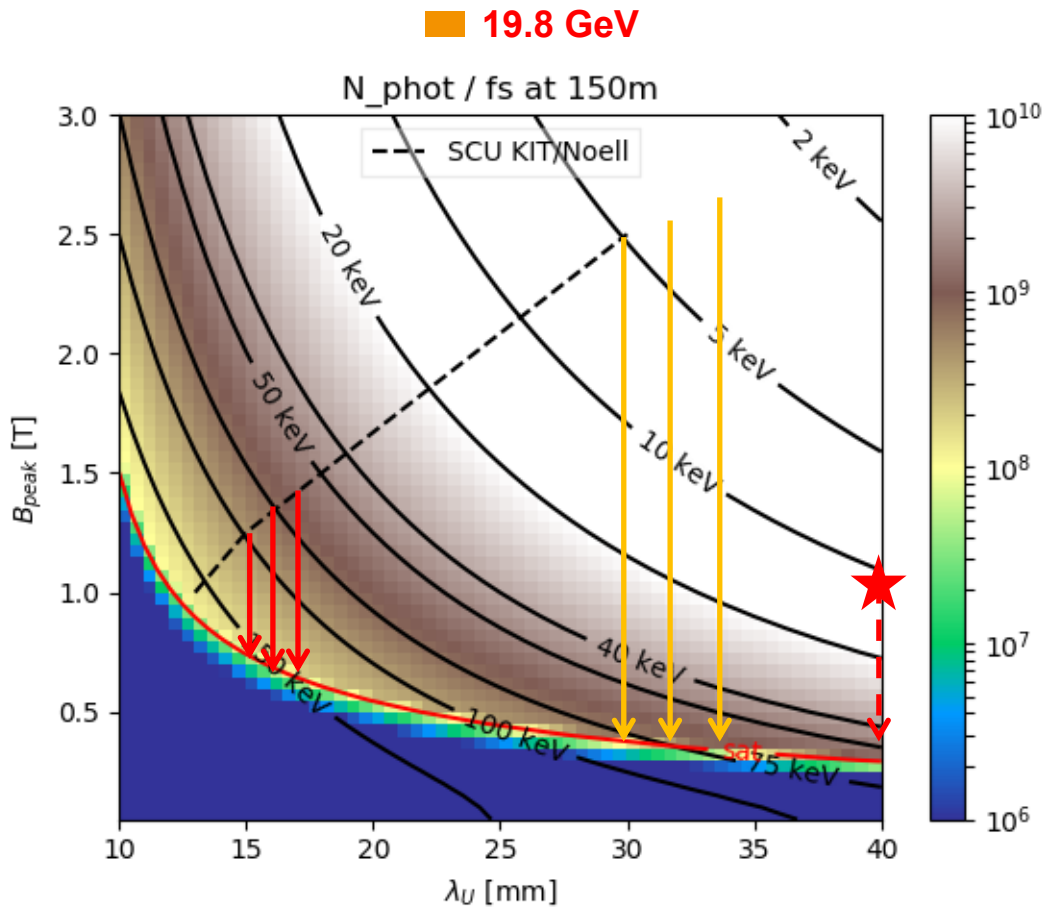
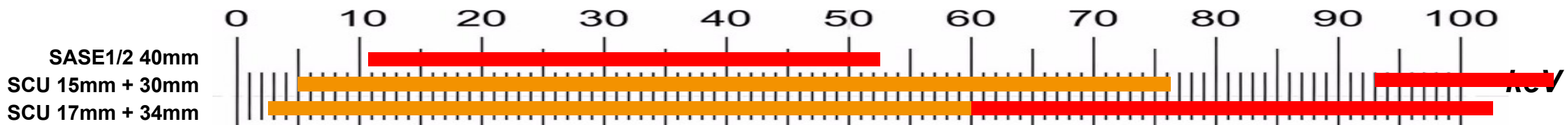


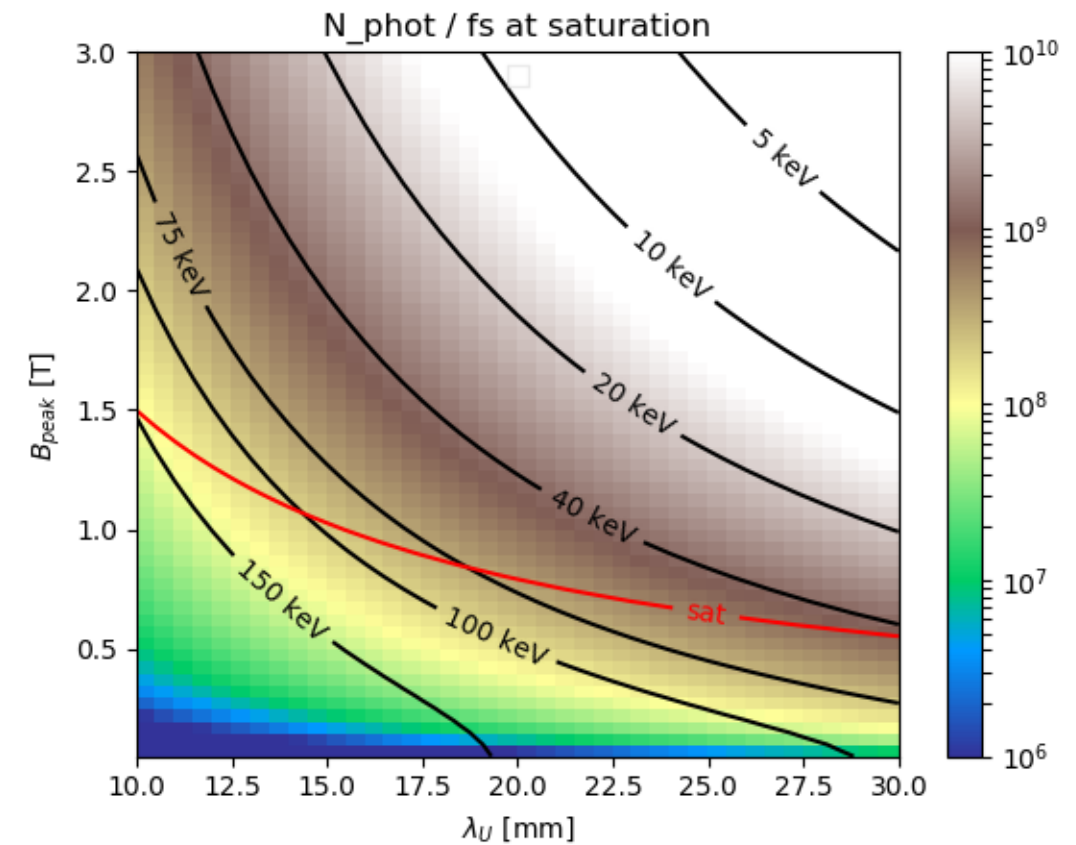
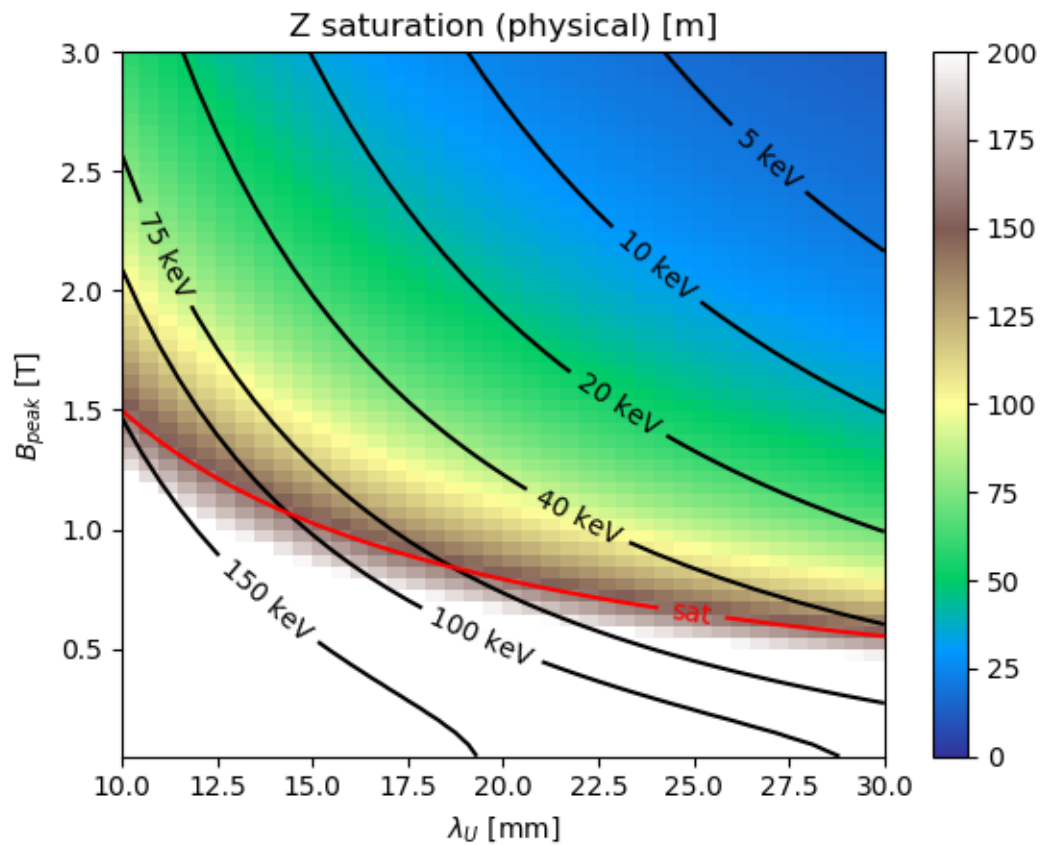
TABLE VI. Beam energy and DF estimated for the upgraded XFEL accelerator.

Operation mode	E_{beam} [GeV]	E_{acc} in ML [MV/m]	Beam-on DF [%]
sp (nominal)	19.8	23.4	0.6
cw	7.8	7.3	100
lp	10	10	53
lp	14	15	23

At optimistic electron energy and emittance parameters one can expect to reach beyond 100keV



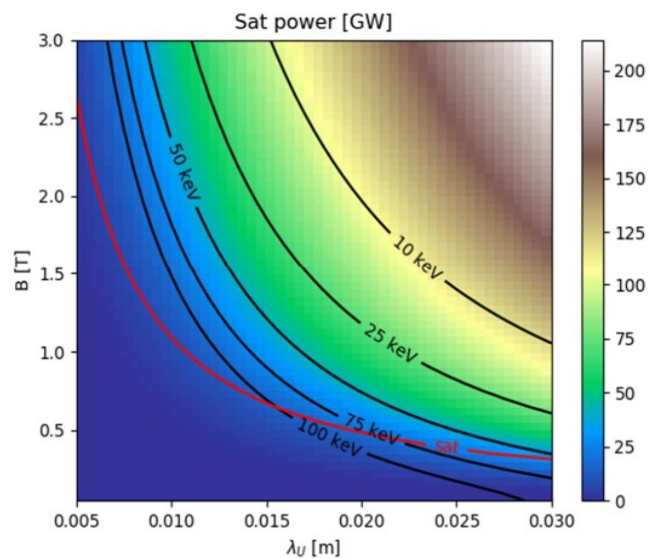
Saturation length and number of photons/femtosecond at saturation



Simplex vs Genesis

■ Good agreement

Ming Xie (SS) vs GENESIS

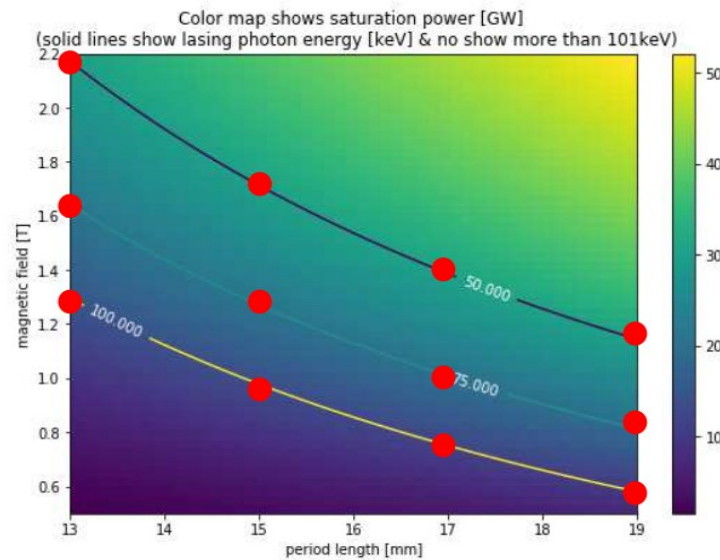


Peak saturation power simulated by GENESIS
(() indicates quantum effect considered)

Mag. Period \ Ph. Energy	50keV	75keV	100keV
13mm	28 GW (8)	17 GW (7)	16 GW (7)
15mm	27 GW (15)	18 GW (11)	13 GW (10)
17mm	27 GW (18)	18 GW (12)	Before satu.
19mm	28 GW (21)	Before satu.?	Before satu.

Ming Xie (TT) vs SIMPLEX

●: simulation point



Peak saturation power simulated by SIMPLEX
(() indicates averaged power)

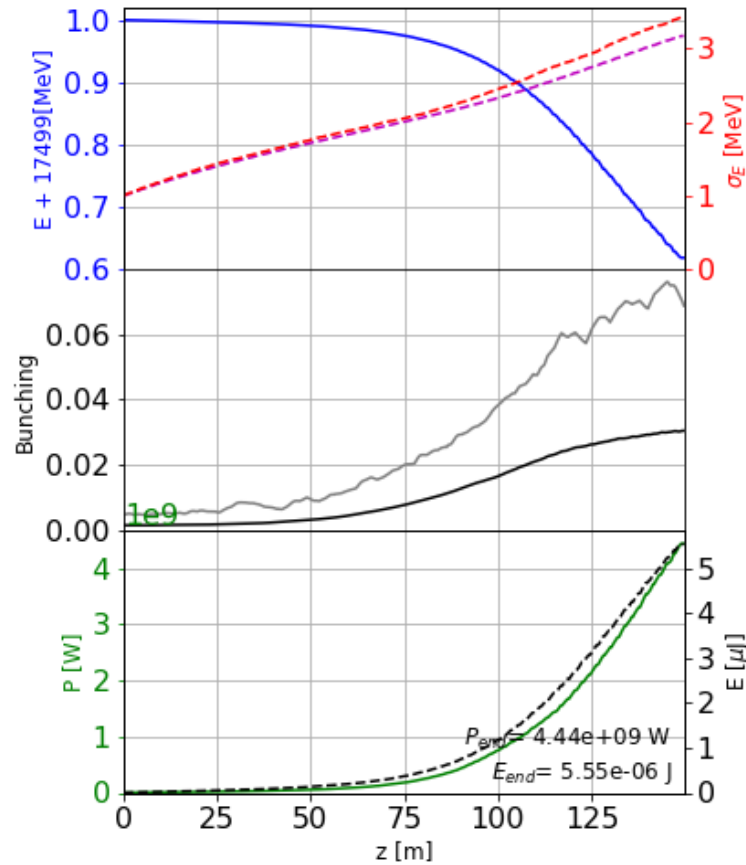
Mag. Period \ Ph. Energy	50keV	75keV	100keV
13mm	26 GW (11)	17 GW (8)	12 GW (4)
15mm	28 GW (11)	19 GW (8)	12 GW (5)
17mm	28 GW (11)	26 GW (7)	14 GW (4)
19mm	28 GW (10)	24 GW (7)	11 GW (3)

Planar vs Helical undulator: 100keV, 17.5 GeV, 15mm period, QF included

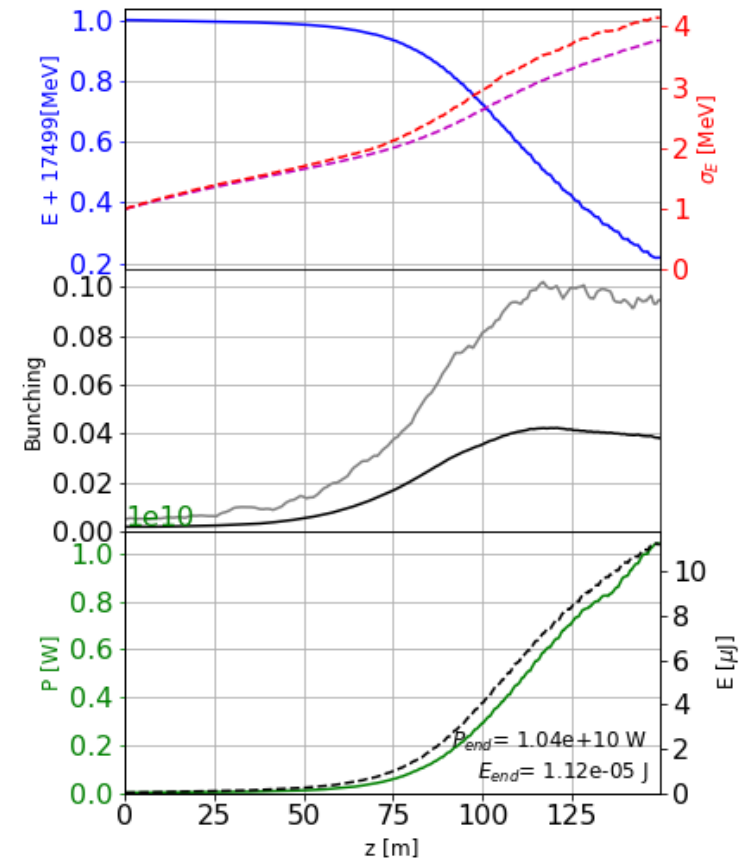
$K_{rms} = 0.97$

$Z_{sat}^{hel} / Z_{sat}^{pl}$
 $\sim (A_{jj}^{pl} / A_{jj}^{hel})^{2/3}$
 ~ 0.9

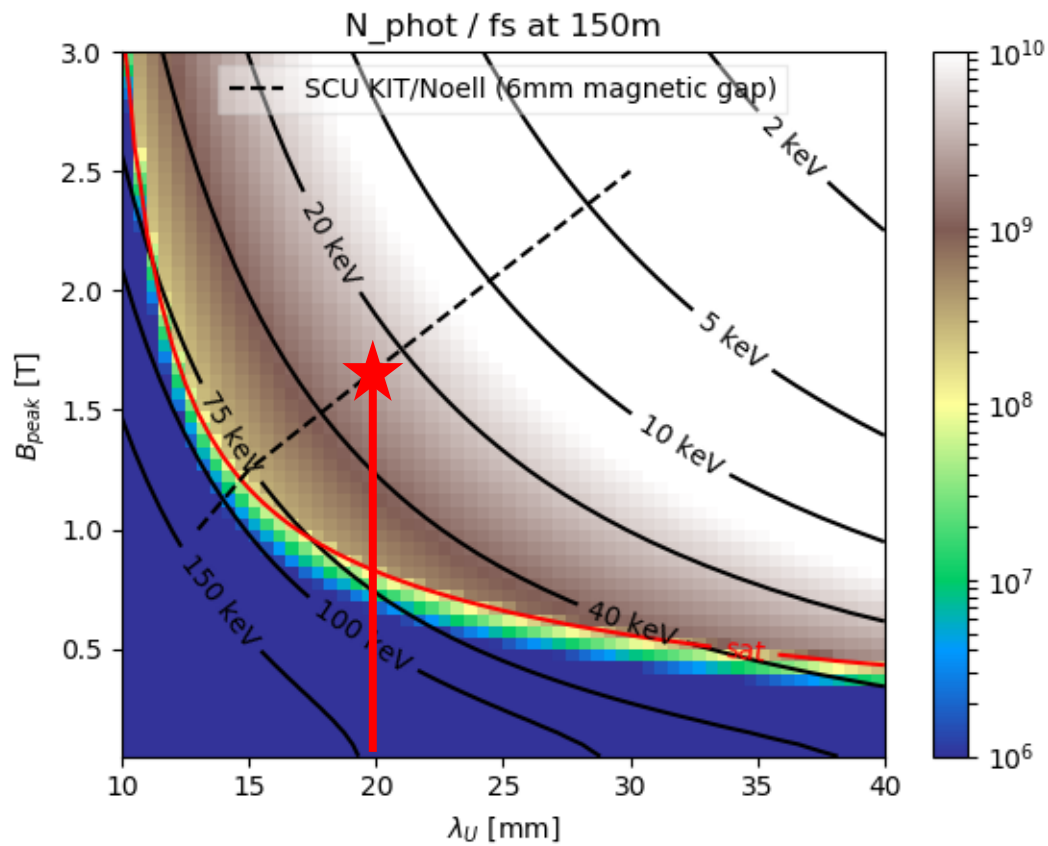
Planar



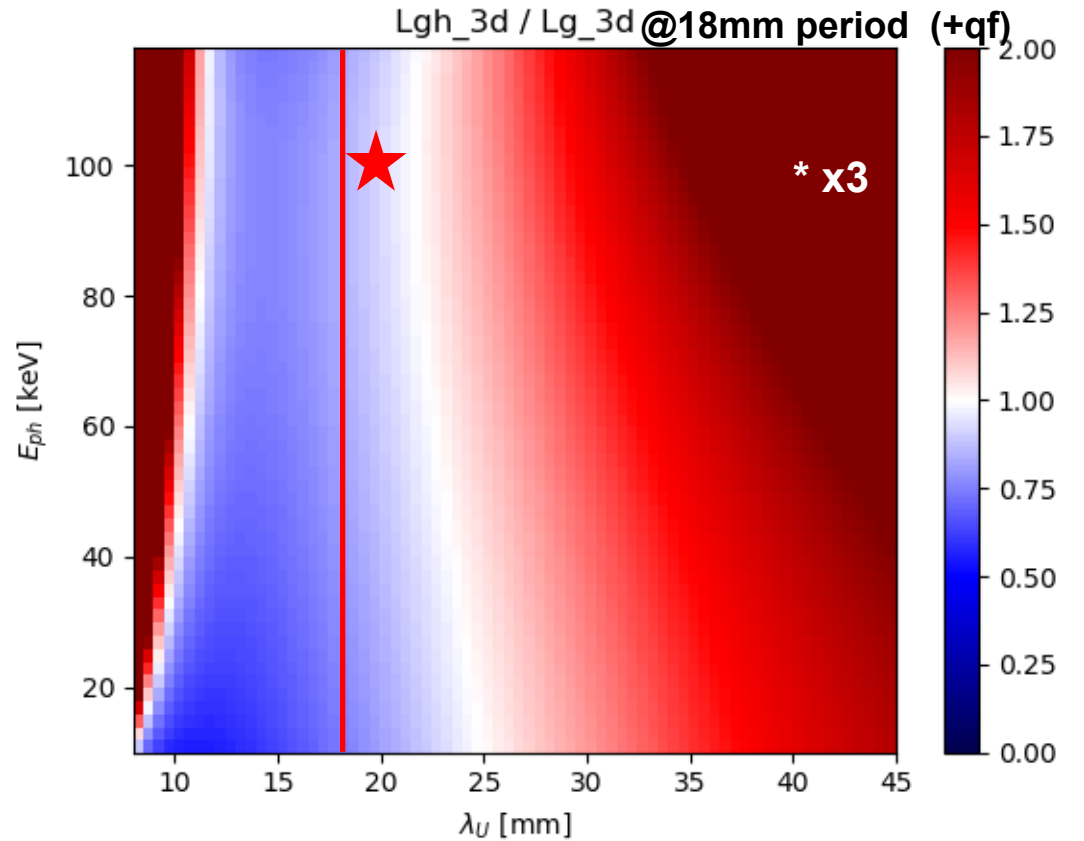
Helical



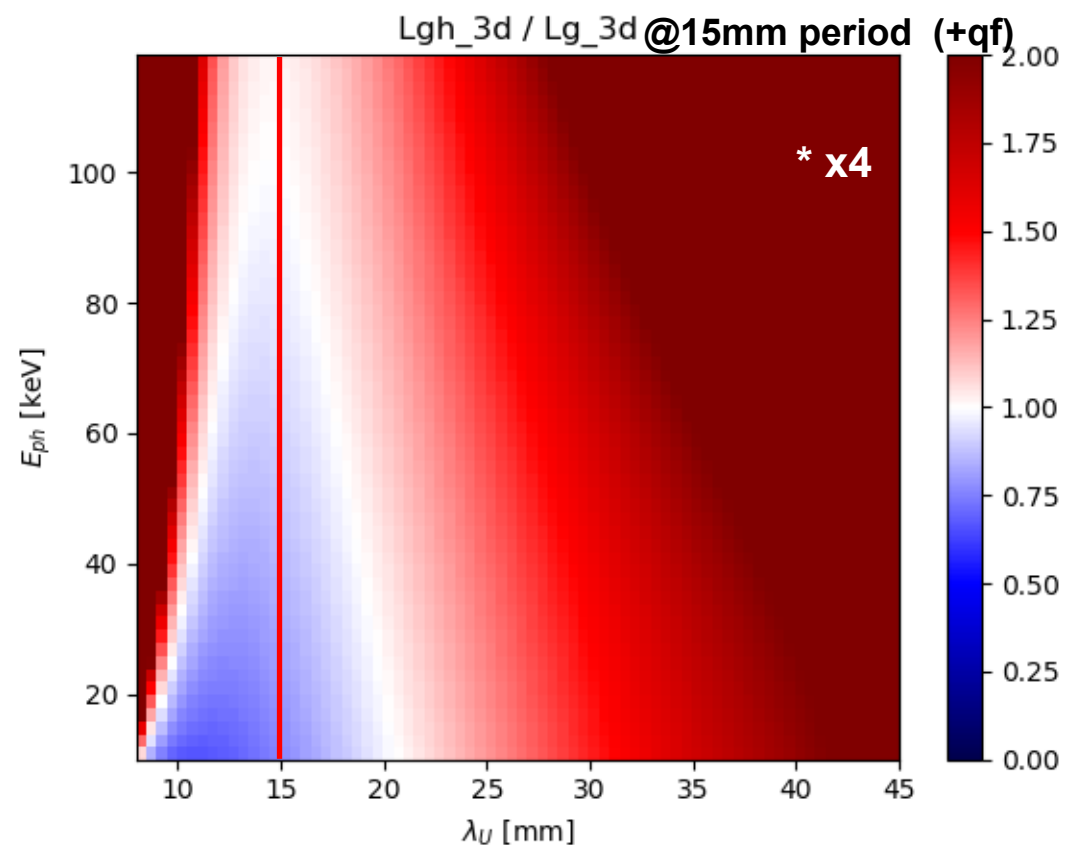
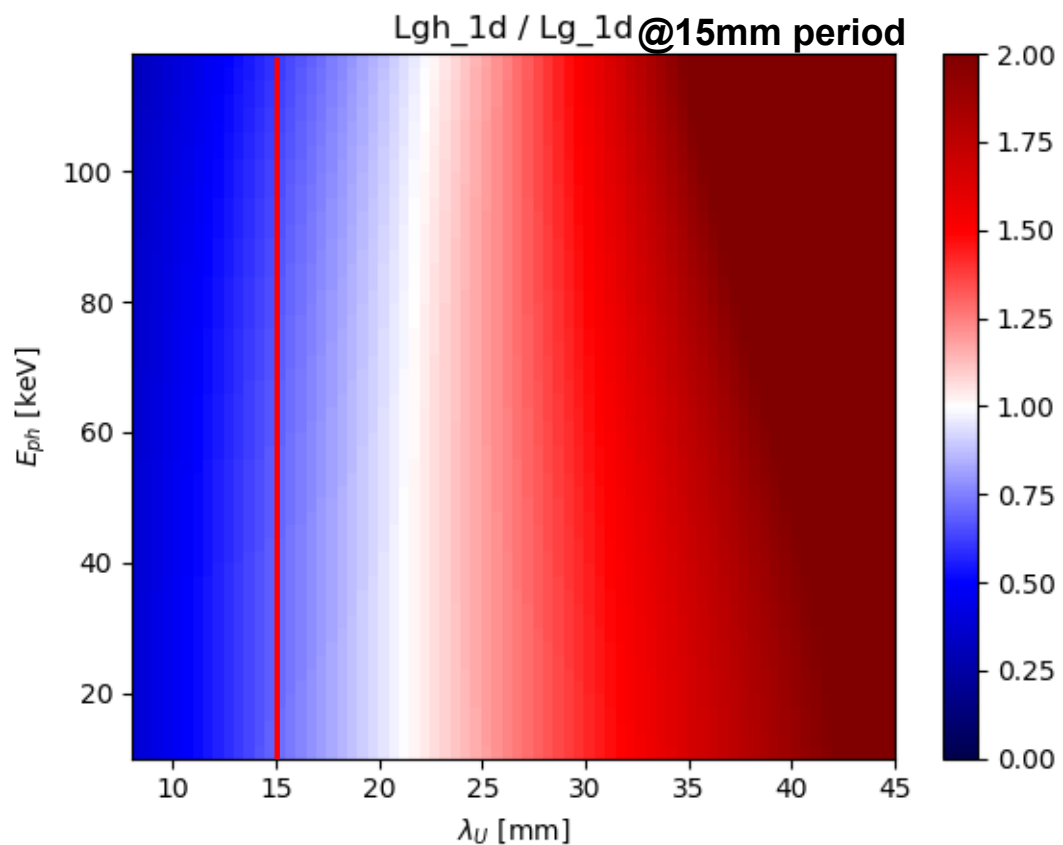
Comparison with harmonic lasing



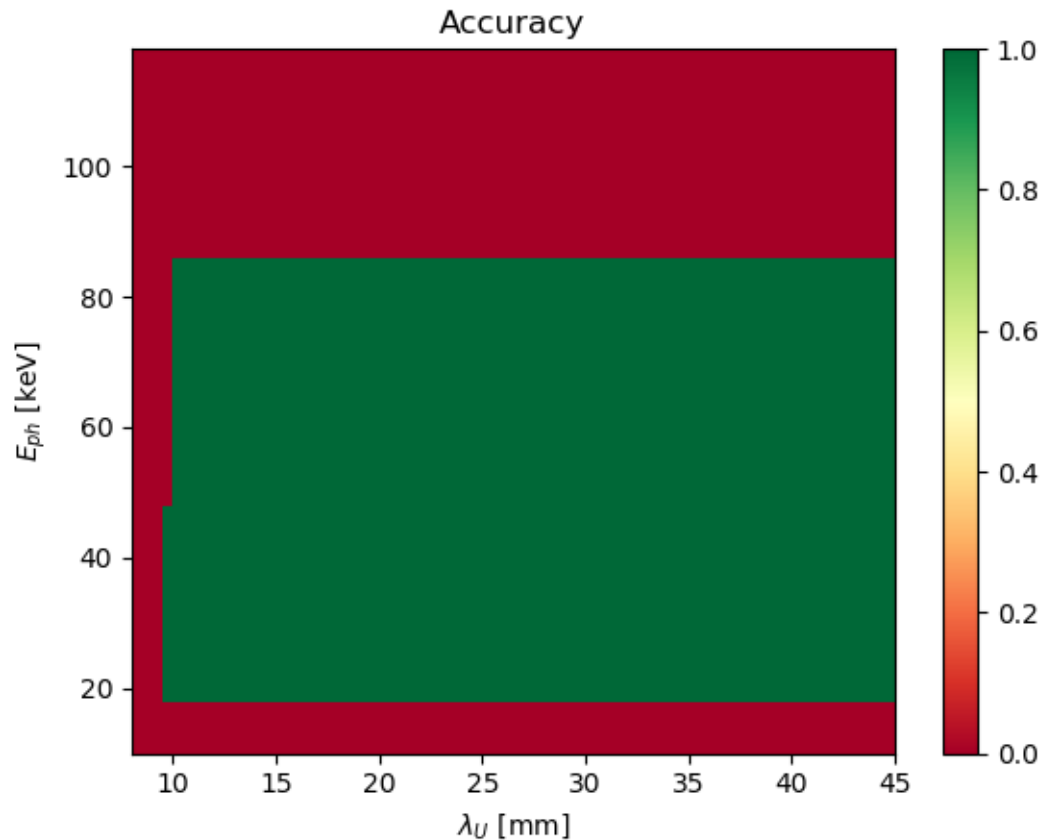
33*3=100



Comparison with harmonic lasing



Comparison with harmonic lasing



Phys. Rev. ST Accel. Beams **15**, 080702 (2012)

The formulas (3)–(5) provide an accuracy better than 5% in the range of parameters

$$1 < \frac{2\pi\epsilon}{\lambda_h} < 5, \quad (6)$$

$$\delta < 2.5 \left\{ 1 - \exp \left[-\frac{1}{2} \left(\frac{2\pi\epsilon}{\lambda_h} \right)^2 \right] \right\}. \quad (7)$$

In fact, the formulas (3)–(5) can also be used well beyond this range, but the above-mentioned accuracy is not guaranteed.

The 2018 Lessons of Radiation Doses on Undulators

Frederik Wolff-Fabris, Nov. 20th, 2018

27

■ SASE1/2 damage slides by Frederik Wolff-Fabris

■ Cell#27, 9.3keV

Using recent User Operation weeks

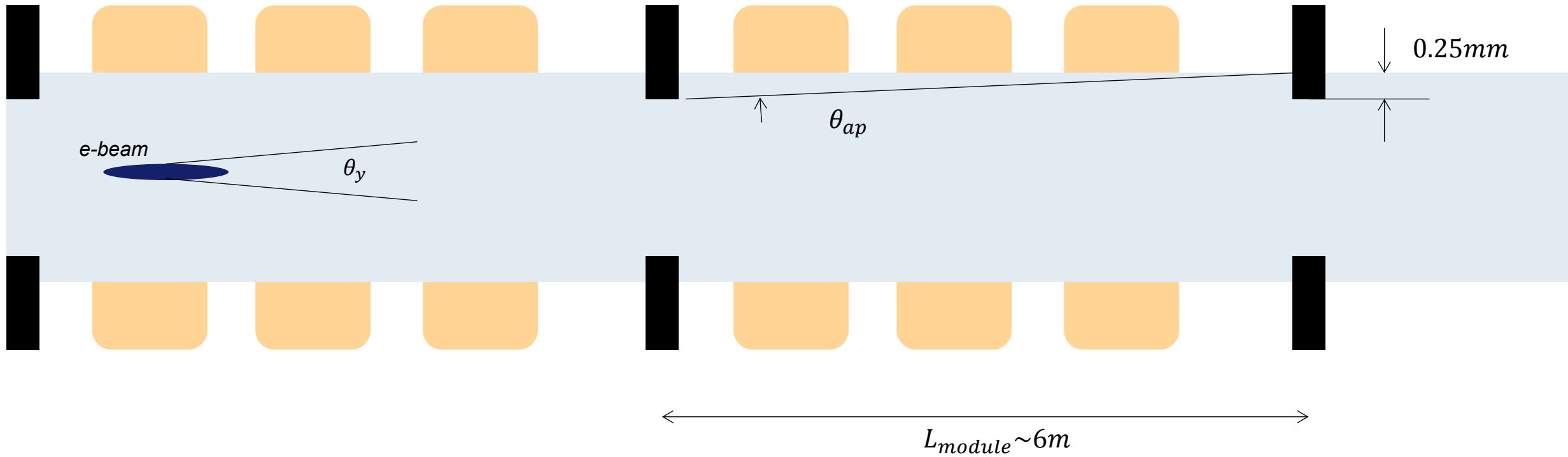
Using 1nC and not 0.25nC

Dose (Gy)	Charge (C)	Bunches	Time (weeks)	Time (weeks)	Time (weeks)
230	14.375	120	81	162-324	40.5-81
500	31.21	120	176	352-704	88-176
1000	62.42	120	352	704-1408	176-352
230	14.375	500	19.4	38.8-77.6	9.7-19.4
500	31.21	500	42.2	84.4-168.8	21.1-42.2
1000	62.42	500	84.4	168.8-337.6	42.2-84.4
230	14.375	1200	8.1	16.2-32.4	4.05-8.1
500	31.21	1200	17.6	35.2-70.4	8.8-17.6
1000	62.42	1200	35.2	70.4-140.8	17.6-35.2
230	14.375	2700	3.6	7.2-14.4	1.8-3.6
500	31.21	2700	7.8	15.6-30.2	3.9-7.8
1000	62.42	2700	15.6	31.2-62.4	7.8-15.6

■ ■ ■ European XFEL

■ ■ ■ European XFEL

SR heating handled with apertures



■ $\theta_{rad}^y \sim \frac{1}{\gamma} = \frac{1}{35000} \sim 30\mu rad$

■ $\theta_{rad}^x = K\theta_{rad}^y$

■ $\theta_{ap}^{xy} = \frac{250\mu m}{6m} \sim 40\mu rad$

SPECTRA – Wiggler model

SPECTRA 10.1 - D:\proj\Mid-term XFEL upgrades\Super-X\Heat_issues_SR\Super-X_wig.prm

File Select Calculation Run Utility Configuration Help

Accelerator Specification

Linac

Bunch Profile: Gaussian Injection Condition: Default

Electron Energy (GeV)	17.5	Energy Spread	0.0000584
Average Current (mA)	2.5e-07	β_x (m)	30
Pulses/sec	1	β_y (m)	30
σ_z (mm)	6	η_x (m)	0
Bunch Charge (nC)	0.25	η_y (m)	0
Peak Current (A)	4.98333	$1/\gamma$ (mrad)	0.0291999
Natural Emittance (m.rad)	9e-12	σ_x (mm)	0.01162
Coupling Constant	1	σ_y (mm)	0.01162
ϵ_x (m.rad)	4.5e-12	$\gamma\sigma_x'$	0.01326
ϵ_y (m.rad)	4.5e-12	σ_x' (mrad)	3.873e-04
		σ_y' (mrad)	3.873e-04
		$\gamma\sigma_y'$	0.01326

Light Source Description

Wiggler

Link Gap & Field

Gap Value	20	σ_{rx} (mm)	0.01021	σ_{rx}' (mrad)	0.01772
B(T)	0.898905	σ_{ry} (mm)	0.01003	σ_{ry}' (mrad)	0.01742
Periodic Length (cm)	1.5	Σ_x (mm)	0.01547	Σ_x' (mrad)	0.01773
Total Length (m)	2.0	Σ_y (mm)	0.01535	Σ_y' (mrad)	0.01743
Number of Periods	133	Critical Energy (eV)	183074		
K Value	1.259	Critical Wavelength (nm)	0.00677234		
		Total Power (kW)	7.80869e-08		

SPECTRA – Wiggler model – far zone calculation

Spatial Dependence (Along Axis) - Power Density

Observation

Observation Point in Angle

Distance from the Source (m) 30

$\Sigma_{px'}$ (mrad) 0.0276495

$\Sigma_{py'}$ (mrad) 0.0206547

Minimum θ_x (mrad) -0.07

Maximum θ_x (mrad) 0.07

Mesh x 101

Minimum θ_y (mrad) -0.07

Maximum θ_y (mrad) 0.07

Mesh y 101

Filtering Generic Filter

Numerical Conditions

Zero Emittance

Accuracy Level 3

Output File Settings

Print Header

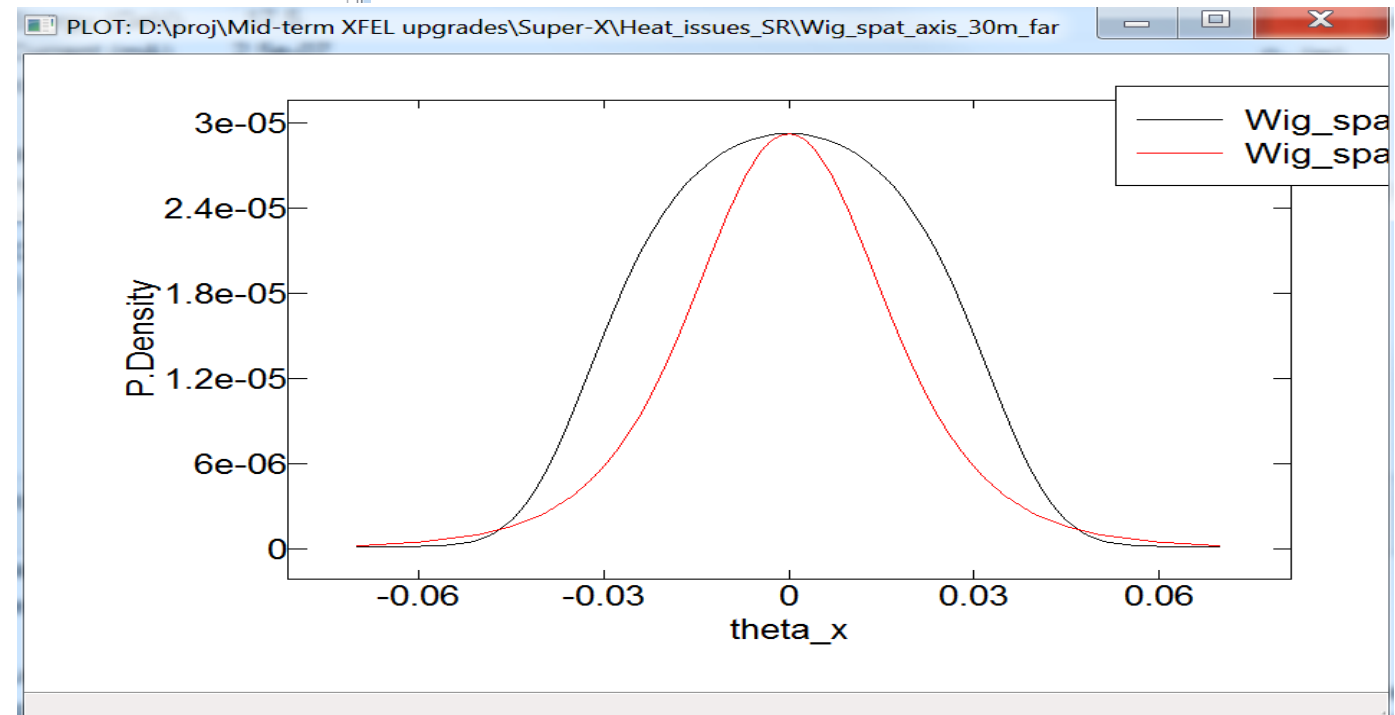
Print Unit

Suffix (X Axis) dtx

Suffix (Y Axis) dty

Target Item	Unit
Power Density	kW/mrad ²

- $R = \theta_x \cdot \text{Distance from source}$
- Source is in the MIDDLE of the ID



SPECTRA – Wiggler model – near zone calculation (2.2 m from source)

Near Field: Spatial Dependence (Along Axis) - Power Density

Observation Point in Angle

Distance from the Source (m) 2.2

Σ_{px} (mrad) 0.0281467

Σ_{py} (mrad) 0.0213157

Minimum θ_x (mrad) -0.06

Maximum θ_x (mrad) 0.06

Mesh x 51

Minimum θ_y (mrad) -0.06

Maximum θ_y (mrad) 0.06

Mesh y 51

Numerical Conditions

Zero Emittance

Accuracy Level 3

Output File Settings

Print Header

Print Unit

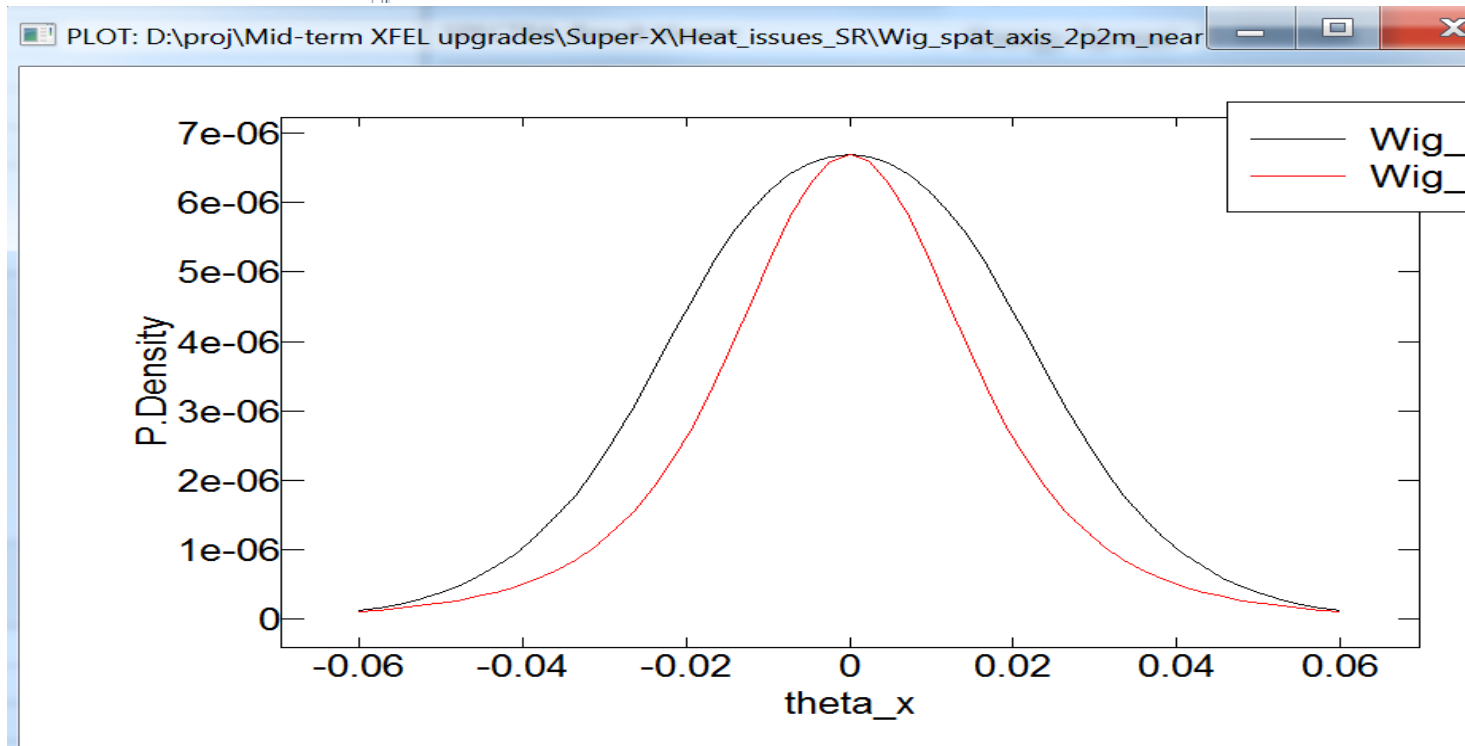
Suffix (X Axis) dtx

Suffix (Y Axis) dty

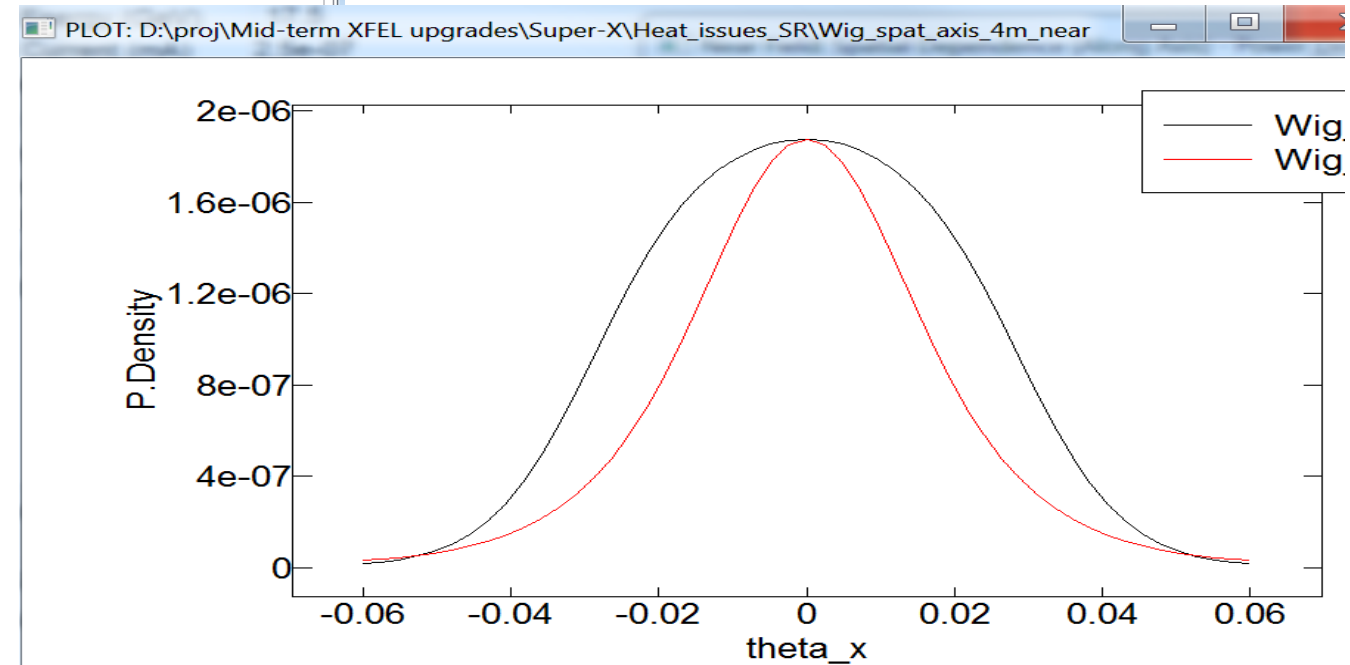
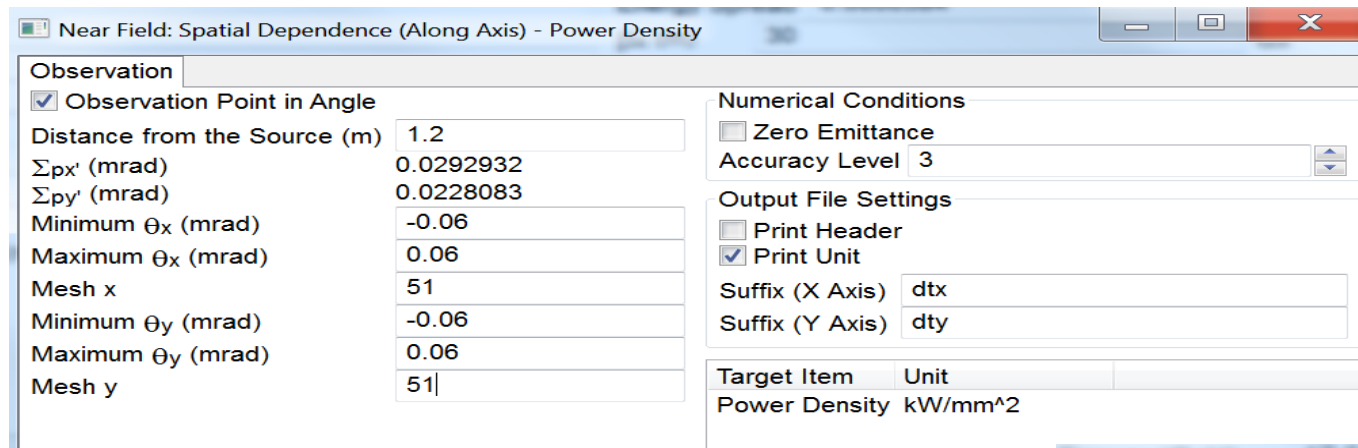
Target Item Unit

Power Density kW/mm²

- R=Theta_x*Distance from source
- In kW/mm² → (2.2)²=4.84 wrt previous

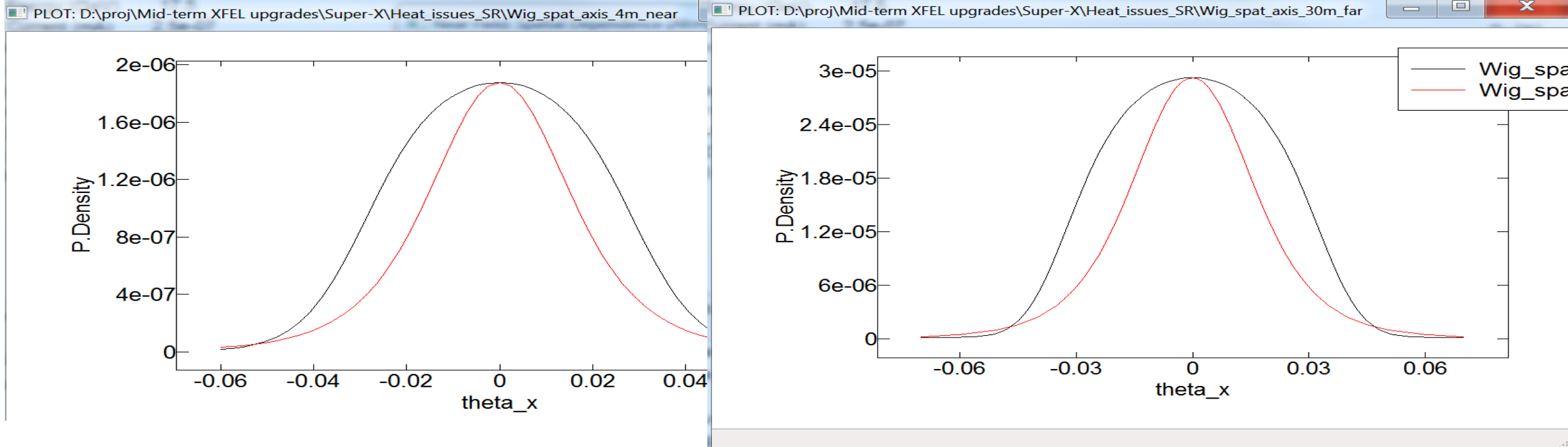


SPECTRA – Wiggler model – near zone calculation (4 m from source)

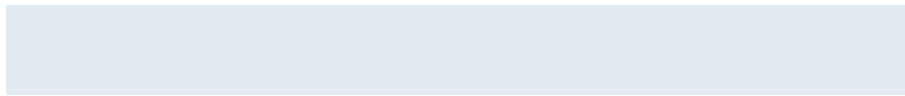


- R=Theta_x*Distance from source
- In kW/mm² → (4)²=16 wrt previous

Receipt



■ Since not too much difference after a couple of meters use the following model:



Undulator of variable length L_w

SPECTRA – Undulator model

SPECTRA 10.1 - D:\proj\Mid-term XFEL upgrades\Super-X\Heat_issues_SR\Super-X_undu.prm

File Select Calculation Run Utility Configuration Help

Accelerator Specification

Linac

Bunch Profile: **Gaussian** Injection Condition: **Default**

Electron Energy (GeV)	17.5	Energy Spread	0.0000584		
Average Current (mA)	2.5e-07	β_x (m)	30	α_x	0
Pulses/sec	1	β_y (m)	30	α_y	0
σ_z (mm)	6	η_x (m)	0	η_x'	0
Bunch Charge (nC)	0.25	η_y (m)	0	η_y'	0
Peak Current (A)	4.98333	$1/\gamma$ (mrad)	0.0291999		
Natural Emittance (m.rad)	9e-12	σ_x (mm)	0.01162	σ_x' (mrad)	3.873e-04
Coupling Constant	1	σ_y (mm)	0.01162	σ_y' (mrad)	3.873e-04
ϵ_x (m.rad)	4.5e-12	$\gamma\sigma_x'$	0.01326	$\gamma\sigma_y'$	0.01326
ϵ_y (m.rad)	4.5e-12				

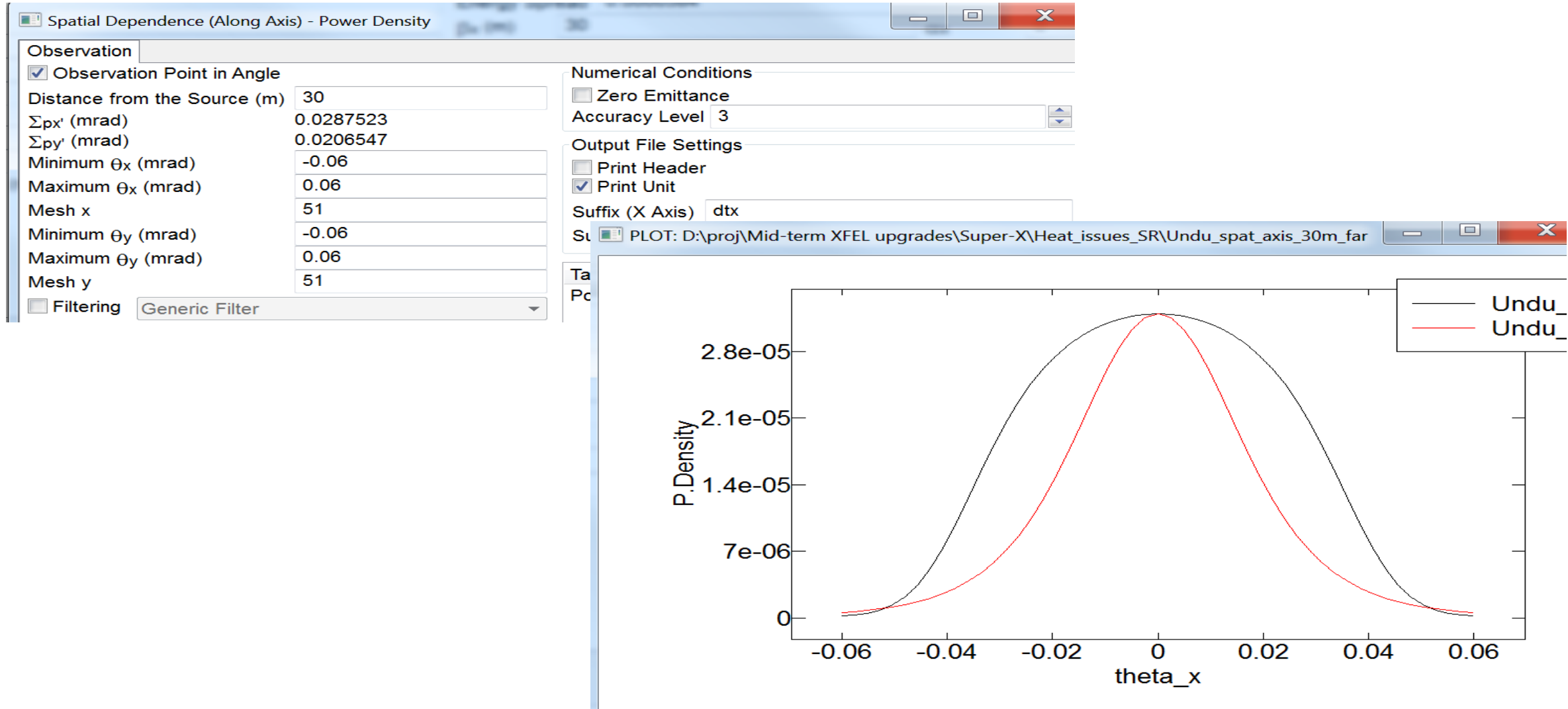
Light Source Description

Linear Undulator

Link Gap & Field
 Segmented Undulator
 Special Magnet Setup

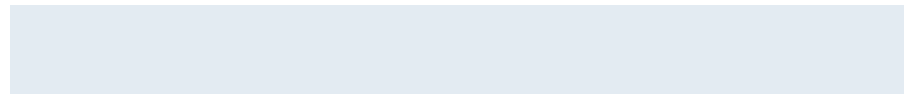
Gap Value	20	σ_r (mm)	5.597e-04	σ_r' (mrad)	1.763e-03
B(T)	0.978157	Σ_x (mm)	0.01163	Σ_x' (mrad)	1.805e-03
Periodic Length (cm)	1.5	Σ_y (mm)	0.01163	Σ_y' (mrad)	1.805e-03
Total Length (m)	2.0	λ_{1st} (nm)	0.012396		
Number of Periods	133	ϵ_{1st} (peak:eV)	100005		
K Value	1.37	ϵ_{3rd} (peak:eV)	300008		
ϵ_{1st} (eV)	100020	Flux _{1st}	1.72445e+06		
		Brilliance _{1st}	9.91211e+13		
		Peak Brilliance	1.97581e+24		
		Bose Degeneracy	0.00156919		
		Total Power (kW)	9.2463e-08		

SPECTRA – Undulator model – far-zone calculation



Therefore:

- No big difference between undulator and wiggler model
- Far zone starts to be ok for a distance a few times the ID length
- Use wiggler model, far zone
- Assume e.g. 5m from the exit of a wiggler of variable length
- Study as a function of the wiggler length

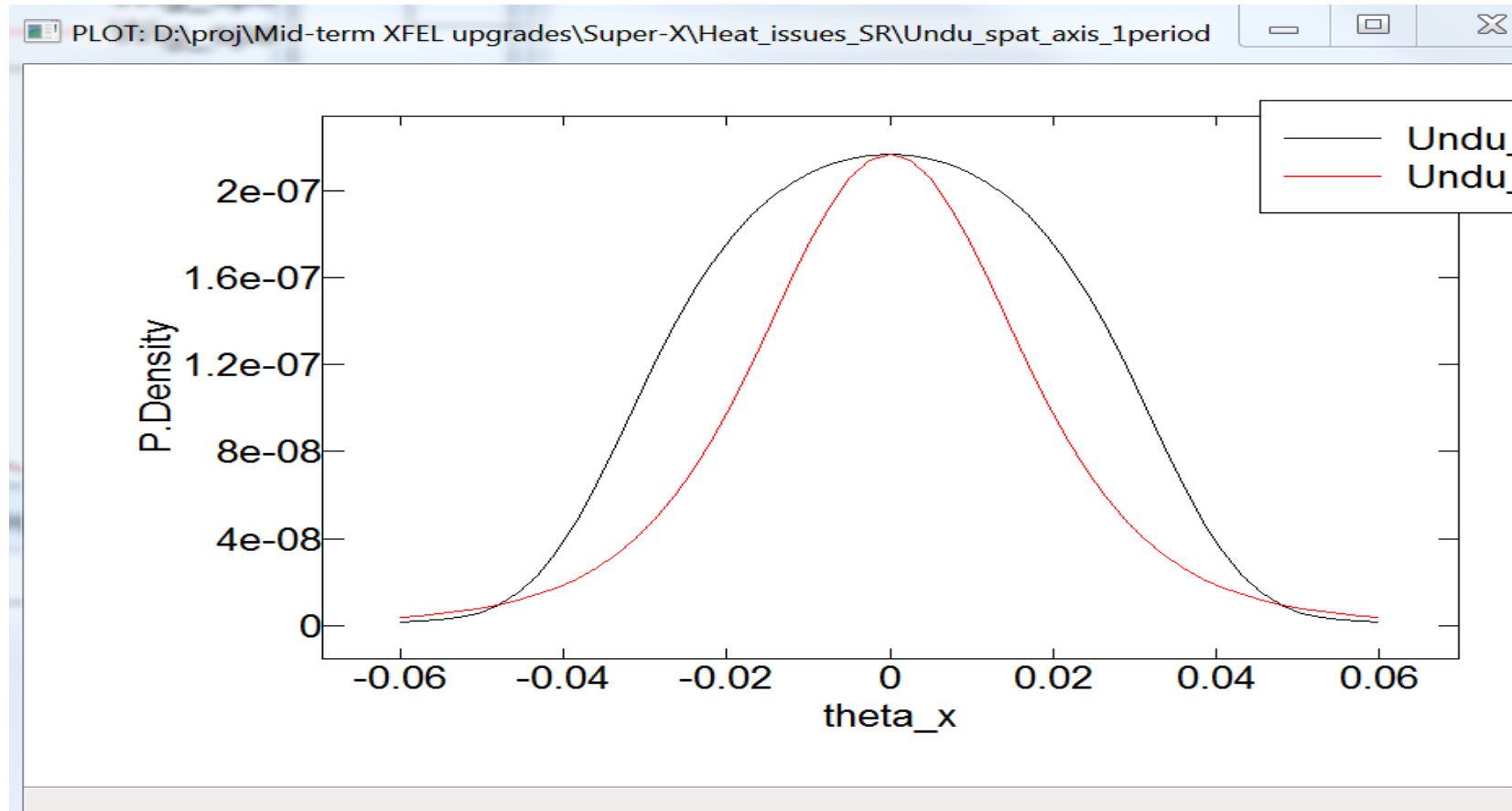


Undulator of variable length L_w



Observation position fixed at 5 m from the exit

Selecting 1 period just divides the full flux by #periods



File Select Calculation Run Utility Configuration Help

Accelerator Specification

Linac

Bunch Profile: **Gaussian** Injection Condition: **Default**

Electron Energy (GeV)	17.5	Energy Spread	0.0000584
Average Current (mA)	2.5e-07	β_x (m)	30
Pulses/sec	1	β_y (m)	30
σ_z (mm)	6	η_x (m)	0
Bunch Charge (nC)	0.25	η_y (m)	0
Peak Current (A)	4.98333	$1/\gamma$ (mrad)	0.0291999
Natural Emittance (m.rad)	9e-12	σ_x (mm)	0.01162
Coupling Constant	1	σ_y (mm)	0.01162
ϵ_x (m.rad)	4.5e-12	$\gamma\sigma_x'$	0.01326
ϵ_y (m.rad)	4.5e-12	σ_x' (mrad)	3.873e-04
		σ_y' (mrad)	3.873e-04
		$\gamma\sigma_y'$	0.01326

Light Source Description

Wiggler

Link Gap & Field

Gap Value	20	σ_{rx} (mm)	1.415e-04	σ_{rx}' (mrad)	0.01772
B(T)	0.898905	σ_{ry} (mm)	8.153e-05	σ_{ry}' (mrad)	0.01742
Periodic Length (cm)	1.5				
Total Length (m)	0.015				
Number of Periods	1				
K Value	1.259				

Spatial Dependence (Mesh: x-y) - Power Density

Observation

Observation Point in Angle

Distance from the Source (m)

$\Sigma_{px'}$ (mrad)

$\Sigma_{py'}$ (mrad)

Minimum θ_x (mrad)

Maximum θ_x (mrad)

Mesh x

Minimum θ_y (mrad)

Maximum θ_y (mrad)

Mesh y

Filtering

Numerical Conditions

Zero Emittance

Accuracy Level

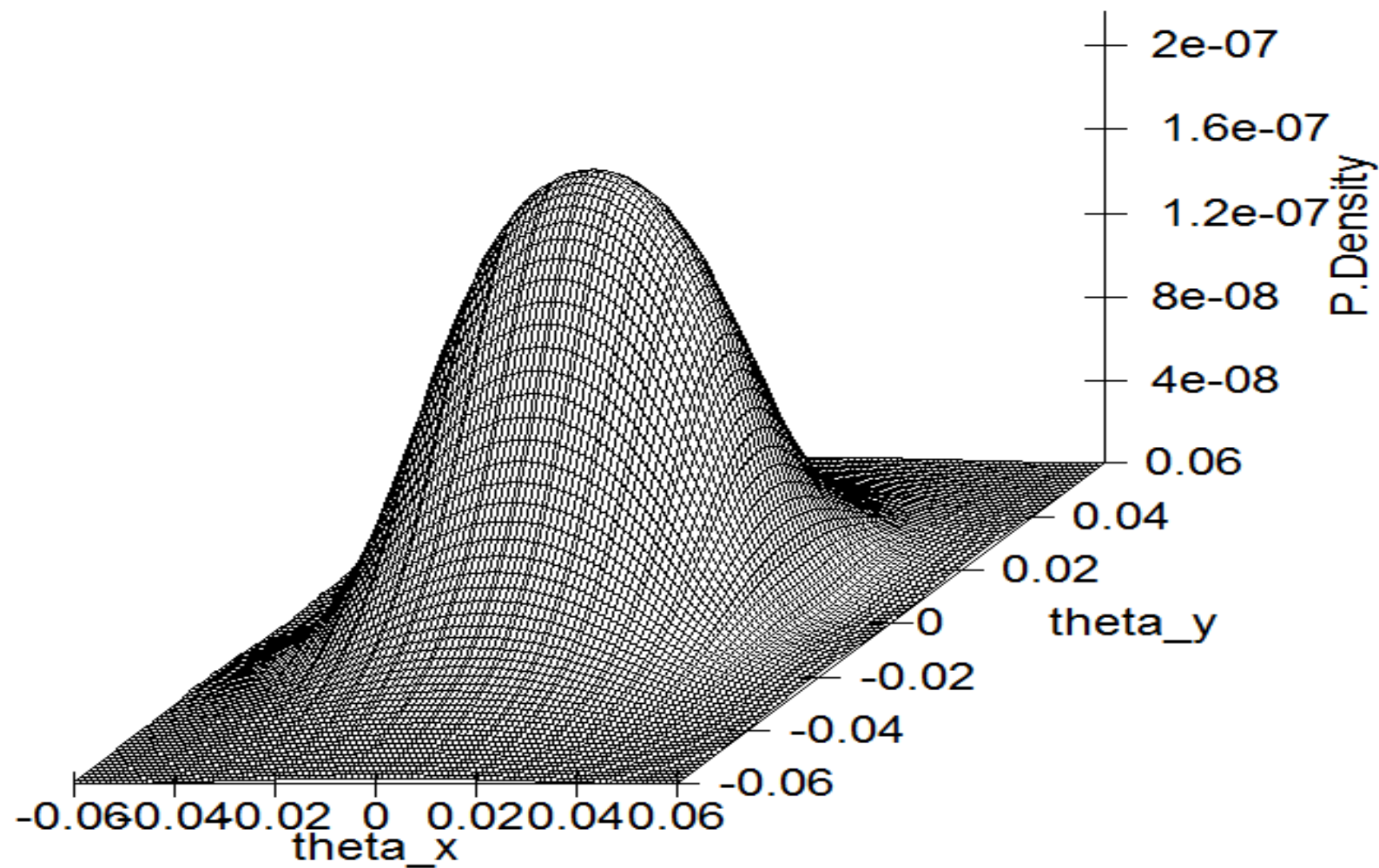
Output File Settings

Print Header

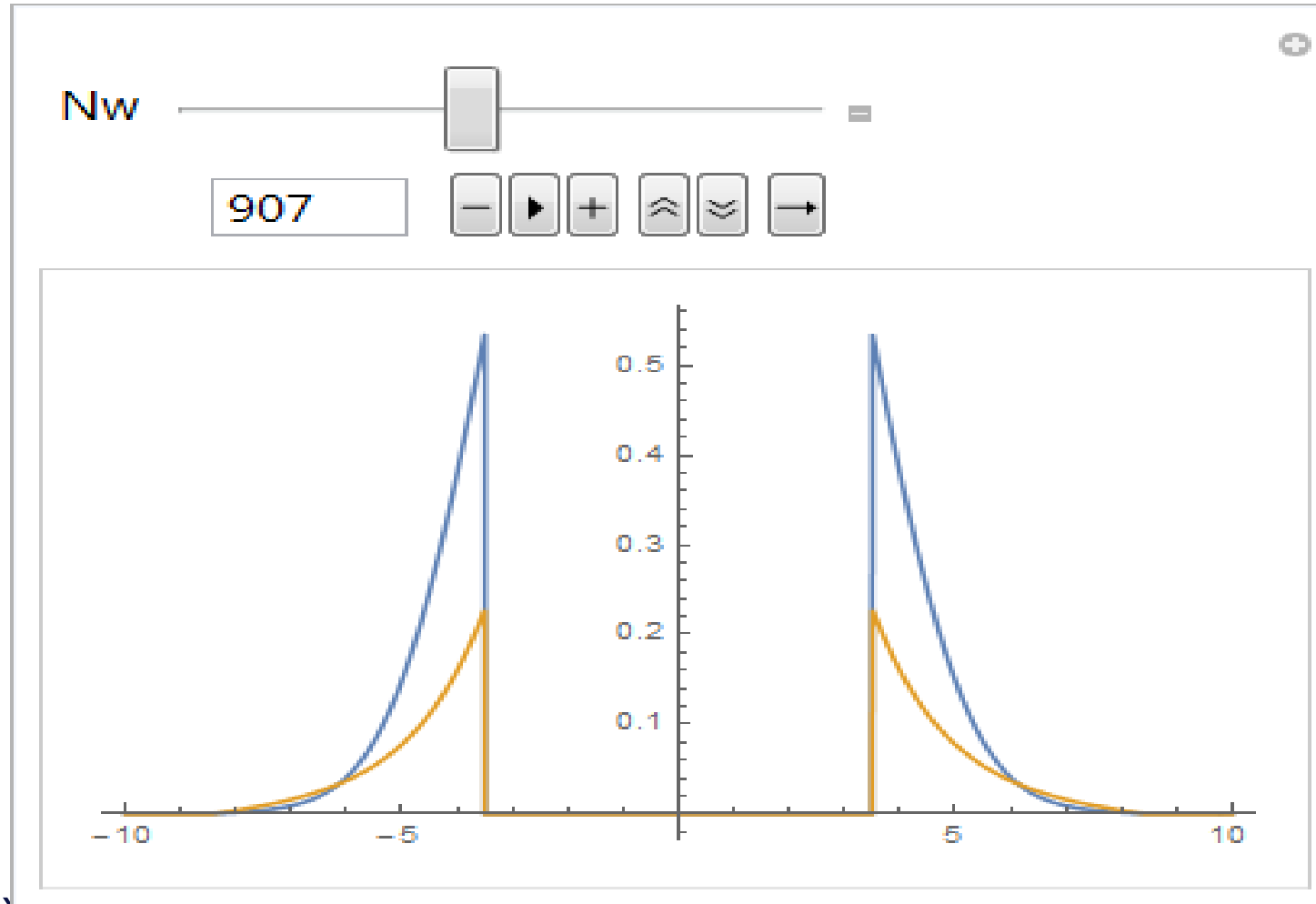
Print Unit

Suffix

Target Item	Unit
Power Density	kW/mrad^2



Example after about 907 periods (see Analysis.nb)



Harmonic Lasing Basic Fitting Formulas

Harmonic Lasing Basic Fitting Formulas

PHYSICAL REVIEW SPECIAL TOPICS - ACCELERATORS AND BEAMS **15**, 080702 (2012)

Harmonic lasing in x-ray free electron lasers

E. A. Schneidmiller* and M. V. Yurkov

$L_g \simeq L_{g0}(1 + \delta)$ Field gain length

$$L_{g0} = 1.67 \left(\frac{I_A}{I} \right)^{1/2} \frac{(\epsilon_n \lambda_w)^{5/6} (1 + K^2)^{1/3}}{\lambda_h^{2/3} h^{5/6} K A_{JJh}}$$

$$\delta = 131 \frac{I_A}{I} \frac{\epsilon_n^{5/4}}{\lambda_h^{1/8} \lambda_w^{9/8}} \frac{h^{9/8} \sigma_\gamma^2}{(K A_{JJh})^2 (1 + K^2)^{1/8}}$$

$$A_{JJh}(K) = J_{(h-1)/2} \left(\frac{hK^2}{2(1 + K^2)} \right) - J_{(h+1)/2} \left(\frac{hK^2}{2(1 + K^2)} \right)$$

$$\beta_{\text{opt}} \simeq 11.2 \left(\frac{I_A}{I} \right)^{1/2} \frac{\epsilon_n^{3/2} \lambda_w^{1/2}}{\lambda_h h^{1/2} K A_{JJh}} (1 + 8\delta)^{-1/3}$$

$$L_g(\beta) \simeq L_g(\beta_{\text{opt}}) \left[1 + \frac{(\beta - \beta_{\text{opt}})^2 (1 + 8\delta)}{4\beta_{\text{opt}}^2} \right]^{1/6} \quad \text{for } \beta > \beta_{\text{opt}}.$$

$$2\pi \frac{\epsilon}{\lambda} > 1$$

Harmonic Lasing vs. SCU

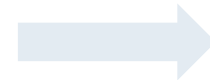
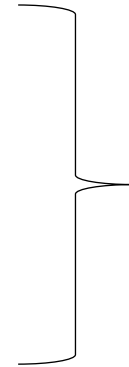
Target Wavelength $\lambda_t = \lambda_w \frac{1 + K^2}{2\gamma^2}$

$\lambda_t = \lambda_h$ fixed

γ fixed

λ_w variable

K (*rms*) variable



$\lambda_w(1 + K^2) = \text{constant}$

- Note the difference with the “retuning” case, where the period is fixed too (see PRSTAB 15, 080702 Appendix A)

Therefore

$$\lambda_{wh}(1 + K_h^2) = \lambda_{wSC}(1 + K_{SC}^2)$$

Index “h” → Harmonic lasing

Index “SC” → Superconducting Undulator

Harmonic Lasing vs. SCU

~~$$\lambda_{wh}(1 + K_h^2) = \lambda_{wSC}(1 + K_{SC}^2)$$~~

~~$$L_{g0SC} = 1.67 \left(\frac{I_A}{I} \right)^{1/2} \frac{(\epsilon_n \lambda_{wSC})^{5/6} (1 + K_{SC}^2)^{1/3}}{\lambda_t^{2/3} K A_{JJSC}}$$~~

~~$$L_{g0h} = 1.67 \left(\frac{I_A}{I} \right)^{1/2} \frac{(\epsilon_n \lambda_{wh})^{5/6} (1 + K_h^2)^{1/3}}{\lambda_t^{2/3} h^{5/6} K A_{JJh}}$$~~

~~$$\frac{L_{g0h}}{L_{g0SC}} = \frac{\lambda_{wh}^{1/2} K_{SC} A_{JJSC}}{h^{5/6} K_h A_{JJh} \lambda_{wSC}^{1/2}}$$~~

Harmonic Lasing vs. SCU

Get the K for SC and HL case

$$K_{sc} = \frac{\sqrt{2 \gamma^2 \lambda_{target} - \lambda_{usc}}}{\sqrt{\lambda_{usc}}}; \quad K_h = \frac{\sqrt{2 h \gamma^2 \lambda_{target} - \lambda_{uh}}}{\sqrt{\lambda_{uh}}};$$

Use the above expressions with

$$\frac{L_{g0h}}{L_{g0SC}} = \frac{\lambda_{wh}^{1/2} K_{SC} A_{JJSC}}{h^{5/6} K_h A_{JJh} \lambda_{wSC}^{1/2}}$$

$$\text{FullSimplify} \left[h^{-5/6} \frac{\lambda_{uh}^{1/2} K_{sc}}{\lambda_{usc}^{1/2} K_h} \frac{(\text{BesselJ}[0, K_{sc}^2 / (2 + 2 K_{sc}^2)] - \text{BesselJ}[1, K_{sc}^2 / (2 + 2 K_{sc}^2)])}{(\text{BesselJ}[(h-1)/2, h K_h^2 / (2 + 2 K_h^2)] - \text{BesselJ}[(h+1)/2, h K_h^2 / (2 + 2 K_h^2)])} \right]$$

$$\frac{\lambda_{uh} \sqrt{2 \gamma^2 \lambda_{target} - \lambda_{usc}} \left(\text{BesselJ}\left[0, \frac{1}{2} - \frac{\lambda_{usc}}{4 \gamma^2 \lambda_{target}}\right] - \text{BesselJ}\left[1, \frac{1}{2} - \frac{\lambda_{usc}}{4 \gamma^2 \lambda_{target}}\right] \right)}{h^{5/6} \sqrt{2 h \gamma^2 \lambda_{target} - \lambda_{uh}} \lambda_{usc} \left(\text{BesselJ}\left[\frac{1}{2}(-1+h), \frac{h}{2} - \frac{\lambda_{uh}}{4 \gamma^2 \lambda_{target}}\right] - \text{BesselJ}\left[\frac{1+h}{2}, \frac{h}{2} - \frac{\lambda_{uh}}{4 \gamma^2 \lambda_{target}}\right] \right)}$$

Set the gain length ratio



`LOHdivLOSC[h_, λtarget_, λuh_, λusc_] =`

$$\frac{\lambda_{uh} \sqrt{2 \gamma^2 \lambda_{target} - \lambda_{usc}} \left(\text{BesselJ}\left[0, \frac{1}{2} - \frac{\lambda_{usc}}{4 \gamma^2 \lambda_{target}}\right] - \text{BesselJ}\left[1, \frac{1}{2} - \frac{\lambda_{usc}}{4 \gamma^2 \lambda_{target}}\right] \right)}{h^{5/6} \sqrt{2 h \gamma^2 \lambda_{target} - \lambda_{uh}} \lambda_{usc} \left(\text{BesselJ}\left[\frac{1}{2}(-1+h), \frac{h}{2} - \frac{\lambda_{uh}}{4 \gamma^2 \lambda_{target}}\right] - \text{BesselJ}\left[\frac{1+h}{2}, \frac{h}{2} - \frac{\lambda_{uh}}{4 \gamma^2 \lambda_{target}}\right] \right)}$$

Harmonic Lasing vs. SCU

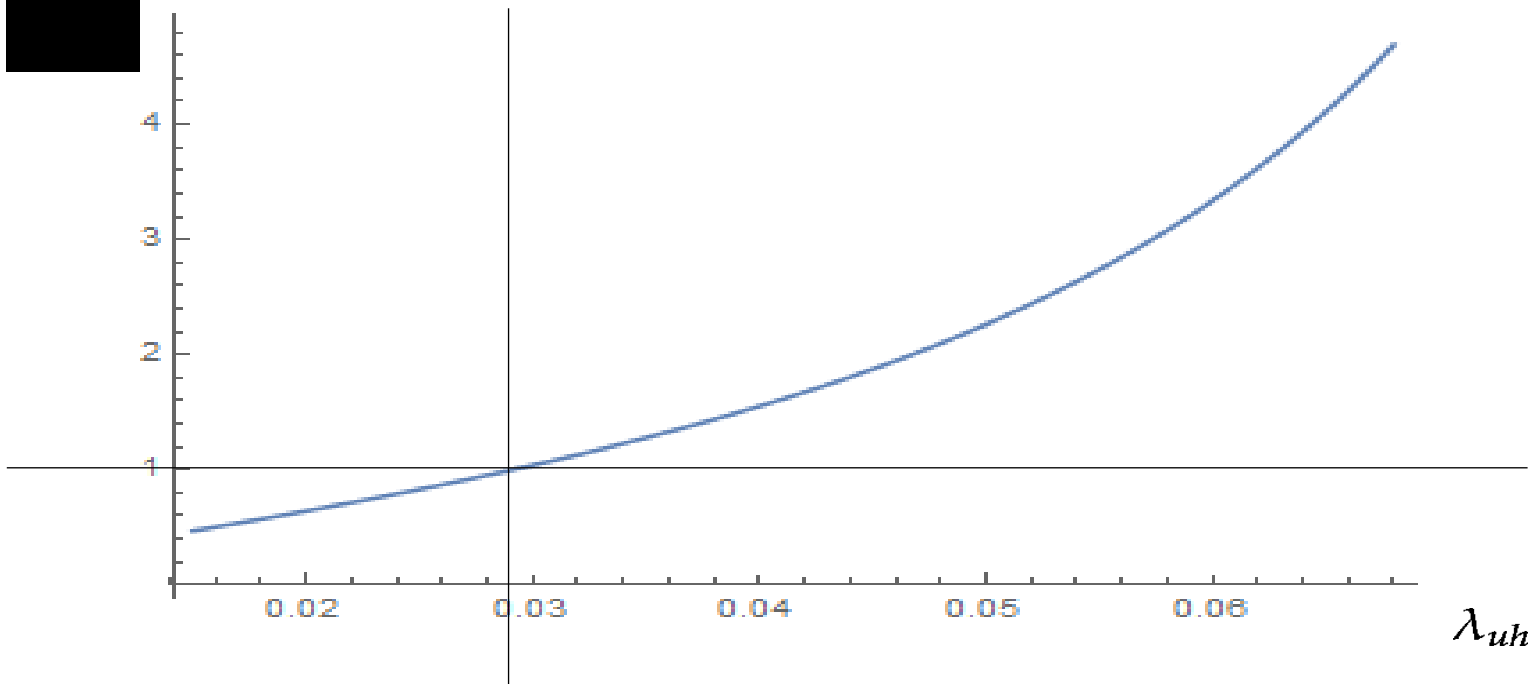
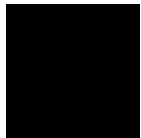
So we indicated with `LOHdivLOSC[h_, λtarget_, λuh_, λusc_]` the ratio



Now set

`λtarget = 0.0155 * 10-9` `γ = 17500 / 0.511` `h = 3`

`λusc = 0.015` 15mm period SCU!



Harmonic Lasing has longer gain-length

for undulator periods > 30mm

Energy-spread modifications
make the situation worse for HL

Harmonic Lasing vs. SCU

Energy-spread modifications make the situation much worse for HL

$$L_g \simeq L_{g0}(1 + \delta) \quad \delta = 131 \frac{I_A}{I} \frac{\epsilon_n^{5/4}}{\lambda_h^{1/8} \lambda_w^{9/8}} \frac{h^{9/8} \sigma_\gamma^2}{(KA_{JJh})^2 (1 + K^2)^{1/8}}$$

$$\text{In[1]} := \delta[\epsilon_n, \lambda_u, h, \sigma_\gamma, Ku, AJJh] =$$

$$131 * IA / Ip * \epsilon_n^{(5/4)} / (\lambda_{target}^{(1/8)} * \lambda_{uh}^{(9/8)}) * h^{(9/8)} * \sigma_\gamma^2 / ((Ku * AJJh)^2 * (1 + Ku^2)^{(1/8)})$$

$$\text{Out[1]} = \frac{131 h^{9/8} IA \epsilon_n^{5/4} \sigma_\gamma^2}{AJJh^2 Ip Ku^2 (1 + Ku^2)^{1/8} \lambda_{target}^{1/8} \lambda_{uh}^{9/8}}$$

$$\gamma = 17500 / 0.511 \quad \lambda_{target} = 0.0155 * 10^{-9} \quad \epsilon_n = 0.3 * 10^{-6}$$

$$IA = 17000; Ip = 5000; h = 3; \sigma_\gamma = 2.; Ku = \frac{\sqrt{2 h \gamma^2 \lambda_{target} - \lambda_{uh}}}{\sqrt{\lambda_{uh}}};$$

$$AJJh = \text{BesselJ}[(h - 1) / 2, h Ku^2 / (2 + 2 Ku^2)] - \text{BesselJ}[(h + 1) / 2, h Ku^2 / (2 + 2 Ku^2)];$$

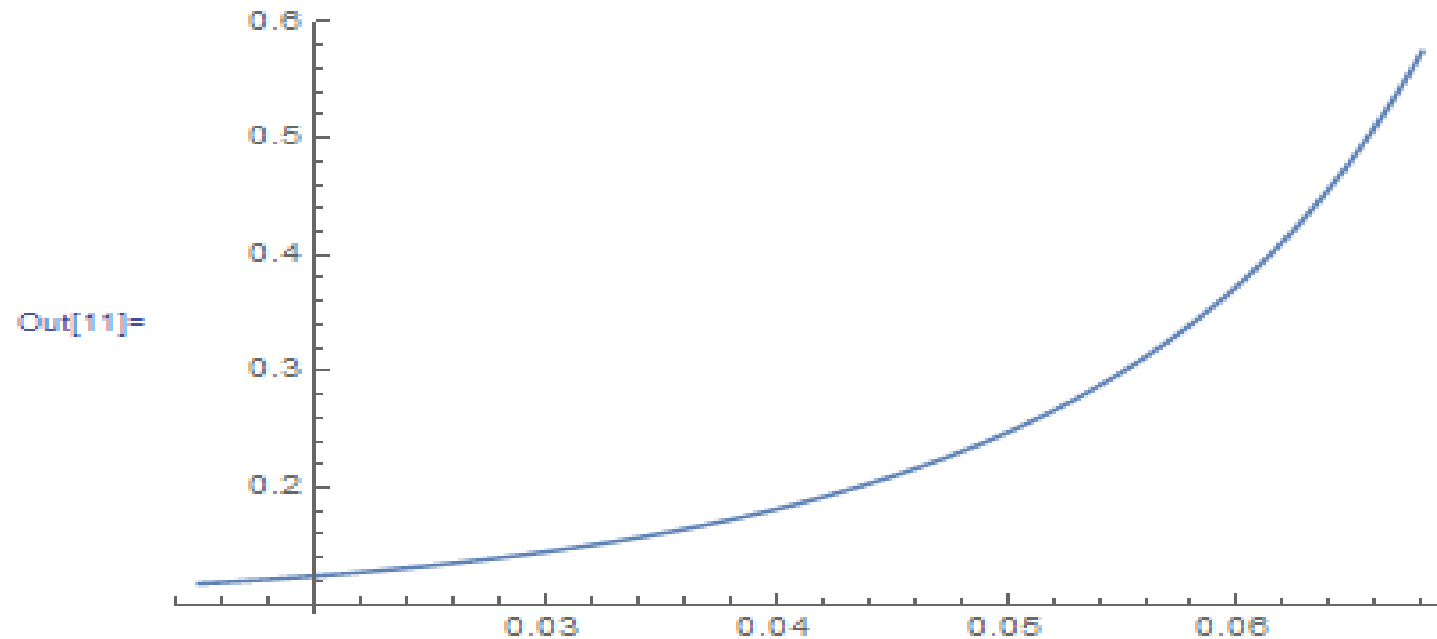
Harmonic Lasing vs. SCU

Energy-spread modifications make the situation much worse for HL

```
In[10]:= h = 3
```

```
Out[10]= 3
```

```
In[11]:= Plot[δ[en, λuh, h, σγ, Ku, AJJh], {λuh, 0.015, 0.068}]
```



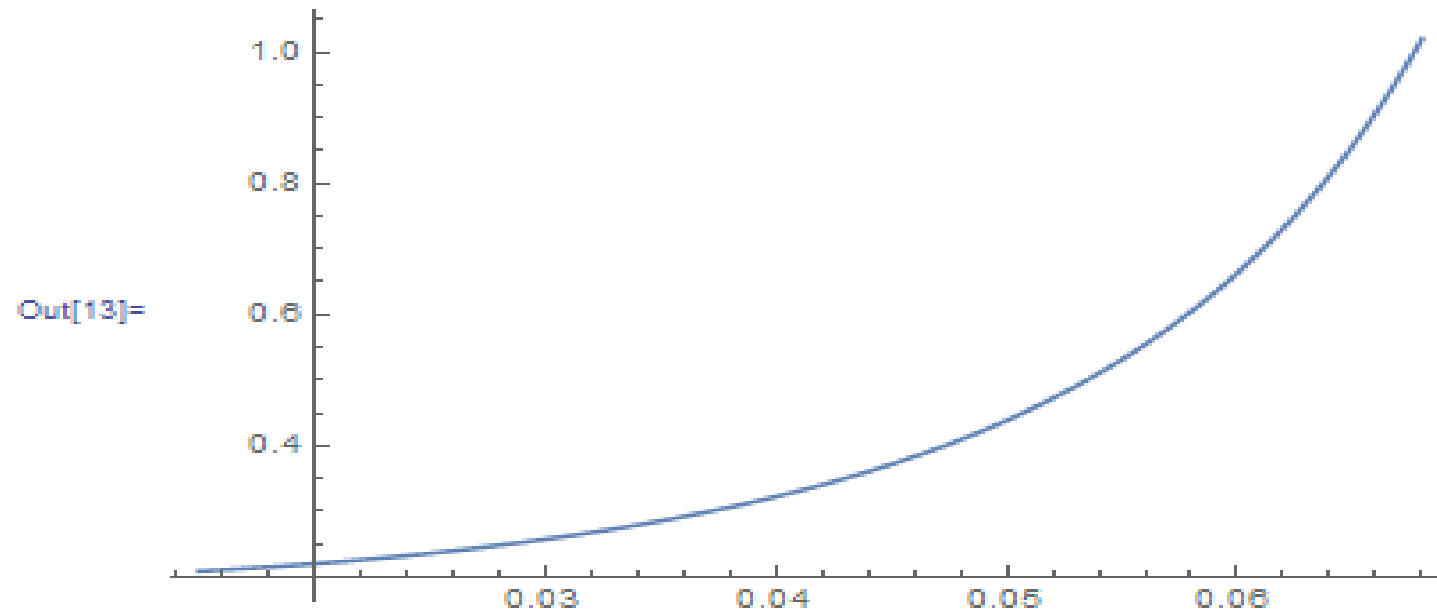
Harmonic Lasing vs. SCU

Energy-spread modifications make the situation much worse for HL

```
In[12]:= h = 5
```

```
Out[12]= 5
```

```
In[13]:= Plot[δ[εn, λuh, h, σγ, Ku, AJJh], {λuh, 0.015, 0.068}]
```



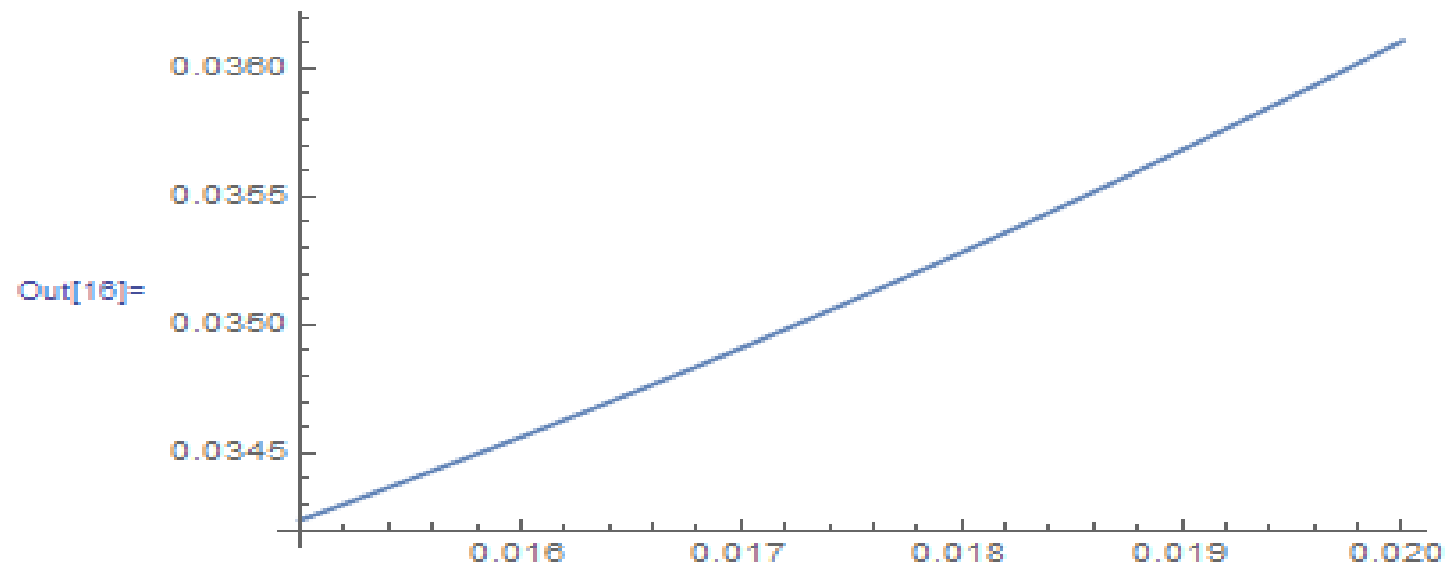
Harmonic Lasing vs. SCU

Energy-spread modifications make the situation much worse for HL

```
In[15]:= h = 1
```

```
Out[15]= 1
```

```
In[16]:= Plot[ $\delta[\epsilon_n, \lambda_{uh}, h, \sigma_\gamma, K_u, A_{JJh}]$ , { $\lambda_{uh}$ , 0.015, 0.02}]
```



No large influence for the case of SCU!

Harmonic Lasing Seeding vs. SCU

HLSS → Use part (A) of the undulator tuned directly at λ_t , part (B) tuned at a sub-harmonic
Conceptually the same as pSASE

Two different undulator periods are used for the two undulator parts

Then assume part (A) is the same as in the SCU case

And

Part (B) is like in the harmonic lasing case

Assume a fraction $0 < f < 1$ of the total length is (A) tuned directly at λ_t as SCU

The total gain length can be then written (assuming perfect suppression of the sub-harmonic fundamental in (B) as

$$L_g = fL_{gSC} + (1 - f)L_{gh} > L_{gSC} \text{ for } L_{gh} > L_{gSC}$$

Usually part (A) is shorter than (B), so $f < 0.5$ typically

Conclusions

Harmonic Lasing

Unless a short-period undulator is used, gain length is longer than for an optimized SCU

Example:

Case 40mm vs. SCU with 15mm: $L_{g0h} = 1.55L_{g0SC}$

Energy spread (1MeV rms)

$$L_{gSC} \simeq L_{g0SC}$$

$$h = 3 : L_{gh} \simeq 1.18L_{g0h} \longrightarrow L_{gh} \simeq 1.83L_{gSC}$$

$$h = 5 : L_{gh} \simeq 1.32L_{g0h} \longrightarrow L_{gh} \simeq 2L_{gSC}$$

HLSS

Is also longer as $L_g = fL_{gSC} + (1 - f)L_{gh} > L_{gSC}$ for $L_{gh} > L_{gSC}$ a small part

Important notes:

→ All this assuming perfect suppression of the fundamental in HL (or HLSS), worse in reality

→ The extra “budget” due to SCU can be used e.g. for tapering

→ Moreover: HL or HLSS are better with short periods. And SCUs produce large magnetic field

So they are best for tuning at sub-harmonic of the fundamental. One could install SCUs as baseline and still employ HL and HLSS to increase the spectral brightness, this time with a better gain length (energy spread effect still there, but short period)